



Winter Term Design Report

Project E4 - Tent Mountain Pumped Hydro Energy Storage Civil Engineering Design - ENCI 570

4 April 2024

Authors:

Monique Beaulieu - Technical

Patrick DeNault - Project Manager

Jack Dietze - Technical

Maxwell Machacek - Research

Matthew Zuidema - Technical

Dustin Thiessen - Project Manager

Navkaran Kang - Research

Melissa Erkmen - Technical

Sylvan Burdett - Technical

Advisors:

Dr. Simon Papalexiou – Academic

Dr. Alain Pietroniro – Academic

Mr. Andrew Szojka – Industry

Executive Summary

This report presents the final design selections and findings for the Tent Mountain Pumped Hydro Energy Storage (TM-PHES) project, located near the Crowsnest Pass of Alberta. During the Fall Term, the primary objectives were to optimize a design to enhance the Tent Mountain Upper Reservoir, size the Lower Reservoir, and design the North and South dams to enable a 16-hour continuous operation. The investigation focused on the water level, intake structure placement, and seepage losses of the Upper Reservoir. Among the options considered, the elevation (El.) of 1803.3 m for the Normal Maximum Operating Level (NMOL) was identified as having the least seepage losses, smallest dead storage volume, lowest flooded area at NMOL, and minimized grouting expenses. The Lower Reservoir was sized to accommodate the incoming volume from the Upper Reservoir during the 16-hour operation, where the NMOL El. of 1509 m was selected due to its minimal environmental and social impacts. Finally, the North and South dams were chosen to utilize dams with asphalt cores due to considerations such as the ease of construction, minimal environmental effects, and favorable cost factors.

For the Winter Term, the primary objectives were to conduct a water balance, hydrological analysis, and long-term climate change impact analysis. A Hydrologic Engineering Center – Hydrological Modelling System (HEC-HMS) model was adapted for long-term continuous and event-based simulations of the TM-PHES watershed. A modified Linacre equation was formulated using historical temperature data to calculate the basin's evaporation rate, resulting in an annual mean evaporation of 861.5 mm. Additionally, a GeoStudio seepage model was created for the Upper Reservoir, resulting in a total annual flux of 7.9 mm/year. Furthermore, projected future meteorological forcing data from four climate change scenarios, based on different socioeconomic development trends over the next 75 years, were used to simulate an ensemble of possible future streamflow records and examine the potential effects of climate change on the project. It was found that extreme outflow events, occurring due to an increase in precipitation intensity and rain on snow events, were greatest in Scenario 2 and occurred in May at 5.5 m³/s. Overall storage showed maximum fluctuations of 40,000 m³, corresponding to 150 mm of water level or 6 minutes of electricity production. An Operations Plan was formulated to outline the regulatory framework applicable to the system, the supply-demand dynamics concerning wind and solar generation, and the optimal pumping and generation schedules based on historical pool price data from the Alberta Electric System Operators (AESO). Several generating and pumping schedules were developed based on 2022 pool prices in Alberta, where it was determined that the option with 8 hours of generation to 10 hours of pumping was most advantageous. Finally, the developed Mitigation and Adaptation Plan offered various strategies for dealing with the climate extremes of floods and droughts, such as spillway management for the former and Aquacaps and Shade Balls for the latter.

Table of Contents

1	Introduction	1
1.1	Background	1
1.2	Fall Term Design Summary	1
1.3	Winter Term Scope of Work	3
1.4	Project Code Repository.....	6
2	Data Analysis	6
2.1	Observed Data Sources	6
2.2	The Ensemble Meteorological Dataset for North America	8
3	Water Balance	11
3.1	General	11
3.2	Basin Delineation	12
3.3	Precipitation.....	13
3.4	Evaporation and Evapotranspiration	13
3.5	Change in Reservoir Storage	16
3.6	Groundwater Seepage.....	17
3.7	Runoff.....	19
3.8	Results	20
4	Hydrological Modelling	20
4.1	Forcing Data	20
4.2	Model Workflow	20
5	Long-Term Climate Change Scenarios	24
5.1	Introduction	24
5.2	Scenario Overview	25
5.3	Temperature.....	26
5.4	Precipitation.....	31
5.5	Projected Outflow.....	36
5.6	Projected Storage.....	42
6	Design Event Estimation	47
6.1	Frequency Analysis	47
6.2	Probable Maximum Precipitation.....	48
6.3	Probable Maximum Flood.....	51
7	Design Updates.....	54
7.1	Spillway.....	54
7.2	Riparian Outlet	55

8	Operational Plan	56
8.1	Project Initialization	56
8.2	Power Generation in Alberta	56
8.3	Production and Pumping Plan	58
8.4	Operating Schedule	59
9	Mitigation and Adaptation.....	62
9.1	Extreme Drought Events	62
9.2	Extreme Excess Water Events.....	65
9.3	Recommendations	66
10	Conclusion.....	68
11	References	70
12	Appendix A	72

Tables

Table 1 – Fall Term Design Summary	1
Table 2 – Winter Term Deliverable Summary	5
Table 3 – TMCCP Climate Scenario Data Issue Summary.....	11
Table 4 - Monthly and Annual Evaporation Results Summary	16
Table 5 – Upper Reservoir Seepage Parameters	19
Table 6 – Original HEC-HMS Model Summary.....	21
Table 7 – Adapted HEC-HMS Models Summary (Continuous Simulation)	22
Table 8 – Adapted HEC-HMS Models Summary (Event-Based Simulation)	23
Table 9 - Summary of Storage Fluctuations.....	45
Table 10 – Frequency Analysis Summary.....	47
Table 11 – IDF Event-Based Model Results.....	51
Table 12 – Lower Reservoir Spillway Width Sensitivity Analysis.....	54
Table 13 – Monthly Riparian Flow Summary - Historical.....	55
Table 14 – Monthly Riparian Flow Summary – Scenario 2.....	55
Table 15 - Turbine design discharges [1]	59
Table 16 – List of most profitable pool price hours in Alberta for 2022 [24]	60
Table 17 – Net revenue and annual % difference of the maximum and set options.	61
Table 18 – Monthly % difference between generating and pumping pool prices for Alberta in 2022	62
Table 19 – Design Summary (Fall and Winter Terms)	68

Figures

Figure 1 - ECCC Weather Station Locations Near Tent Mountain Watershed Map	7
Figure 2 - Data Availability for Nearby ECCC Stations	7
Figure 3 - Streamflow Gauge Locations Near Tent Mountain.....	8
Figure 4 - Tent Mountain Catchment in EMDNA Grid	9
Figure 5 - Tent Mountain Water Balance.....	11
Figure 6 - Tent Mountain Delineated Catchment Areas	12
Figure 7 - Mean Monthly Evaporation and Precipitation.....	16
Figure 8 - GeoStudio SEEP/W Model of E-W Cross-Section	18
Figure 9 - GeoStudio SEEP/W Model of E-W Cross-Section with Waste Dump Pile	18
Figure 10 - GeoStudio SEEP/W Model of N-S Cross-Section	19
Figure 11 – HEC-HMS Model Workflow Chart.....	21
Figure 12 - Climate Change Scenario Summary [5]	25
Figure 13 - Average Historical Monthly Temperature with Range.....	26
Figure 14 - Average Projected S1 Monthly Temperature with Range	27
Figure 15 - Average Projected S2 Monthly Temperature with Range	28
Figure 16 - Average Projected S3 Monthly Temperature with Range	28
Figure 17 - Average Projected S4 Monthly Temperature with Range	29
Figure 18 - Box Plot of Monthly Temperature for All Scenarios Excluding Outliers	30
Figure 19 - Average Historical Daily Precipitation per Month with Maximum	31
Figure 20 - Average Projected S1 Daily Precipitation per Month with Maximum.....	32
Figure 21 -Average Projected S2 Daily Precipitation per Month with Maximum.....	32
Figure 22 - Average Projected S3 Daily Precipitation per Month with Maximum.....	33
Figure 23 - Average Projected S4 Daily Precipitation per Month with Maximum.....	34
Figure 24 - Box Plot of Daily Precipitation per Month for All Scenarios Excluding Outliers	34
Figure 25 - Bar Graph of Average Cumulative Monthly Precipitation for All Scenarios.....	35
Figure 26 - Average Historical Daily Outflow per Month with Maximum	37
Figure 27 - Average Projected S1 Daily Outflow per Month with Maximum.....	38
Figure 28 - Average Projected S2 Daily Outflow per Month with Maximum	38
Figure 29 - Average Projected S3 Daily Outflow per Month with Maximum.....	39
Figure 30 - Average Projected S4 Daily Outflow per Month with Maximum.....	40
Figure 31 - Box Plot of Daily Outflow per Month for All Scenarios Excluding Outliers	40
Figure 32 - Box Plot of Daily Outflow per Month for All Scenarios Including Outliers.....	41

Figure 33 - Reservoir Storage for All Scenarios 2020-2100.....	43
Figure 34 - Daily S1 Projection of Average Reservoir Storage with Range from 2031-2100.....	43
Figure 35 - Daily S2 Projection of Average Reservoir Storage with Range from 2031-2100.....	44
Figure 36 - Daily S3 Projection of Average Reservoir Storage with Range from 2031-2100.....	44
Figure 37 - Daily S4 Projection of Average Reservoir Storage with Range from 2031-2100.....	45
Figure 38 - Monthly Average Reservoir Storage for All Scenarios	46
Figure 39 - Spatial Distribution of PMP Values at 24-hour, 10 km ²	50
Figure 40 – Upper Reservoir Storage, Flow, and Water Elevation (PMF 1)	52
Figure 41 – Lower Reservoir Storage, Flow, and Water Elevation (PMF 1).....	52
Figure 42 – Upper Reservoir Storage, Flow, and Water Elevation (PMF 2)	53
Figure 43 – Lower Reservoir Storage, Flow, and Water Elevation (PMF 2).....	53
Figure 44 – Lower Reservoir Storage, Flow, and Water Elevation (PMF 2, 15 m Spillway).....	55
Figure 45 – Wind and Solar Generation as a Function of Pool Price (April 2023).....	58
Figure 46 – Shade Balls [25].....	63
Figure 47 – Aquacaps on Reservoir [26].....	63

Appendix A Figures

Appendix A Figure 1 - Elevation of ECCC Weather Stations	72
Appendix A Figure 2 - Monthly Correlation Stations with 5+ Years Overlapping Data.....	72
Appendix A Figure 3 - EMDNA Data Creation Methodology and Example [4].....	73
Appendix A Figure 4 - Sample of EMDNA Historic Data Tent Mountain.....	73
Appendix A Figure 5 - Sample Scenario Output Data with Calculated Evaporation	74
Appendix A Figure 6 - Overall Leapfrog Model of the Tent Mountain Site (Plan View)	75
Appendix A Figure 7 - Sample HEC-HMS Output.....	76
Appendix A Figure 8 -Box Plot of Monthly Temperature for all Scenarios with Outliers	76
Appendix A Figure 9 - Average Historical Monthly Precipitation Excluding 0 Precipitation Days	77
Appendix A Figure 10 - Average Projected S1 Daily Precipitation Excluding 0 Precipitation Days.....	77
Appendix A Figure 11 - Average Projected S2 Daily Precipitation Excluding 0 Precipitation Days.....	78
Appendix A Figure 12 -Average Projected S3 Daily Precipitation Excluding 0 Precipitation Days.....	78
Appendix A Figure 13 - Average Projected S4 Daily Precipitation Excluding 0 Precipitation Days.....	79
Appendix A Figure 14 - Box Plot of Daily Precipitation per Month, All Scenarios Including Outliers....	79
Appendix A Figure 15 – Box Plot of Daily Outflow per Month Excluding Outliers (2010-2040).....	80
Appendix A Figure 16 - Box Plot of Daily Outflow per Month Excluding Outliers (2041-2071)	80
Appendix A Figure 17 – Box Plot of Daily Outflow per Month Excluding Outliers (2072-2100).....	81

1 Introduction

1.1 Background

The Tent Mountain Renewable Energy Complex (TM-REX), formerly a coal mine in southwestern Alberta, is undergoing evaluation for transformation into a pumped hydro energy storage (PHES) facility, jointly pursued by TransAlta and Evolve Power [1,2]. The goal of this project is to transform the mine pit into a renewable energy storage facility, where water is discharged from the Upper Reservoir for power generation when demand for electricity is high, and water is pumped back up during periods of low electricity demand.

1.2 Fall Term Design Summary

This report builds upon and is intended to be read in that context of the Fall Term Design Report, where initial assessment and scoping were a major component of the project deliverables. A summary of the work presented therein is included in Table 1.

Table 1 – Fall Term Design Summary

Parameter	Value
Upper Reservoir	
Drainage Area	1.311 km ²
Live Storage Volume	7.107 E06 m ³
NMOL	1803.3 masl
NMOL Reservoir Footprint	0.2758 km ²
Dead Storage Volume	2.045 E06 m ³
DSL	1760.0 masl
Seepage Reduction Strategy	Grout curtain and grouted cutoff wall
Containment Structure Minimum Elevation	1806.8 masl
Lower Reservoir	
Drainage Area	5.557 km ²
Live Storage Volume	7.107 E06 m ³
NMOL	1509.0 masl
Dead Storage Volume	0.5268 E06 m ³
DSL	1480.0 masl
South Dam	
Dam Crest Elevation	1513.0 masl
Dam Type	Asphalt core rockfill embankment
North Dam	
Dam Crest Elevation	1512.5 masl
Dam Type	Asphalt core rockfill embankment

During the Fall semester, the primary objectives were to optimize a design to enhance the Tent Mountain Upper Reservoir and size the Lower Reservoir to enable a 16-hour continuous operation for generating 320 MW of clean power for Alberta.

1.2.1 Upper Reservoir

The Upper Reservoir is a decommissioned coal mine pit that filled with water after the cessation of its operations in 1983 and has maintained a water level of around elevation (El.) 1780 m for decades [1]. This suggests that any water entering the reservoir above this elevation escapes via seepage and evaporation, maintaining a consistent equilibrium with precipitation inputs. The topography of the Upper Reservoir is such that the required water volume for 16 hours of electricity generation can be achieved by raising the Normal Maximum Operating Level (NMOL) or lowering the Dead Storage Level (DSL), rather than by expanding the inundated area as is the case with the Lower Reservoir. Three NMOL-DSL pairs were investigated based on the constraints of the Upper Reservoir's topography, where the selection was largely governed by seepage losses, dead storage volume, the flooded area at its NMOL, and associated grouting costs.

The security of the water supply is dependent on the reduction of seepage from the reservoir walls, this is imperative in the context of this project as water is the “fuel” source of the system. The seepage losses were modelled and quantified using the GeoStudio SEEP/W module, based upon cross-sections taken from the Leapfrog geological model provided by TransAlta for the site. Using N-S and E-W cross-section models, flux values ($\text{m}^3/\text{s}/\text{m}^2$) were computed, adjusting boundary conditions to reflect each design's NMOL. These values were averaged across the submerged reservoir surface, resulting in six flux values. The use of a grout barrier vertical cutoff wall was identified as the best solution for preventing seepage through the waste material; moreover, for the non-waste material, polyurethane (PU) curtain grouting was selected. The choices were determined by site constraints, suitability, constructability, minimal waste production, permeability resistance, eco-friendliness, and cost-effectiveness, according to literature about reducing seepage of hazardous materials on mine sites. Overall, the elevation (El.) 1803.3 m NMOL option was found to be the most cost-effective due to the lowest flux ($4.85\text{E-}03 \text{ m}^3/\text{s}$) of the three options, and thus requiring less exterior grouting, and as a result, a shorter vertical cutoff wall. The low cutoff wall height not only leads to the lowest construction costs by reducing the grouting required, but it also mitigates overtopping or slope failure risks due to additional topography surrounding the final water level and less force along the reservoir walls. Moreover, it minimizes the dead storage volume, making use of the maximum proportion of retained water. With the associated low flux and flooded area, this enhances the operational resilience against drought by reducing seepage and evaporation losses, respectively.

1.2.2 Lower Reservoir

For the Lower Reservoir, the main goal was to size the reservoir to be able to accommodate the incoming volume from the Upper Reservoir during this 16-hour operation. It can be noted that the Lower Reservoir's location and sizing are constrained by its proximity to the Alberta-British Columbia provincial border and its encroachment onto Crown Land. Additional selection criteria considered included maximizing the catchment area while minimizing the following: inundated area, environmental impacts, haul distances based on existing access roads, average ground slope, and dam width when selecting dam locations. These factors guided the decision to fix the South Dam location in place near the BC border and explore alternative locations for the North Dam. Subsequently, the variations in water level and the necessary dam dimensions were assessed for each alternative. Three NMOL options for the Lower Reservoir were evaluated: El. 1500 m, El. 1505m and El. 1509 m. The 1509 m NMOL El. option was selected primarily due to the lowest Crown Land encroachment, smallest flooded area, and minimal environmental and social impacts.

Finally, three alternative rockfill embankment dam types for the North and South Dams were considered. A sheet pile core dam, an asphalt core dam, and a concrete-faced dam were researched and assessed for suitability. To maximize the ease of material acquisition, all three dam types were based on a rockfill embankment dam which can take advantage of the local abundance of rocky materials in the area. Additional deciding factors included maximizing the sustainability of the materials and constructability of the dam, while minimizing transportation impacts, lifecycle environmental impacts, construction costs, and operational costs. After incorporating all constraints into the design, the rockfill embankment dam with an asphalt core was selected based on its superior comparative scores regarding constructability, reduced environmental impacts, and favourable costs.

1.3 Winter Term Scope of Work

Winter Term deliverables analyze the TM-PHES Project based on the fixed design of the Fall Term parameters such as reservoir size, reservoir location, and seepage rates. This analysis focuses on modelling the site's water balance, future climate scenarios, and operational scenarios. Values from the analysis are utilized to inform the spillway and riparian outlet design, along with climate mitigation techniques, and recommendations for the site's operation. The motivation behind these deliverables was to inform stakeholders about the projected future behaviour of the site. This scope reduces risk by considering extreme values before construction, which reduces the likelihood of failure or a future re-design, improving sustainability and cost-effectiveness. Moreover, it also allows stakeholders to gauge project feasibility before significant capital investment. Thus, an informed design decision during the conceptual design stage can be made when scope change is comparatively cheap. The remainder of this section will describe each deliverable, its purpose, and the potential issues they address.

- 1. Initial Water Balance:** The initial water balance assesses the current water levels, storage capacity, and inflow/outflow dynamics of the reservoirs at the project site for the various phases of filling, balancing, and operating the PHES system. This investigation analyzes historical data on inflows and outflows to understand natural hydrological patterns. The deliverables generated include parameters for each water balance component, such as evaporation and seepage, historical data sets, and an overarching water balance analysis. These documents address design considerations concerning the reservoir fill time and furnish historical data crucial for informed design decisions.
- 2. Hydrological Modelling:** The hydrological model investigates the water cycle, temperature variations, and precipitation patterns at Tent Mountain, projecting how these factors will impact both outflow and water storage at the location. The outcome of this section is a tailored HEC-HMS model, specifically designed for the site, which emulates the operations of the TM-PHES project. By integrating future climate projections, this model will help address design considerations related to the anticipated behaviour of reservoir storage and outflow, informing decisions for the reservoirs.
- 3. Long Term Climate Modelling:** The long-term climate model will project temperature, precipitation, and reservoir behaviour due to four different climate change scenarios until the year 2100. Predicting how changes in climate patterns impact the hydrological cycle and, consequently, the performance of the PHES system. The deliverables for this section include graphs comparing the average and extreme temperature, precipitation, outflow, and storage at Tent Mountain due to the changing climate. These deliverables will help inform the design of the outflow design and the mitigation plan. They will also address stakeholder concerns regarding the future viability of the project concerning potential high outflow or low storage scenarios.
- 4. Outflow Structure Design:** This section encompasses plans for the spillway and riparian outlet components of the project, serving to manage reservoir water levels, ensure repayment of streamflow obligations, and offer an outlet to mitigate the risk of dam failure during extreme outflow occurrences. Drawing upon both historical data and climate scenario projections, the designs will be informed by estimates of probable maximum flood and probable maximum precipitation. The output includes the design specifications for the spillway and riparian outlet, aiming to alleviate stakeholder apprehensions regarding flood risks, dam integrity, and the environmental restoration of water obligations.
- 5. Operational Plan:** The operational plan outlines the day-to-day function of the pumped hydro system, detailing how energy storage and generation can be managed to meet demand. It investigates energy production and price in Alberta to project the best times for the project to refill the Upper Reservoir or produce electricity. The deliverables from this section include a projected pumping and production plan as well as a potential operating schedule. Several operating scenarios

are considered based on alternative electricity production and potential profits. Stakeholder concerns regarding the profitability of the project, the operating schedule of the project, and potential connections with renewable energy generation are also addressed by this deliverable.

6. **Mitigation and Adaptation Plan:** The mitigation and adaptation plan addresses how variations in input parameters or external factors affect the performance of the pumped hydro system. It investigates different technologies and features which could be utilized at the site to reduce the risk of both drought and flooding scenarios. The deliverables for this section consist of investigations into a range of technologies applicable to the TM-PHES project. It will provide stakeholders with an analysis of technologies that can be implemented to increase project resilience and sustainability.

Table 2 – Winter Term Deliverable Summary

Deliverable	Sub-deliverables	Constraints	Exclusions
Historical Hydrological Analysis	<ul style="list-style-type: none"> • Continuous simulation hydrological model adaptation. 	<ul style="list-style-type: none"> • Constrained to the features of the hydrological model. • No hydrometric data available at site. • Inadequate observed weather station data. 	<ul style="list-style-type: none"> • Model calibration. • Lower reservoir seepage.
Projected Future Hydrological Analysis	<ul style="list-style-type: none"> • Projected site storage and outflow response to future climate conditions. 	<ul style="list-style-type: none"> • Constrained to the features of the hydrological model. 	<ul style="list-style-type: none"> • Model calibration. • Lower reservoir seepage.
Long Term Climate Change Scenarios	<ul style="list-style-type: none"> • Climate projection realizations. • Graphs for temperature, precipitation, outflow, and storage. 	<ul style="list-style-type: none"> • Limited data available at site. • Limited project timeframe. • Errors in certain climate realizations. 	<ul style="list-style-type: none"> • Any climate scenario that is not a Tier 1 CMIP6 model.
Outflow Structure Design	<ul style="list-style-type: none"> • Event-based hydrological model adaptation. • Spillway design. • Riparian outlet design. 	<ul style="list-style-type: none"> • The spillway must be able to safely route the Inflow Design Flood. • The riparian outlet must be compatible with average runoff. 	<ul style="list-style-type: none"> • Model calibration. • Structural design. • Cost analysis.
Operational Plan	<ul style="list-style-type: none"> • Predict ideal times to pump based on historical pool prices and peak renewable energy generation. 	<ul style="list-style-type: none"> • Uncertainty around pool price fluctuations and future renewable energy generation. 	<ul style="list-style-type: none"> • Predictions based on forecasted generation data.
Mitigation and Adaptation Plan	<ul style="list-style-type: none"> • Potential mitigation strategies to reduce the risks of flood and drought. 	<ul style="list-style-type: none"> • Geographic constraint of site. 	<ul style="list-style-type: none"> • Cost analysis. • Technology implementation plan.

1.4 Project Code Repository

The scope of work in the winter semester included several deliverables which required coding in R and Python to complete. These deliverables include data wrangling, cleaning, analysis, and visualization, primarily focused on Sections 2 and 5 of the report. A public GitHub repository was created to consolidate all project coding efforts. This repository, available at https://github.com/moniquebeaulieu/TM_PHES.git, provides a comprehensive explanation of the workflow process and analytical methodology used.

2 Data Analysis

2.1 Observed Data Sources

Environment and Climate Change Canada (ECCC) maintains a database of meteorological stations across Canada; among their monitored parameters are temperature and precipitation, which are key to hydrological analysis. Within a 25 km radius of the site, multiple stations exist, and statistical transformations of their data were applied by Hatch and Matrix in previous analyses to estimate historical temperature and precipitation at the site. [1,3].

Hatch also used meteorological data from the Morrissey Ridge station provided by the Pacific Climate Impacts Consortium [1]. This dataset has a high proportion of missing values over the period of record and issues exist regarding data validity; therefore, it was rejected from the analysis described herein.

Several ECCC stations exist near the Tent Mountain site watershed (see Figure 1). These stations provide observed precipitation and temperature data, which could theoretically be interpolated to the site location to model historical weather at Tent Mountain. However, these stations lack overlapping years and several have under 20 years of historical data (see Figure 2). Furthermore, the elevations of most stations are lower than the Tent Mountain site, and the monthly correlation between stations with over five years of data is inconsistent. These factors make interpolating observed data to Tent Mountain difficult, as data reliability and geographical differences would lead to inaccuracies in the interpolation process. Additionally, accurate outflow values for the watershed are required to train and validate the interpolation and stochastic parameters of observed data for the site which was not available at Tent Mountain. Additional data exploration in Appendix A highlights more issues with the observed data.

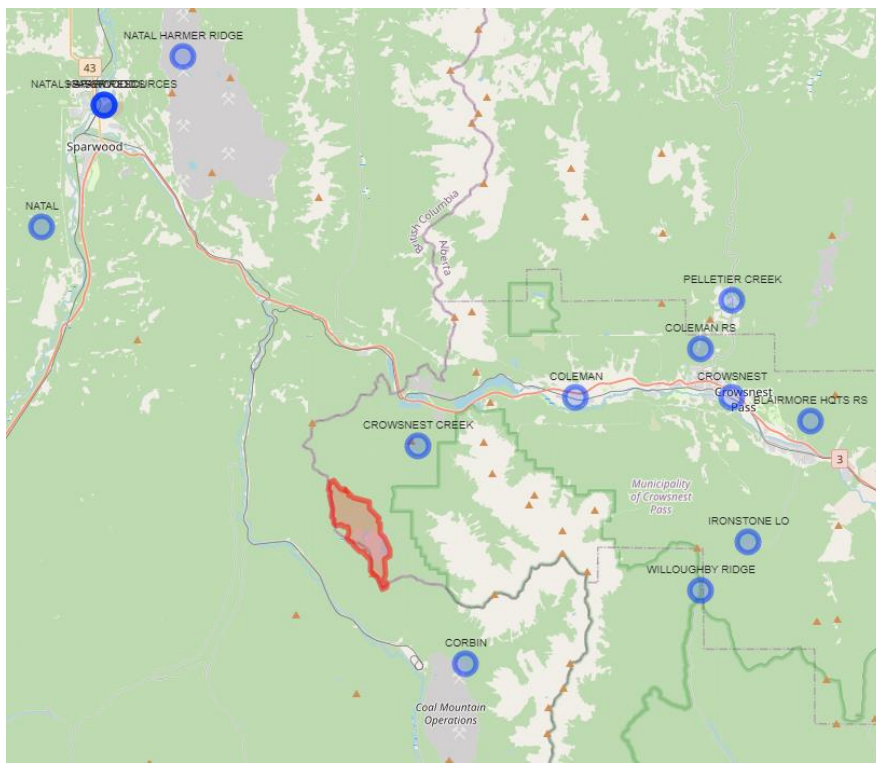


Figure 1 - ECCC Weather Station Locations Near Tent Mountain Watershed Map

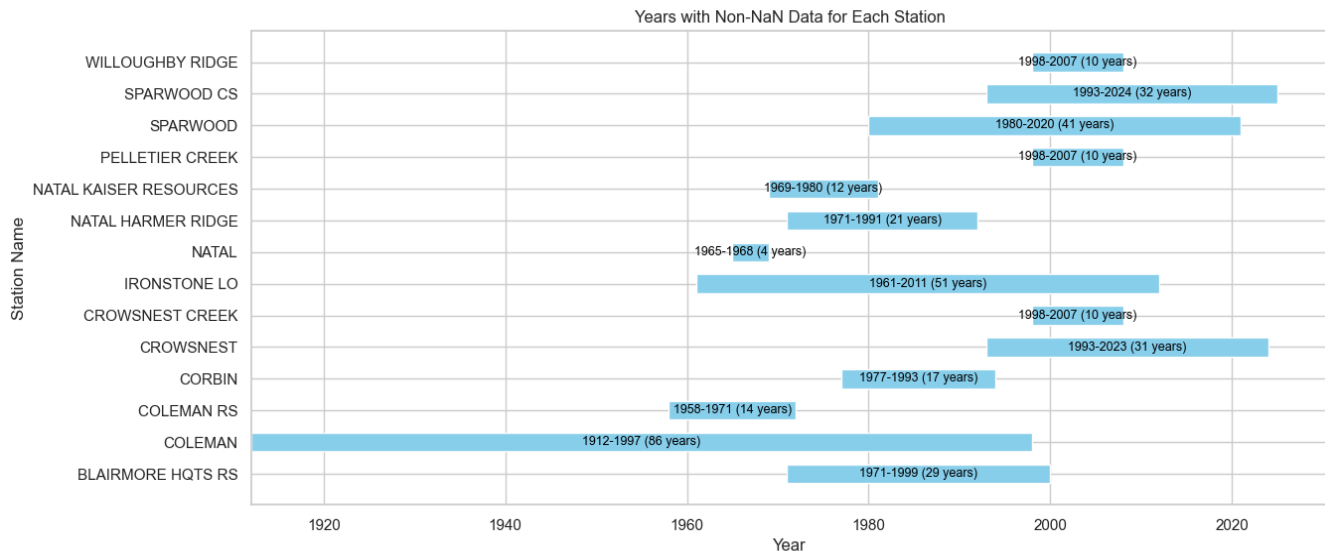


Figure 2 - Data Availability for Nearby ECCC Stations

The Water Survey of Canada (WSC) monitors streamflow and/or water level on thousands of reaches nationwide. Due to Canada's large number of water bodies and relatively low population density, there remains a high proportion of unmonitored streams. Such is the case for the tributary of Crowsnest Creek into which the Tent Mountain site drains. Figure 3 highlights the location of the four nearest streamflow gauges with similar-sized watersheds to Tent Mountain. Matrix's Hydrology Basis used the statistical

relationships between the drainage areas and outflows of these nearby basins to estimate outflow from the Tent Mountain site [3]. However, the transferability of flow information using these methods, particularly in high-relief areas, is often unreliable. The estimated outflow value for Tent Mountain would result in an additional layer of uncertainty and potential bias to the estimate.

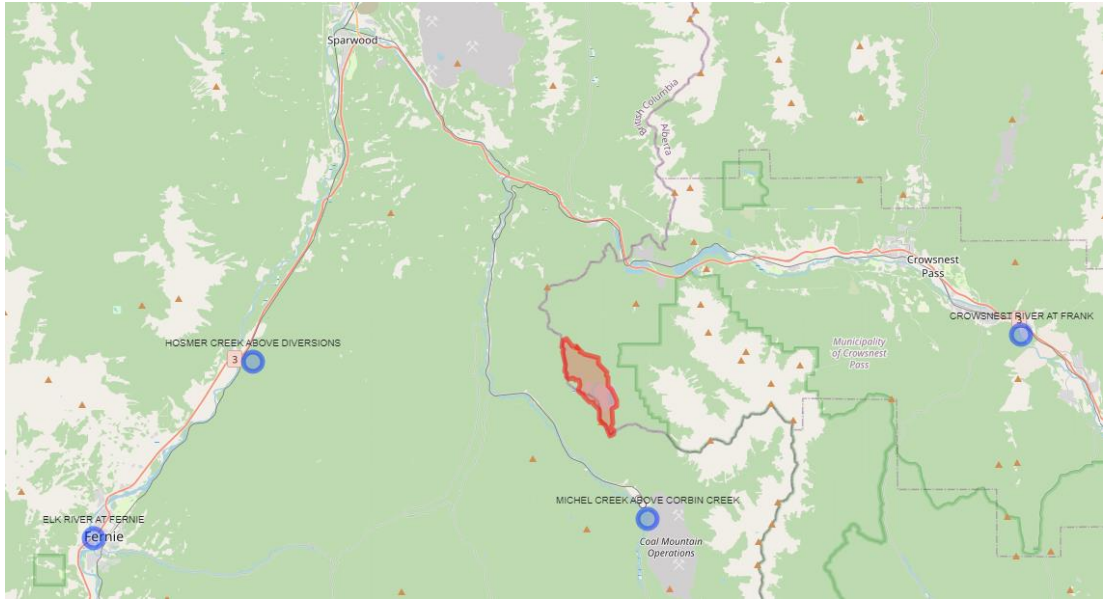


Figure 3 - Streamflow Gauge Locations Near Tent Mountain

Ultimately, the lack of certainty regarding outflow data for the Tent Mountain site made interpolating observed hydrometric data to the site and performing stochastic analysis sub-optimal as an approach. The analysis outlined herein employs a modelling approach to obtain historical data for Tent Mountain, the details of which are discussed below.

2.2 The Ensemble Meteorological Dataset for North America

2.2.1 Current Climate Information

The Ensemble Meteorological Dataset for North America (EMDNA) is a gridded climate dataset that uses point data from multiple meteorological stations and performs probabilistic analysis on this data to produce gridded temperature and precipitation estimates [4]. Missing values and short data durations in this model are supplemented by spatial interpolation from the Serially Complete Dataset for North America (SCDNA). SCDNA uses interpolation, machine learning, and quantile mapping techniques on raw data of temperature and precipitation to complete weather station data in sparsely gauged regions. Distance-weighted weather station data from the nearest 20-30 stations were used to create estimates for temperature and precipitation for a given location at a certain time. Spatial temperature and precipitation were treated as random variables (x) represented by probability density functions (PDFs). Temperature (T_{mean} & T_{range}) was approximated using a normal distribution, while precipitation was approximated by a PDF with the following equation:

$$F_X(x) = (1 - p_0)F_{X|>0}(x) + p_0 \quad (1)$$

Equation 1 accounts for precipitation being both highly skewed and bounded at zero. The term $F_{X|>0}(x)$ is the cumulative distribution function (CDF) for precipitation in a region if precipitation occurs, and p_0 is the probability of zero precipitation, $(1 - p_0)$ is the probability of precipitation (PoP) [4]. The mean (μ) and standard deviation (σ) of space and time-varying temperature and precipitation values, as well as the elevation-based PoP were used to create a gridded estimate for a region. The grids are 0.1° resolution (approximately 11 km) and use latitude, longitude, and elevation as predictor variables. EMDNA then used Optimal Interpolation (OI) to merge data from the multiple weather stations for specific locations, and advanced bias correction and error adjustments were performed. Finally, a spatially correlated random field (SCRF) was created to sample temperature and precipitation at any location within any grid. EMDNA data from 1979 to 2014 exists for all of North America. A summary of this process and an example of the methodology used to produce this stochastic data is provided in Appendix A.

EMDNA data was peer-reviewed and proven to represent spatial temperature and precipitation throughout North America accurately [4]. Therefore, it was used at Tent Mountain instead of the observed weather station data because it remedied the lack of site-specific temperature and precipitation values. The entire Tent Mountain catchment area is within the $49.50\text{--}49.60^\circ\text{N}$ by $114.70\text{--}114.80^\circ\text{W}$ EMDNA grid, as seen in Figure 4. This grid was used to obtain the site-specific temperature and precipitation values used throughout this report. A sample of the output data is in Appendix A. This current climate data was used by the water balance estimation in Section 3, and the HEC-HMS model in Section 4.

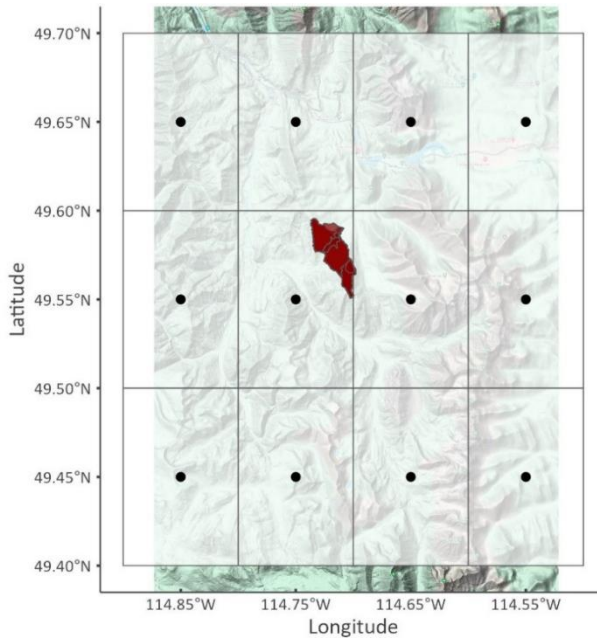


Figure 4 - Tent Mountain Catchment in EMDNA Grid

2.2.2 Future Climate Projections

The EMDNA database provided complete and accurate historical temperature and precipitation data for the Tent Mountain site. Accurate data for variables such as seepage, windspeed, evaporation, and outflow were unavailable for this site, and the assumptions made to incorporate these variables in the analysis are explained throughout this report. To produce projections for future climate scenarios the historical data from the EMDNA database was used to bias correct climate change scenarios and realizations obtained from The Coupled Model Intercomparison Project Phase 6 (CMIP6) [4,5,6]. Four scenarios were investigated, with each scenario describing the projected climate implications of different environmental policies. Each scenario is represented by several CMIP6 realizations, each with slightly altered internal parameters to encompass climate variability. The Tent Mountain-specific climate projection data produced by bias correcting the CMIP6 models with Tent Mountain EMDNA data is referred to as the Tent Mountain Climate Change Projection (TMCCP) throughout this report. The TMCCP data incorporates several bias-corrected realizations for each of the four CMIP6 climate change scenarios. An in-depth summary of the climate scenarios, as well as the results and analysis from the TMCCP data, are in Section 5.

A few data integrity issues emerged with the TMCCP data. Each realization was supposed to produce predicted temperature and precipitation values from January 1st, 2015, to December 31st, 2100. These dates were chosen because the first year provided by the climate realizations was 2015, while 2100 is a common ending point for similar climate models. However, many TMCCP realizations had missing dates over their 85-year spans. When a missing date occurred between dates with known values it was considered a minor issue. The missing date was added, and the missing precipitation and temperature values were linearly interpolated. It was assumed this linear interpolation did not significantly impact data integrity, and realizations with this issue were kept in the analysis.

Some TMCCP realizations produced data that ended before the December 31st, 2100, deadline. This problem was a major issue as it created inconsistencies in end dates and impacted seasonality. When more than a couple of months of data were missing at the end of a realization, an unknown error would shift the temperature and precipitation values forward by the number of missing days, so January would be projected to experience summer-like temperatures while July experienced winter conditions. An extreme example of this was a realization that ended on May 24th, 2097, which projected temperatures of 11°C on January 15th, 2015, and -30°C on July 15th, 2015. This issue of inverted seasonality would create major data integrity problems; therefore, any realization with an end date earlier than October 31st, 2100, was assumed to have inaccurate seasonality and was removed from the analysis. Two months of missing data was the maximum amount achievable without producing noticeable inconsistencies. Data integrity was still deemed acceptable

because each climate change scenario had 25 or more TMCCP realizations with complete data or only minor issues. Table 3 summarizes the total realizations, and realizations used for each future climate scenario.

Table 3 – TMCCP Climate Scenario Data Issue Summary

Climate Scenario	Total Realizations	Realizations with Major Issues	Realizations Used (Minor or No Issues)
Scenario 1	34	8	26
Scenario 2	36	7	29
Scenario 3	31	6	25
Scenario 4	40	10	30

3 Water Balance

3.1 General

A water balance involves a systematic assessment of input, output, and storage aspects within a hydrological system, including precipitation, evapotranspiration, outflow, groundwater outflow, and catchment storage. This method, also known as a water budget, is crucial in hydrology for monitoring water movement and distribution over a defined period. It considers factors like rainfall, evaporation, runoff, groundwater recharge, and changes in water levels to gauge water availability and movement, aiding in water resource management and environmental impact prediction. Figure 5 illustrates the parameters used in the Tent Mountain water balance and their interconnections within the geographical area.

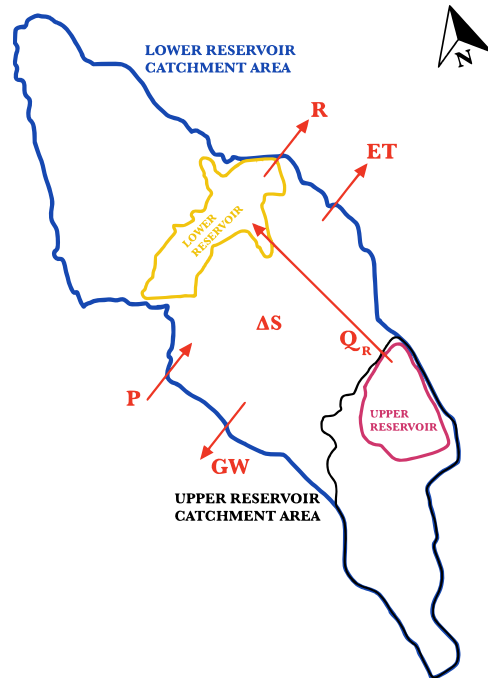


Figure 5 - Tent Mountain Water Balance

The following equation was used to approximate the water balance for the site:

$$P - ET - \Delta S - GW = R \quad (2)$$

In equation 2, P is precipitation, ET is evapotranspiration from the reservoirs and terrestrial areas, ΔS is change in reservoir storage, GW is groundwater seepage, and R is runoff, which is approximately equal to streamflow from the riparian outlet under normal operating conditions. Various assumptions were made to approximate the complexity of the TM-PHES basin for the hydraulic model and are discussed in each of the respective subsequent sections.

3.2 Basin Delineation

The Upper and Lower Reservoir subbasins were delineated using Global Mapper, a geographic information system (GIS) program, using the Create Watershed command, which facilitates watershed analysis on loaded terrain data, identifying stream paths and delineating watershed areas draining into specified stream sections. This method utilizes the eight-direction pour point algorithm (D-8) to compute flow direction at individual locations, coupled with a bottom-up strategy for assessing flow direction across flat terrain, and a specialized algorithm for filling depressions in the terrain data. By setting the overall area, the stream size, the cell count, resolution, and stream threshold it then populated catchment areas for the two reservoirs.

The Resolution section allows for the adjustment of the sampling resolution of terrain data, balancing calculation speed with detail level. The Stream Threshold section dictates the water flow required for a cell to be classified as part of a stream, influencing the delineation of significant water flow areas.

Section 1.2 discusses the selection of the upper and lower reservoir NMOLs, which contributed to the final catchment areas used, depicted in Figure 6.

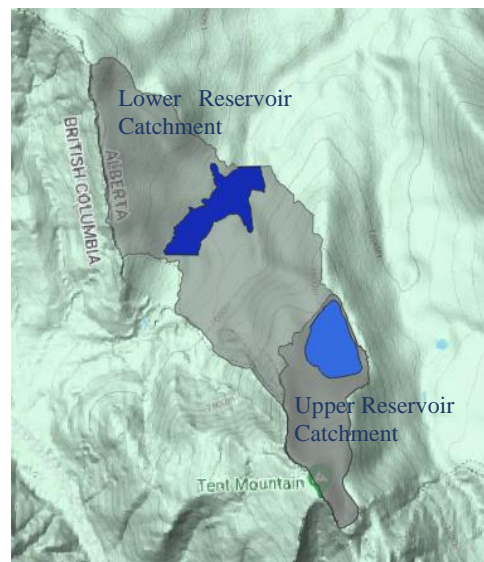


Figure 6 - Tent Mountain Delineated Catchment Areas

3.3 Precipitation

EMDNA gridded precipitation data was used for reasons discussed in Section 2.2. The basin mean annual precipitation for the historical period was 1149 mm. Figure 7 compares the basin mean annual precipitation with the mean annual evaporation, and illustrates seasonal fluctuations in both evaporation and precipitation, aiding in identifying peak months for each factor.

3.4 Evaporation and Evapotranspiration

3.4.1 Background

Due to the limited meteorological data in the area, calculations for evaporation and evapotranspiration were restricted to equations that rely solely on temperature, or other assumptions. Previous feasibility studies utilized the Morton Method (Matrix, 2020) [3,7] and the Linacre Method (Hatch, 2022) [1,8].

The Morton Method was derived to assess evaporation rates at 20 different locations across Alberta, so Matrix extrapolated to the Tent Mountain region by averaging data from Lethbridge (lower elevation; similar latitude) and Jasper (higher elevation; further north). Using this method, estimates of mean annual gross evaporation rates were reported for Jasper as 663 mm/year, for Lethbridge as 1062 mm/year, and for Tent Mountain as 929 mm/year. These findings have shown their reliability in estimating conditions in the prairie regions of Alberta, serving as a precise benchmark for comparison. Nevertheless, a more thorough examination is necessary to ascertain a precise evaporation estimate for the mountainous terrain where Tent Mountain is situated.

The Linacre equation, a modified version of the Penman formula, does not require radiation or humidity data, rather it relies solely on temperature, as defined below:

$$E_0 = \frac{\frac{Q T_m}{100 - A} + 15(T - T_d)}{80 - T} \quad (3)$$

In equation 3, Q is an empirically derived constant that describes the relationship between radiation and albedo, $T_m = T + 0.006h$ is the sea-level equivalent mean temperature, h is elevation in meters, T is the mean temperature, A is the latitude in degrees, and T_d is the mean dewpoint temperature. If dewpoint temperature data is unavailable, $T - T_d$ can be approximated using the following relationship shown by equation 4, provided the precipitation is at least 5 mm per month and $T - T_d$ is at least 4°C:

$$T - T_d = 0.0023h + 0.37T + 0.53R + 0.35R_{ann} - 10.9^\circ\text{C} \quad (4)$$

In equation 4, R is the daily temperature range and R_{ann} is the difference between the mean temperature of the hottest and coldest months.

Using the Linacre Method and input data from 1983-2021 at the Pacific Climate Impacts Consortium's (PCIC) Morrissey Ridge station, Hatch estimated a mean annual evaporation rate of 752 mm/year, the majority of which occurred from April to October [1]. This work could not be replicated. Independently, their HEC-HMS model calibration process yielded an evapotranspiration value of 710 mm/year. These estimates represent approximately 64% and 62% of the annual precipitation, respectively, and correspond to an overall runoff rate of roughly 37% – which is reasonable based on the orography of the basin.

3.4.2 Application

To integrate the EMDNA dataset and conduct a comprehensive assessment of long-term climate impacts, the Linacre equation stood out as the optimal choice.

Linacre's description of the R_{ann} variable, used to estimate the difference in temperature and dew point temperature ($T - T_d$), was subject to various interpretations but lacked clarity on which is correct. Two reasonable interpretations were employed in the equation and compared against the Matrix and Hatch findings to establish correctness. The interpretations are as follows:

1. R_{ann} = the absolute annual range (difference) of the hottest and coldest months (one value per year).
2. R_{ann} = the absolute mean monthly range, based on daily R values (one value per month).

Ultimately, the second option was chosen as it provides a more comprehensive consideration of the region's seasonal variations.

The Linacre formula was used with historical EMDNA data from 1979-2014 as inputs. While not a perfect match to the Morrissey Ridge period of record (used by Hatch), the two contain 32 overlapping years (1983-2014), for which the coefficient of determination is $R^2 = 0.943$. They also have very similar mean annual precipitation values, at 1155 mm/year and 1149 mm/year for Morrissey Ridge and EMDNA, respectively. The mean annual evaporation rate for this analysis was 1485 mm/year, approximately double Hatch's estimate, and corresponds to a physically unrealistic negative runoff rate. In an attempt to replicate Hatch's estimate, the Linacre formula was applied to the Morrissey Ridge data. The resulting mean annual evaporation rate was 1376 mm/year, approximately 8% less than the EMDNA value. This analysis demonstrates the consistency of the Linacre formula across comparable data sets. Additional analysis was conducted to reproduce Hatch's results; nevertheless, all endeavors resulted in similarly unrealistic outcomes, leading the team to pursue a different approach.

3.4.3 Adaptation

The Linacre equation was developed using data from Africa, Australasia, and 52 locations in South America [8]. The paper discusses the regression analysis conducted to estimate the difference between the monthly mean temperature and dewpoint, ($T - T_d$). It highlights that the difference between the daily maximum and

minimum temperatures (R) serves as a measure of nocturnal cooling, which is influenced by atmospheric temperature and humidity; therefore, the drier the air (i.e., the lower the dewpoint, T_d), the greater the R . The cold, arid winters in the Tent Mountain region render this situation less than ideal, requiring the following assumptions:

- Mean daily temperatures (T) below 0°C do not contribute to evaporation.
- The selected elevation will be the minimum point within the catchment area (1426 masl).
- For any day with a $T - T_d$ less than 4°C, the equation becomes invalid, resulting in an evaporation value of 0 mm.

Finally, by connecting the net-radiation intensity (Q_n) to a grass surface with the global radiation flux intensity (Q_s), for cloudless and totally overcast conditions, Linacre describes the following relationship:

$$Q_n = (0.75 - \alpha)Q_s \text{ cal.cm}^{-2}\text{s}^{-1} \quad (5)$$

In equation 5, α is the albedo of the surface. For the α of water (0.05) a Q of 700 was derived and for the α of well-watered vegetation (0.25) a Q of 500 was derived. However, since the catchment is mostly composed of forest and vegetation, neither of the α values described above would accurately represent the basin. Using a weighted average of the total reservoir area (0.7118 km²; 12%) to the total terrestrial catchment area (4.8452 km²; 88%), as well as the α values used by Linacre, an α for the Tent Mountain catchment area was determined as follows:

$$\alpha_{tent\ mountain} = 0.05 \cdot 12\% + 0.25 \cdot 88\% = 0.226 \quad (6)$$

From equations 5 and 6, Q for the Tent Mountain basin was found to be 524. Finally, from the modified Linacre equation, daily evaporation was calculated, and applied to the hydraulic model, as described in Section 4.

3.4.4 Results

The analysis produced monthly mean evaporation rates ranging from 1.9 mm/day in January to 184.7 mm/day in July, with an annual mean of 861.5 mm. Corresponding mean temperatures ranged from -8.4°C in January to 13.8°C in July. These results, summarized in Table 4, underscore the significant seasonal variability in evaporation rates and temperature, essential for understanding the hydrological dynamics of the Tent Mountain region. Figure 7 illustrates the mean monthly evaporation and precipitation for the Tent Mountain region over the course of a year.

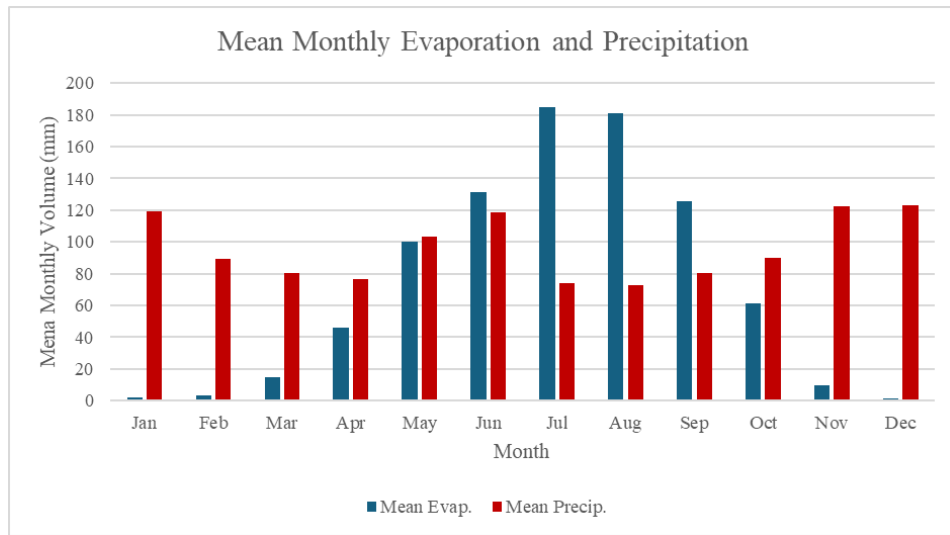


Figure 7 - Mean Monthly Evaporation and Precipitation

The plot underscores the seasonal fluctuations in both evaporation and precipitation, enabling the identification of peak months for each. This graph facilitates a better comprehension of seasonal water availability and the identification of periods at risk of droughts or floods. Furthermore, it aids in evaluating how evaporation and precipitation patterns may impact local ecosystems. These variations in water availability have the potential to affect vegetation growth, soil moisture levels, and the overall health of ecosystems.

Table 4 - Monthly and Annual Evaporation Results Summary

Quantity	Jan	Feb	Mar	Apr	May	Jun	Jul	Aug	Sep	Oct	Nov	Dec	Annual
Mean Evap. (mm/day)	1.9	3.4	14.9	45.7	100.0	131.4	184.7	181.2	125.7	61.2	9.8	1.7	861.5
Mean Temp. (°C)	-8.4	-6.8	-2.9	1.4	6.3	10.1	13.8	13.2	8.7	2.9	-4.1	-8.8	2.1

3.5 Change in Reservoir Storage

It is plausible to assume, based on the historical behavior of the system, that there is no significant change in reservoir storage over an extended period. The HEC-HMS model outlined in Section 4.2 provides a means to verify this assumption. It also allows for the assessment of any future climate on the basin water budget. Calculations using the modeled reservoir storage volumes from the historical simulation indicated that once the storage volumes in each reservoir reached stability, the average annual change in reservoir storage equated to 1.9 mm/year across the entire catchment area. This slightly more conservative value is adopted in the final water balance calculation.

3.6 Groundwater Seepage

3.6.1 GeoStudio Model Setup

GeoStudio 2023's SEEP/W module was utilized to analyze seepage on developed Upper Reservoir models. The E-W and N-S profiles of the upper reservoir were developed using the Leapfrog geological model provided by TransAlta. Hatch's Prefeasibility Study supplied permeability coefficients for Tent Mountain's rock formations, used in the GeoStudio model (see Figure 8, Figure 9, and Figure 10) [2]. In this simplified model, each material was considered isotropic. Additionally, a separate model was prepared to illustrate the seepage pathways observed through the waste dump pile around the intake structure, which has an approximate permeability of 10^{-3} m/s which is 4-5 orders of magnitude larger than the hard rock permeabilities. Therefore, the model shows all water seeping through the dump material as it is the path of least resistance. However, given that a vertical cutoff wall will be implemented to prevent seepage through the waste material, the models excluding the waste dump (see Figure 8 and Figure 10) were utilized for all flux calculations to identify losses through the rest of the reservoir.

The modeled reservoir's total water head at El. 1803 m was used as a boundary condition. The proposed grouted surface spanning from the historical reservoir level of El. 1780 m to the design NMOL of El. 1803 m was included as a boundary condition, with a hydraulic conductivity of 1×10^{-8} m/s [9]. Another boundary condition was used to represent the potential seepage faces with a zero-flux boundary. The "Pit 4 Cross Section Lower Bound" in the E-W model (see Figure 8 & Figure 9) considers a total water head of El. 1627 m, aligning with the natural water body elevation to the east of Pit 4 along the chosen cross-section. For the N-S model (see Figure 10), the Upper Reservoir level and zero flux boundary conditions are also utilized. The water level higher up the mountain (Pit 2) is included as a source of inflow to the Upper Reservoir; its water level is based on monitoring well data. The elevation of the natural waterbody within the area of the proposed Lower Reservoir is also included as a total water head condition, valued at 1479 m, which approximately represents its minimum water level. The saturation regime was modeled to reflect a partial saturation, which can be seen by the dashed blue phreatic lines, that differentiate the dry and saturated regimes (see Figure 8 and Figure 10). Ultimately, the GeoStudio modeling provided an understanding of seepage pathways through the Upper Reservoir and helped determine graphical water flux profiles that could be used to approximate total losses. Subsequent work is recommended to increase the validity of the models, which could be achieved through 3D modeling software for greater accuracy and correlation with observed data gathered from the site.

Color	Name	Hydraulic Material Model
Yellow	JF	Saturated / Unsaturated
Blue	JKKA	Saturated / Unsaturated
Magenta	JKKH	Saturated / Unsaturated
Orange	JKKMn	Saturated / Unsaturated
Red	JKKMU	Saturated / Unsaturated

Color	Name	Category	Kind	Parameters
Dark Blue	Pit 4 Cross Section Lower Bound	Hydraulic	Water Total Head	1,627 m
Cyan	Upper Reservoir (Pit 4) Water Level	Hydraulic	Water Total Head	1,810 m
Black	Zero Flux	Hydraulic	Water Flux	0 m/sec

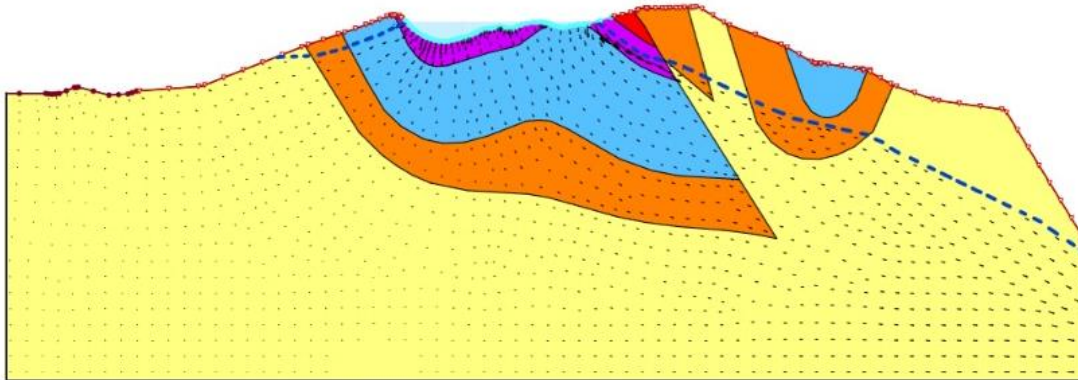


Figure 8 - GeoStudio SEEP/W Model of E-W Cross-Section

Color	Name	Hydraulic Material Model	Sat Kx (m/sec)
Yellow	JF	Saturated Only	4.7e-08
Blue	JKKA	Saturated Only	1.7e-07
Magenta	JKKH	Saturated Only	7e-07
Orange	JKKMn	Saturated Only	2.4e-07
Red	JKKMU	Saturated Only	1.8e-07
Magenta	Waste Dump Material	Saturated Only	0.001

Color	Name	Category	Kind	Parameters
Dark Blue	Pit 4 Cross Section Lower Bound	Hydraulic	Water Total Head	1,627 m
Cyan	Upper Reservoir (Pit 4) Water Level	Hydraulic	Water Total Head	1,810 m
Black	Zero Flux	Hydraulic	Water Flux	0 m/sec

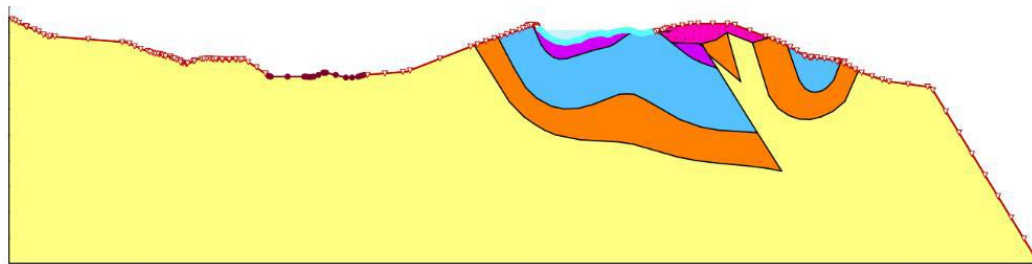


Figure 9 - GeoStudio SEEP/W Model of E-W Cross-Section with Waste Dump Pile

Color	Name	Category	Kind	Parameters
[Green]	Lower Reservoir	Hydraulic	Water Total Head	1,479 m
[Blue]	Pit 2 Water Level	Hydraulic	Water Total Head	2,070 m
[Cyan]	Upper Reservoir Water Level	Hydraulic	Water Total Head	1,803 m
[Dark Red]	Zero Flux	Hydraulic	Water Flux	0 m/sec

Color	Name	Hydraulic Material Model
[Yellow]	JF	Saturated / Unsaturated
[Light Blue]	JKKA	Saturated / Unsaturated
[Purple]	JKKH	Saturated / Unsaturated
[Orange]	JKKMm	Saturated / Unsaturated
[Red]	JKKMU	Saturated / Unsaturated

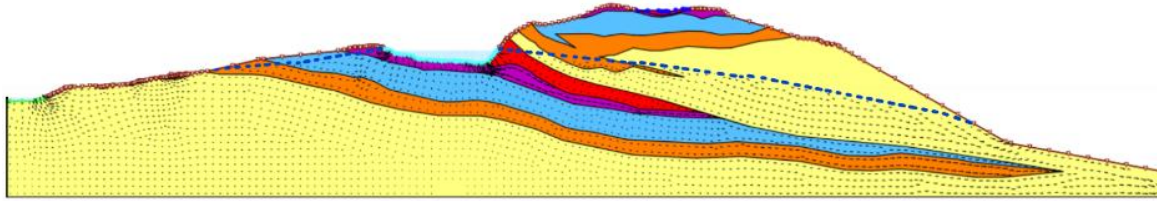


Figure 10 - GeoStudio SEEP/W Model of N-S Cross-Section

3.6.2 Seepage Methodology

Flux calculations were used to quantify the seepage out of the Upper Reservoir as an input for the HEC-HMS model in Section 4. Using N-S and E-W cross-section models, flux values ($\text{m}^3/\text{s}/\text{km}^2$) were computed, accounting for the grouted and vertical cut-off wall seepage reduction methods. The flux values were computed across the entire submerged surface, resulting in two values for each cross-section, which were then averaged. It is important to note that the N-S model was modified to be more conservative, as the inflow from the south wall was ignored and only losses from the reservoir were accounted for. Total flux values (m^3/s) were then calculated using the total wall surface area multiplied by the average flux. All the subsequent values are summarized in Table 5.

Table 5 – Upper Reservoir Seepage Parameters

N-S Flux ($\text{m}^3/\text{s}/\text{m}^2$)	E-W Flux ($\text{m}^3/\text{s}/\text{m}^2$)	Average Flux ($\text{m}^3/\text{s}/\text{m}^2$)	Wall Surface Area (km^2)	Total Flux (m^3/s)	Total Flux (mm/year)
1.63E-08	2.26E-10	8.26E-09	1.38E-01	1.14E-03	7.95

Due to a lack of geotechnical information, lower reservoir seepage was assumed to be accounted for in the HEC-HMS outflow values created in Section 4 and thus was not calculated in this project. A future analysis of the lower reservoir seepage with up-to-date information is recommended.

3.7 Runoff

Given the lack of observed hydrometric data for the tributary of Crowsnest Creek that flows from the project site, runoff was generated using the HEC-HMS model as described in Section 4.2. It is assumed that the calculated runoff approximates the expected streamflow.

3.8 Results

In summary, equation 2 was used to approximate the water balance for the site:

$$P - ET - \Delta S - GW = R \quad (2)$$

Values were calculated as outlined in the preceding subsections, yielding the following annual runoff value:

$$R = 1149 \text{ mm} - 861 \text{ mm} - 1.9 \text{ mm} - 7.9 \text{ mm} = 278 \text{ mm} \quad (2)$$

This result corresponds to an average flow of $0.049 \text{ m}^3/\text{s}$. Assuming an Upper Reservoir water level of El. 1780 m and a completely dry Lower Reservoir, the initial combined total and live storage are $4,900,000 \text{ m}^3$ and $2,328,200 \text{ m}^3$, respectively. Given these conditions, it will take approximately 3.1 years to achieve the specified live storage volume of $7,107,000 \text{ m}^3$ for 16 hours of continuous generation. The time required to achieve a live storage volume corresponding to 8 hours of continuous generation ($3,553,500 \text{ m}^3$) is 0.8 years. Note that seasonal variability will have a greater impact on the accuracy of filling time estimates over the short term, and less on estimates that are greater than one year.

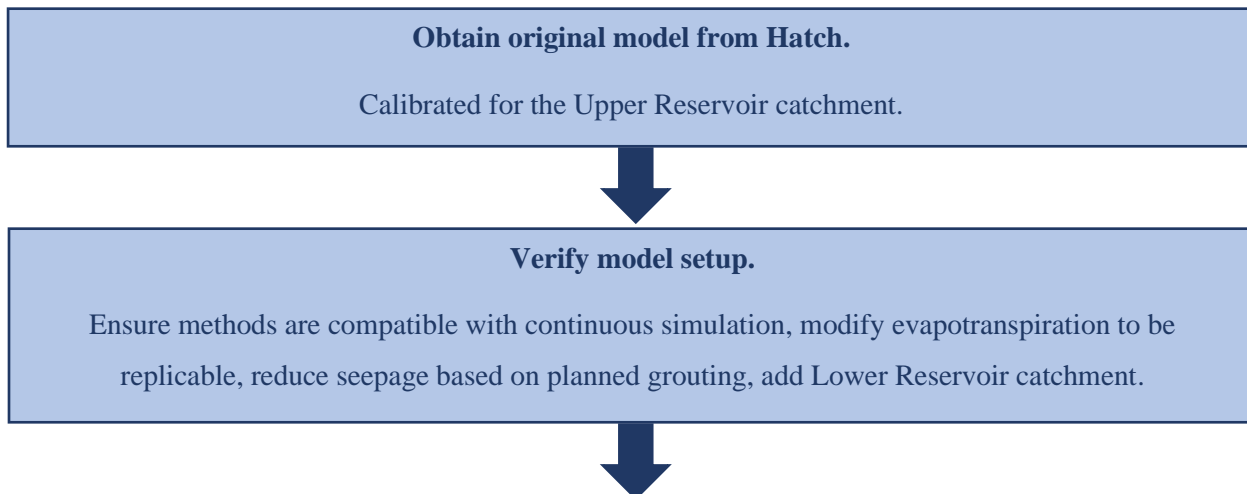
4 Hydrological Modelling

4.1 Forcing Data

Meteorological forcing data, encompassing daily temperature and precipitation records, was utilized in the analysis, as outlined in Section 2.2. The dataset utilized comprised historical EMDNA data spanning from 1979 to 2014, alongside TMCCP realizations pertaining to climate change scenarios 1 through 4, spanning the period from 2015 to 2100, explained in Section 5.2.

4.2 Model Workflow

The Hydrologic Engineering Center's Hydrologic Modeling System (HEC-HMS) was used to develop a set of hydrological models for the Tent Mountain basin. The workflow is as follows:



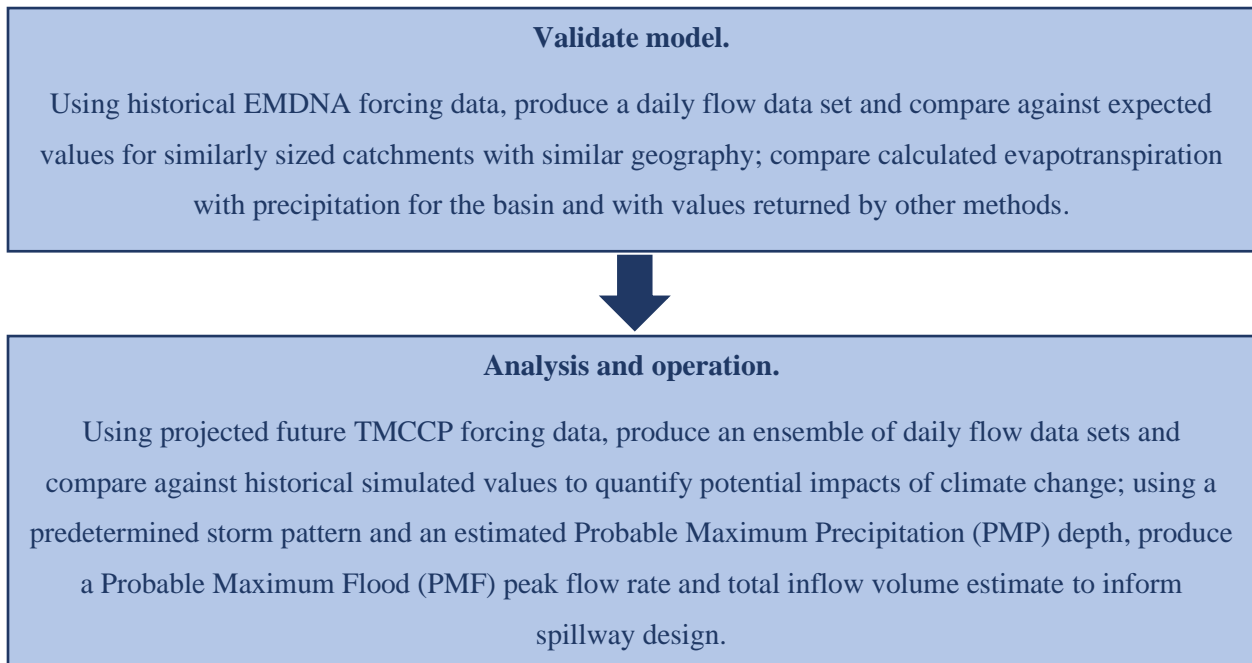


Figure 11 – HEC-HMS Model Workflow Chart

Each of the models referenced in Figure 11 are described in greater detail below. Model outputs are discussed in the following Sections:

- 3.8 Water Balance - Results
- 5.5 Projected Outflow
- 5.6 Projected Storage
- 6.1 Frequency Analysis
- 6.3 Probable Maximum Flood

4.2.1 Original HEC-HMS Model

As part of the pre-feasibility study, Hatch developed a HEC-HMS model for the Upper Reservoir. This model was set up as shown in Table 6.

Table 6 – Original HEC-HMS Model Summary

Aspect	Description
Meteorological Input Data	Observed daily temperature and precipitation.
Catchment Area	1.356 km ² (marginally larger than the Fall Report's delineated catchment area of 1.311 km ²).
Calibration Process	Calibrated to three years of open water season water level records (2018-2020).
Evapotranspiration	Monthly constant, established through the calibration process. Validated by Linacre method.

Seepage	Seasonal: June-October 0.006 m ³ /s, November-May 0.012 m ³ /s.
Snow Method	Temperature Index. This method accumulates snow based on temperature and precipitation input data. When temperatures exceed a set threshold, snowmelt begins. The melting rate is affected by the degree-day factors, which are derived from the temperature data.
Loss Method	Soil Moisture Accounting. This method keeps track of soil moisture with a physically based water balance approach, considering precipitation, evapotranspiration, and changes in storage.
Transform Method	SCS Unit Hydrograph. 39 min lag time.
Time Step	Daily.

4.2.2 Adapted HEC-HMS Model Setup (Continuous Simulation)

Using the parameterization established in Hatch's calibrated HEC-HMS model, a model was created for each of the Upper and Lower Reservoirs to run long-term historical and projected future simulations in order to establish a water balance for the basin and examine the anticipated effects of climate change on that water balance (see Section 3). The adapted model is summarized in Table 7.

Table 7 – Adapted HEC-HMS Models Summary (Continuous Simulation)

Aspect	Description	
	Upper Reservoir	Lower Reservoir
Meteorological Input Data	EMDNA daily temperature and precipitation data.	
Catchment Area	1.311 km ²	4.246 km ²
Calibration Process	None. Assumed calibration of original model is applicable.	
Evapotranspiration	Linacre daily evapotranspiration as described in Section 3.4.	
Seepage	Constant: 0.0014 m ³ /s	None. Assumed all seepage contributes to outflow.
Snow Method	No change from original model.	
Loss Method		
Transform Method	No change from original model.	SCS Unit Hydrograph. 60 min lag time.
Time Step	Daily.	

The similarities observed in land cover, soil types, and slope characteristics between the Upper and Lower Reservoirs provide support for the continued applicability of calibrated parameters for the loss and snow methods. The lag time for the Lower Reservoir's catchment was increased conservatively from the Upper Reservoir's. As addressed in Section 3.4, great importance was placed upon deriving a robust evapotranspiration method that yielded similar results to those used in the original HEC-HMS model. Seepage was modeled as described in Section 3.6.

A broad-crested spillway with a crest El. 1,509.3 m, a width of 30 m, and a spillway coefficient of $1.0 \text{ m}^{0.5}/\text{s}$ was used. It is presumed that this design has negligible impacts on the simulated outflows given their low magnitude during the modeling process. All outflows were modeled through the spillway; moreover, the riparian outlet was excluded from the model to prevent artificial constraints on outflows. Various spillway widths were investigated in the event-based simulation.

4.2.3 Adapted HEC-HMS Model Setup (Event-Based Simulation)

Following best practices, it is recommended to create entirely distinct models with individual calibration procedures for the purposes of continuous and event-based simulations. However, due to time limitations, this approach was not feasible. Nonetheless, substantial adjustments were made to develop a tailored model suitable for estimating the Probable Maximum Flood (PMF). The model setup is outlined in Table 8.

Table 8 – Adapted HEC-HMS Models Summary (Event-Based Simulation)

Aspect	Description	
	Upper Reservoir	Lower Reservoir
Meteorological Input Data	EMDNA daily temperature data. SCS Type II storm.	
Catchment Area	1.311 km ²	4.246 km ²
Calibration Process	None. Assumed calibration of original model is applicable.	
Evapotranspiration	Linacre daily evapotranspiration as described in Section 3.4.	
Seepage	Constant: 0.0014 m ³ /s	None. Assumed all seepage contributes to outflow.
Snow Method	No change from original model.	
Loss Method	Method retained from the original model. Initial conditions set at 100% soil and groundwater saturation to approximate antecedent conditions most conducive to flooding.	
Transform Method	No change from original model.	
Time Step	5 minute.	

The United States Soil Conservation Service (SCS) has developed dimensionless rainfall pattern-based storms intended for use in small watersheds, intended to estimate peak flow and volume for a given storm duration [10]. The geographic distribution of the storms is specified for the contiguous United States, with differentiation typically occurring between three distinct coastal regions and one inland region, regardless of other factors [11]. Although Tent Mountain is not located within the United States, it is assumed that its proximity to the inland northwest validates the use of a Type II storm.

HEC-HMS is limited in its ability to model circular routing (i.e., allowing water to flow from the Upper to the Lower Reservoir and subsequently pumping it back up). As a result, it was necessary to model the two reservoirs separately for the continuous simulation and then merge the model output post-hoc. In the case

of a PMF, it is unlikely that the facility will be operating with any other focus than to attenuate the flood. It is conservatively assumed that no pumping operations would take place during the event, so both reservoirs were modelled together.

The same spillway configuration from the continuous simulation model was used initially. A sensitivity analysis was performed using widths of 15, 20, and 25 m. The results are presented in Section 7.1.

5 Long-Term Climate Change Scenarios

5.1 Introduction

Climate change is projected to have an unprecedented effect on water resources worldwide [12]. Both water scarcity and water-related hazards such as flooding are projected to increase in frequency and intensity. The anticipation of significant variations in water-related impacts across different regions and topographies prompted an extensive investigation to forecast the impact of climate change on Tent Mountain. A consistent water supply is integral for the operation of a pumped hydro energy storage facility. A lack of water would limit the power generation capability of the facility, while extreme excesses of water would threaten reservoir capacity and potentially result in downstream flooding. Thus, it is vital to understand how climatic conditions are projected to change at Tent Mountain. This study will enable a well-informed forecast of outflow and storage patterns within the system. These insights will guide the development of risk management measures like spillways, leading to a climate-resilient, sustainable design that considers future variability.

The climate change scenarios investigated in this analysis were obtained from The Scenario Model Intercomparison Project, and used in climate model scenarios from CMIP6, both of which are professional studies completed by the European Geosciences Union [5,6]. Historic EMDNA data for Tent Mountain was used to bias-correct the scenario models to provide site-specific climate projections for temperature and precipitation. The data acquisition and cleaning processes are explained in Section 2. The projected future temperature and precipitation from the TMCCP realizations were subsequently used as forcing data in the HEC-HMS model of the TM-PHES watershed outlined in Section 4. This model produced the projected water outflow and storage for the Tent Mountain system under climate change conditions. Each scenario has between 25 and 30 realizations utilized in the HEC-HMS model (Table 3); moreover, the monthly mean, maximum, and minimum values for each scenario were calculated based on the ensemble of its realizations. The remainder of this section will investigate the projected temperature, precipitation, outflow, and storage for each climate scenario.

5.2 Scenario Overview

Four climate change scenarios were investigated in this Tier 1 model analysis. Each scenario estimates climate change parameters such as radiative forcing based on different emission and land use variables [5]. These inputs represent societal realizations over the next century based on enacted environmental policies, socioeconomic development, and population growth. Radiative forcing is used to quantify the change in the earth's energy balance due to variables such as greenhouse gases and aerosols. The larger the radiative forcing value, the more radiation energy is trapped by the earth's atmosphere. Figure 12 summarizes the radiative forcing estimated due to society's actions in each scenario.

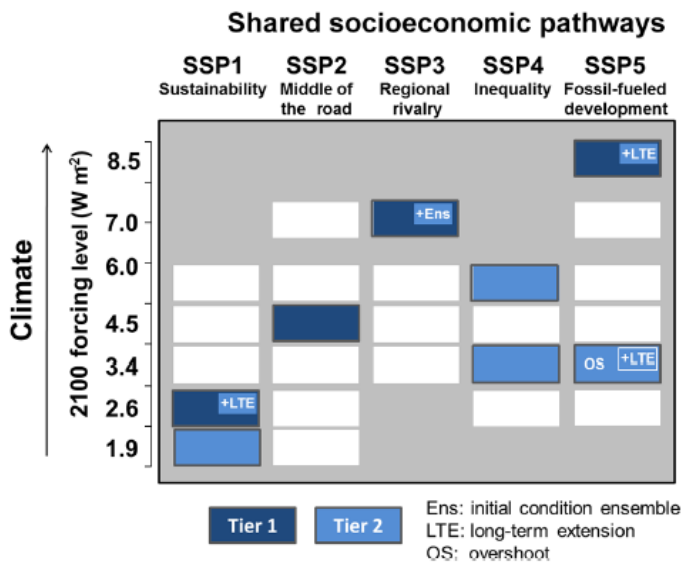


Figure 12 - Climate Change Scenario Summary [5]

Scenario 1 refers to SSP1-2.6 throughout this report. This scenario envisions positive human development and a society that prioritizes economic and institutional growth using sustainable practices such as renewable energies. It predicts the least impactful climate change scenario with the lowest radiative forcing value of 2.6 W m^{-2} in 2100.

Scenario 2 refers to SSP2-4.5 throughout this report. This scenario envisions society maintaining current trends with the adoption of sustainable technologies and economic development occurring at historical rates. It is the most realistic scenario assuming society does not make drastic changes, and thus it is used throughout this report when designs account for future climate trends. It predicts the second least impactful climate change scenario with a radiative forcing value of 4.5 W m^{-2} in 2100.

Scenario 3 refers to SSP3-7.0 throughout this report. This scenario envisions pessimistic human development, with rapid population growth, low education rates, and severe inequality resulting in countries

prioritizing regional security. It predicts the second most impactful climate change scenario with a radiative forcing value of 7.0 Wm^{-2} in 2100.

Scenario 4 refers to SSP5-8.5 throughout this report. This scenario envisions rapid economic growth and institutional improvement through energy-intensive projects utilizing continually increasing fossil fuel development. It predicts the most impactful climate change scenario with a radiative forcing value of 8.5 Wm^{-2} in 2100.

5.3 Temperature

Temperature increase is the most straightforward impact of climate change. Increased greenhouse gas concentrations trap more radiative energy in the earth's system, and this increased energy manifests as increased temperatures [12]. The following line plots represent the historic and projected monthly range and mean for temperature in the Tent Mountain basin. Historical data was obtained from the historical EMDNA predictions, while the scenario data was obtained from the TMCCP scenario realizations. The dark blue line represents the monthly average from all years and realizations for the scenario being analyzed. The light blue shading represents the maximum and minimum values obtained from any year or realization in a certain month. All line plots in Sections 5.3 to 5.6 follow the same format and procedure.

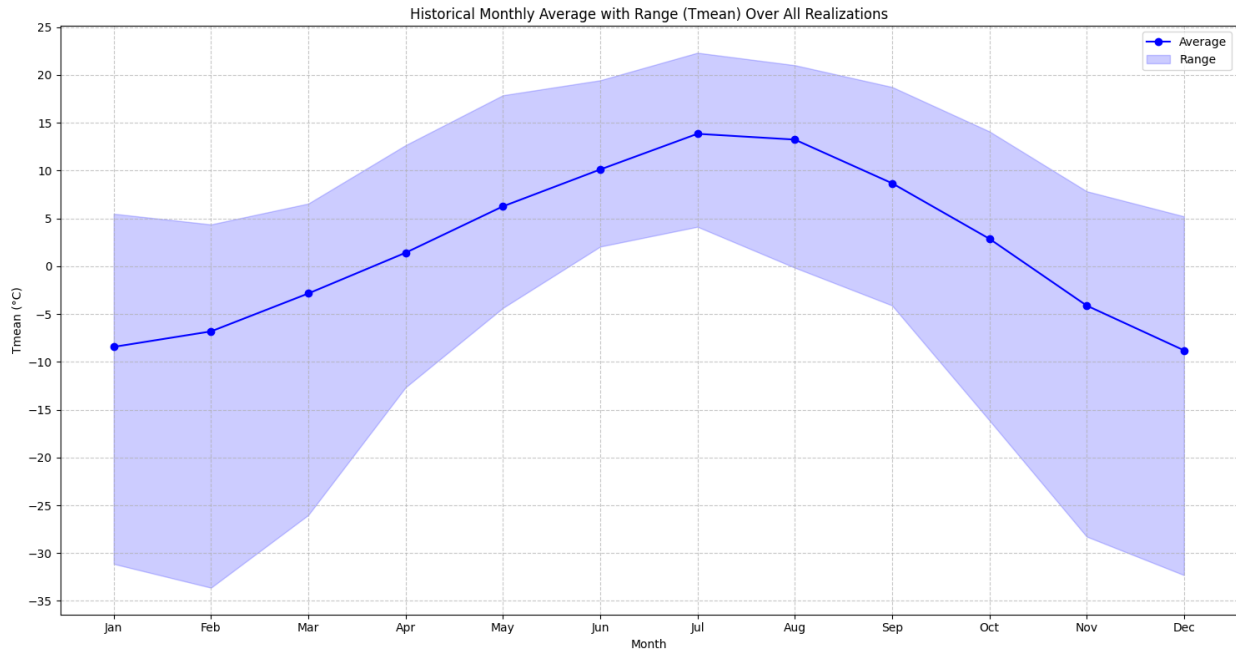


Figure 13 - Average Historical Monthly Temperature with Range

Figure 13 displays the historic temperature data from 1979-2014. The mean monthly temperature fluctuates from a low of approximately $-9 \text{ }^{\circ}\text{C}$ in December to a high of approximately $14 \text{ }^{\circ}\text{C}$ in July. The overall mean

temperature appears to be around 3 °C. The maximum value over this timeframe was approximately 22 °C in July, while the minimum was approximately -33 °C in February.

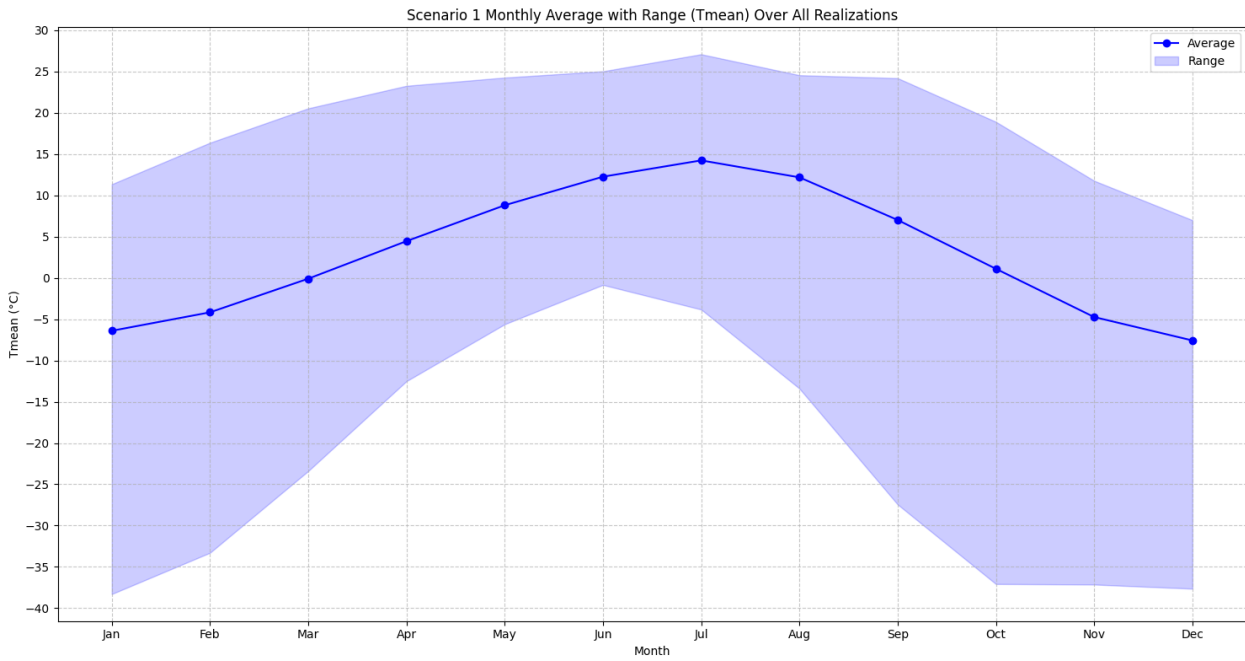


Figure 14 - Average Projected S1 Monthly Temperature with Range

Figure 14 displays the projected future temperature data from 2015-2100 for Scenario 1, the lowest emissions scenario. The mean monthly temperature fluctuates from a low of approximately -7.5 °C in December to a high of approximately 15 °C in July. The overall mean appears to be around 5 °C. The maximum value over this timeframe was approximately 27 °C in July, while the minimum was approximately -38 °C in January.

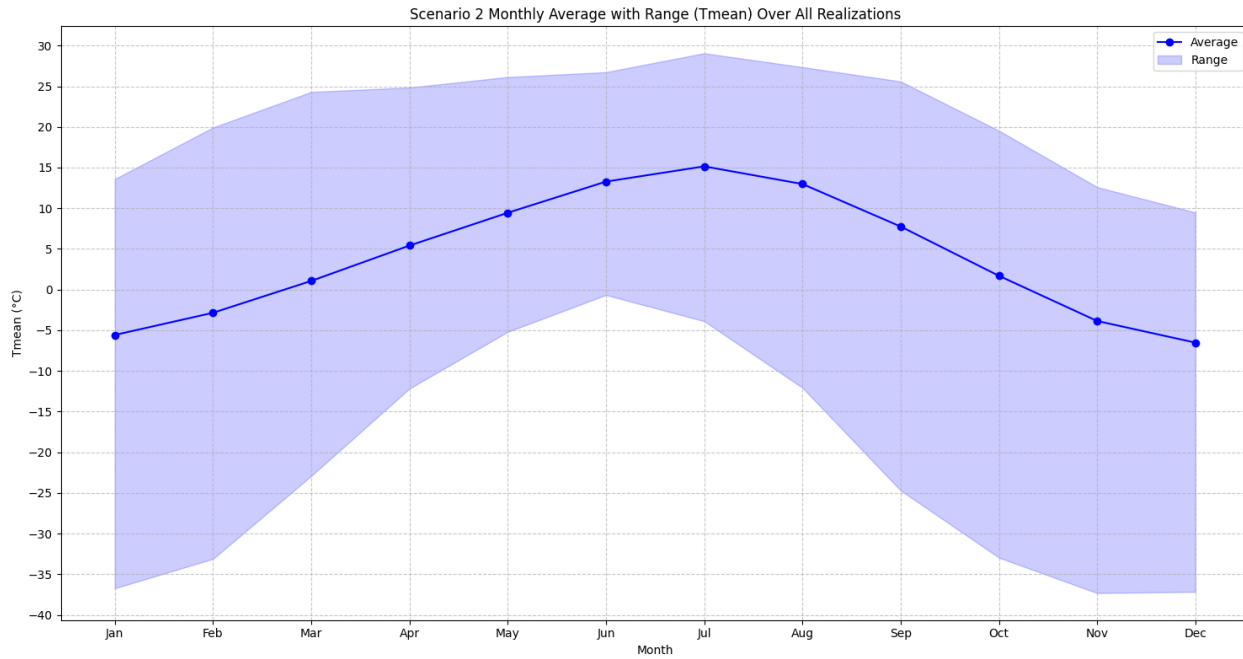


Figure 15 - Average Projected S2 Monthly Temperature with Range

Figure 15 displays the projected future temperature data from 2015-2100 for Scenario 2, the continuation of the current trend's scenario. The mean monthly temperature fluctuates from a low of approximately -6 °C in December to a high of approximately 15 °C in July. The overall mean appears to be around 6 °C. The maximum value over this timeframe was approximately 29 °C in July, while the minimum was approximately -37 °C in December.

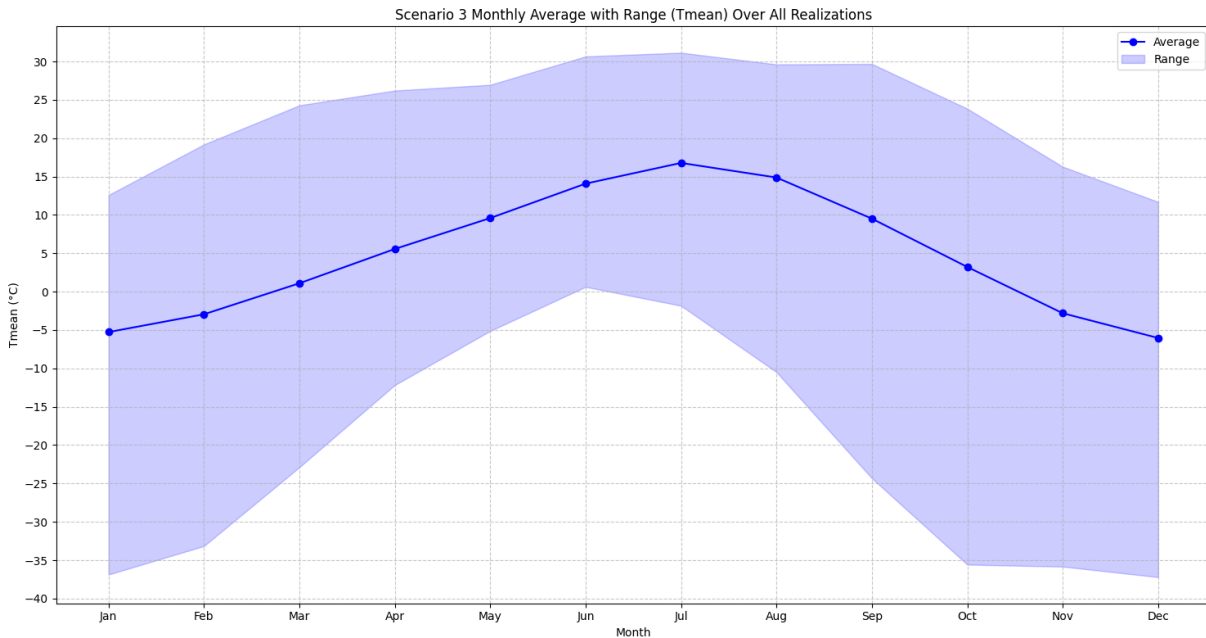


Figure 16 - Average Projected S3 Monthly Temperature with Range

Figure 16 displays the projected future temperature data from 2015-2100 for Scenario 3, the regional conflict scenario. The mean monthly temperature fluctuates from a low of approximately -6 °C in December to a high of approximately 16 °C in July. The overall mean appears to be around 7 °C. The maximum value over this timeframe was approximately 31 °C in July, while the minimum was approximately -37 °C in December.

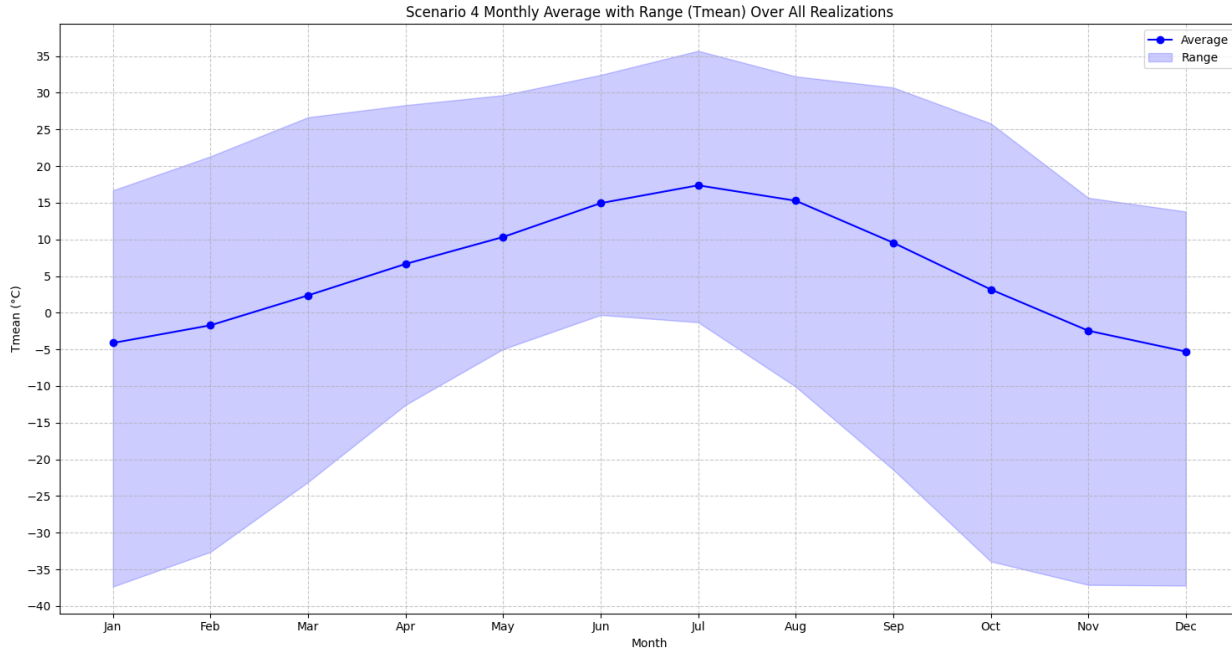


Figure 17 - Average Projected S4 Monthly Temperature with Range

Figure 17 displays the projected future temperature data from 2015-2100 for Scenario 4, the extreme fossil fuel use scenario. The mean monthly temperature fluctuates from a low of approximately -5 °C in December to a high of approximately 17.5 °C in July. The overall mean appears to be around 8 °C. The maximum value over this timeframe was approximately 36 °C in July, while the minimum was approximately -37 °C in January.

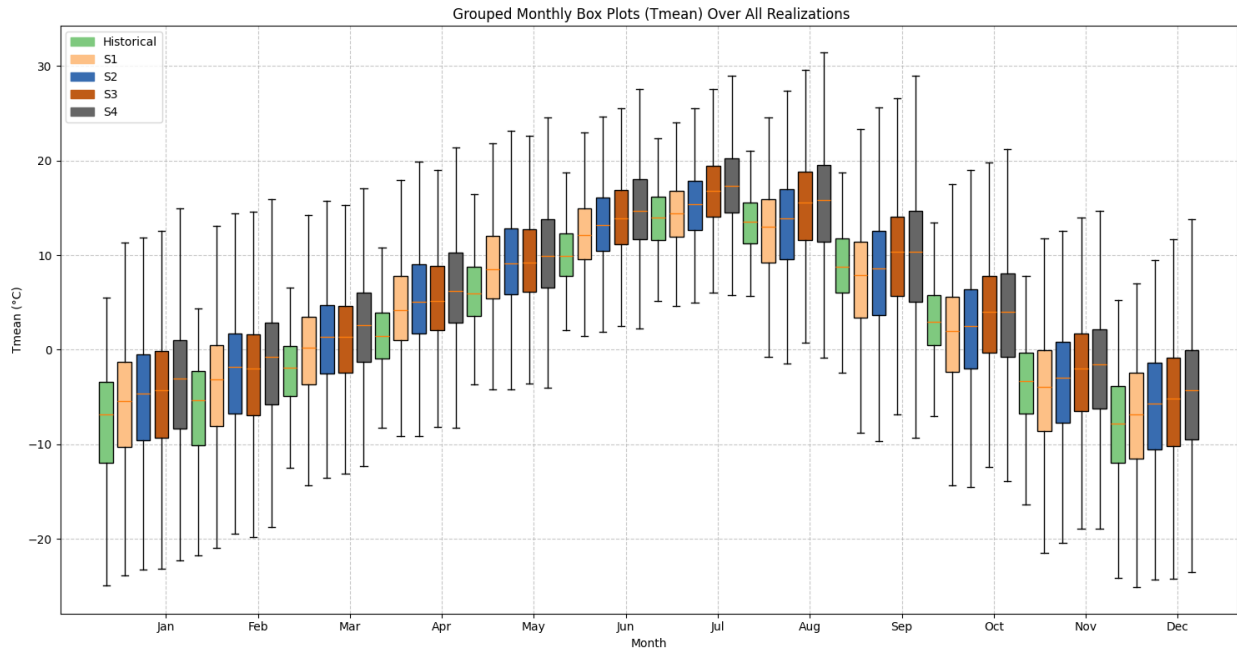


Figure 18 - Box Plot of Monthly Temperature for All Scenarios Excluding Outliers

Figure 18 is a comparative box plot of the monthly temperatures for all scenarios. The median temperature line follows the same trend as the mean values observed in the line graphs, this result is likely due to the tendency for temperature to follow a normal distribution. The box plot whiskers are much smaller than the ranges displayed in the line graph. This outcome is because this box plot does not include outliers, a plot with outliers can be found in Appendix A. The whiskers show the most extreme non-outlier points, which are points that fall within 1.5 times the inter-quartile range (IQR). The whiskers show a maximum value of 31 °C due to Scenario 4 in August, while their minimum temperature would be approximately -26 °C due to the historical data in January. The box plot whiskers provide a likely range of extreme monthly values for each scenario because outliers are not overrepresented.

Ultimately, temperature follows the projected trend with higher emission scenarios resulting in higher mean temperatures and a larger range of temperature values. The overall mean for the scenarios increased from 3 °C in the observed data to 8°C in Scenario 4, an increase of 5 °C and just over 1 °C of warming for every scenario. The range of temperature extremes also got more severe in the higher emission scenarios. The historical data showed a 55 °C range between the overall minimum and maximum values, while Scenario 4 had a range of 73 °C. Increased variability is also shown in the box plot because the whiskers from Scenario 4 are much larger than the observed data whiskers. Thus, increased emission scenarios result in higher mean temperatures and greater fluctuations in temperature extremes. This information will affect the TM-PHES project because higher mean temperatures increase air's capacity to hold moisture, resulting in both more

evaporation and more extreme precipitation events. Extreme temperature variability also increases society's demand for electricity, resulting in a greater need for the project.

5.4 Precipitation

Precipitation variability is expected to be one of the most significant impacts of climate change. Water scarcity and water-related hazards such as floods are both expected to increase in likelihood as increased energy in the earth's system disrupts precipitation patterns [12]. TM-PHES relies on water to produce energy, so it is critical to understand projected precipitation patterns at Tent Mountain to plan for both flood and drought scenarios. The following time series plots present the EMDNA historic and TMCCP scenario daily max and mean precipitation per month at Tent Mountain. Appendix A includes a plot of the average monthly precipitation excluding zero precipitation days, to portray the average monthly intensity of events.

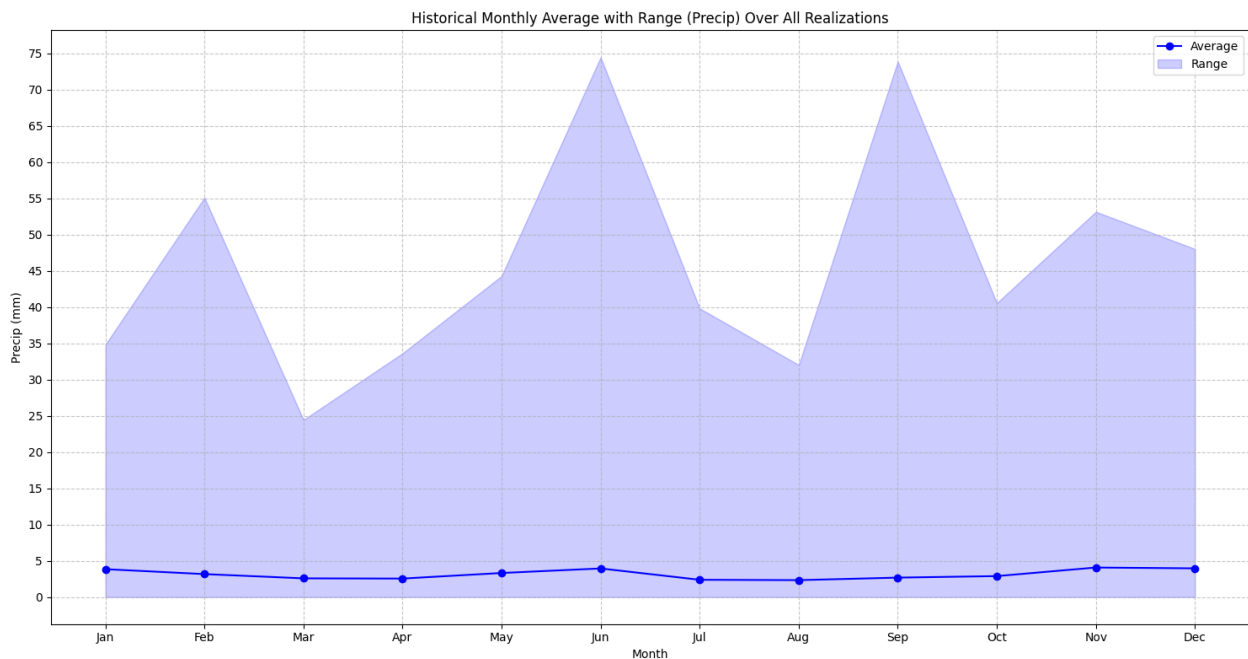


Figure 19 - Average Historical Daily Precipitation per Month with Maximum

Figure 19 displays the historic precipitation data from 1979-2014. The mean monthly precipitation per day fluctuates minorly from a low of approximately 2.5 mm in July to a high of approximately 5 mm in June. The maximum precipitation event over this timeframe was approximately 75 mm in June with a similar peak in September. The monthly maximum precipitation was lowest in March at 25 mm.

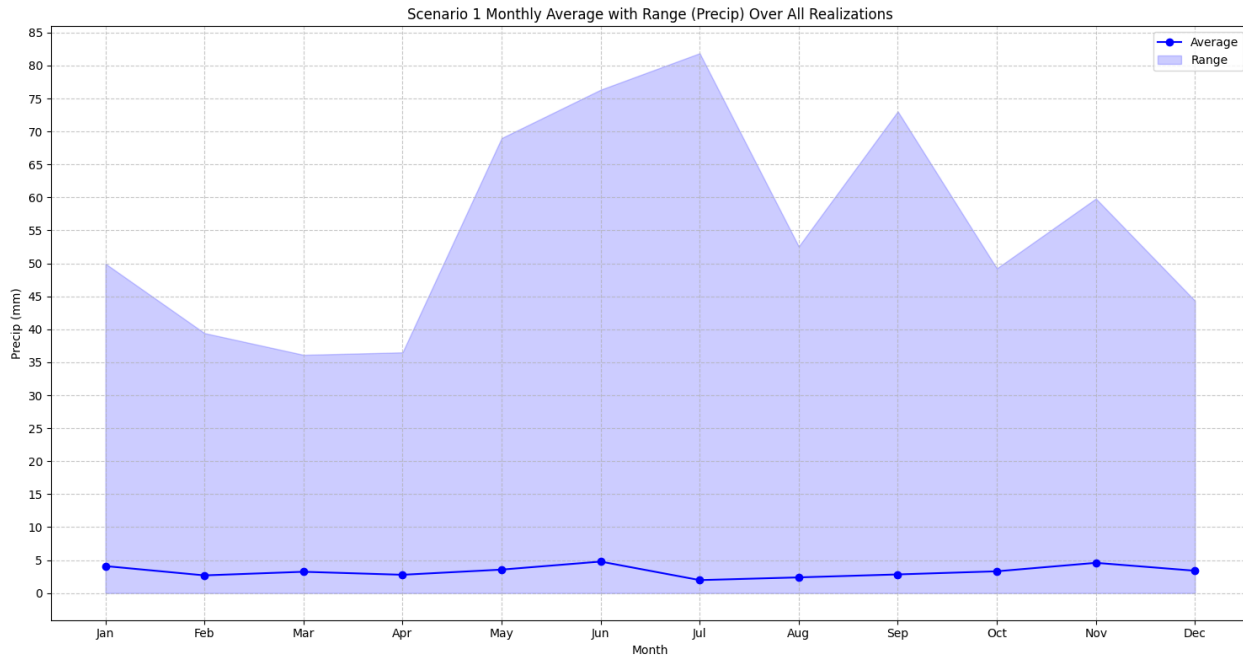


Figure 20 - Average Projected S1 Daily Precipitation per Month with Maximum

Figure 20 displays the projected future precipitation data from 2015-2100 for Scenario 1. The mean monthly precipitation per day fluctuates minorly from a low of approximately 2.5 mm in July to a high of approximately 5 mm in June. The maximum monthly precipitation event over this timeframe was approximately 80 mm in July with 70 mm peaks in September, May, and June. The monthly maximum precipitation was lowest in both March and April at 35 mm.

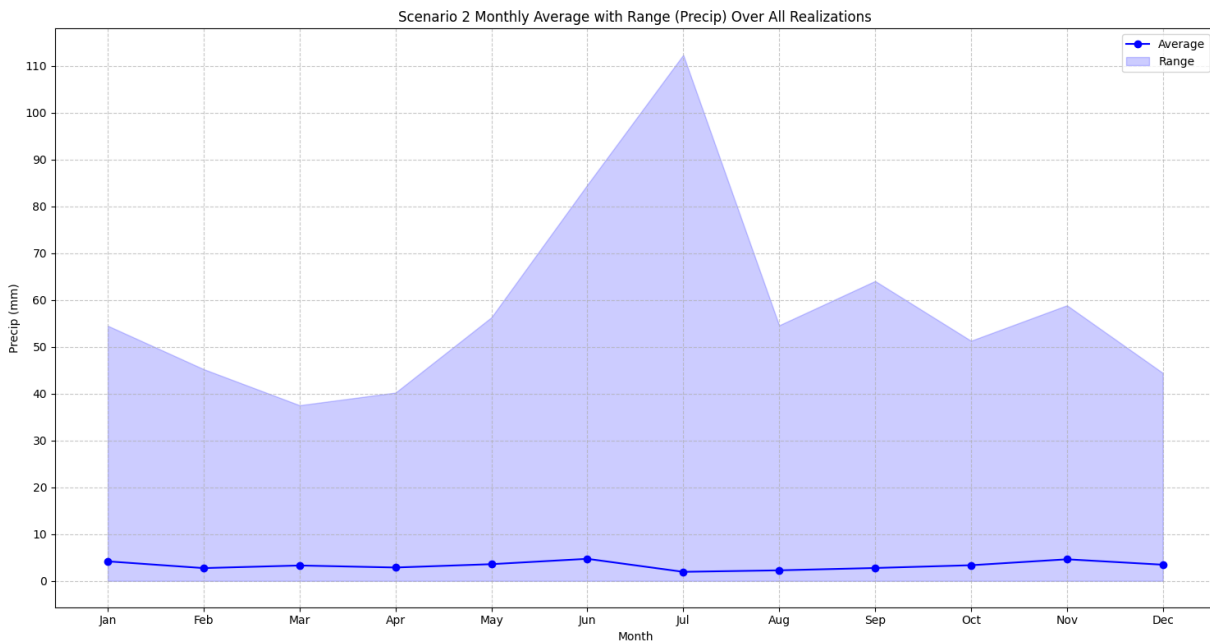


Figure 21 -Average Projected S2 Daily Precipitation per Month with Maximum

Figure 21 displays the projected future precipitation data from 2015-2100 for Scenario 2. The mean monthly precipitation per day fluctuates minorly from a low of approximately 2 mm in July to a high of approximately 5 mm in November. The maximum monthly precipitation event over this timeframe was approximately 110 mm in July followed by 85 mm in June. The monthly maximum precipitation was lowest in both March and April at around 40 mm.

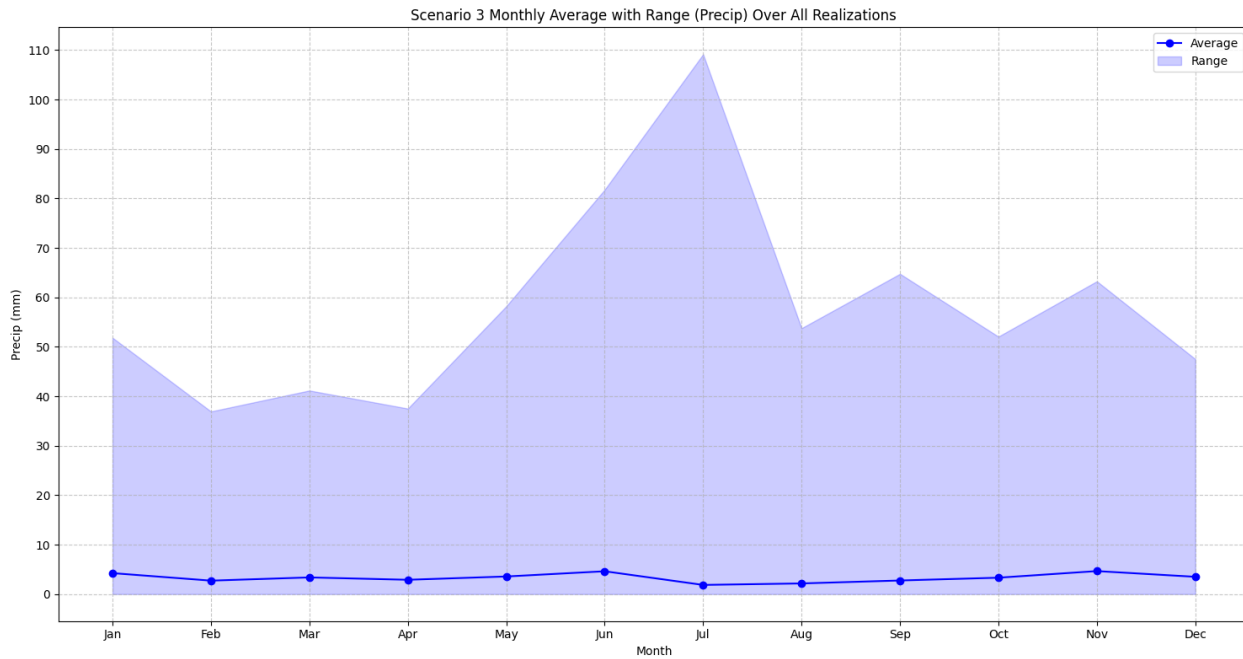


Figure 22 - Average Projected S3 Daily Precipitation per Month with Maximum

Figure 22 displays the projected future precipitation data from 2015-2100 for Scenario 3. The mean monthly precipitation per day fluctuates minorly from a low of approximately 2 mm in July to a high of approximately 5 mm in November. The maximum monthly precipitation event over this timeframe was approximately 110 mm in July followed by 80 mm in June. The monthly maximum precipitation was lowest in February and April at around 37.5 mm.

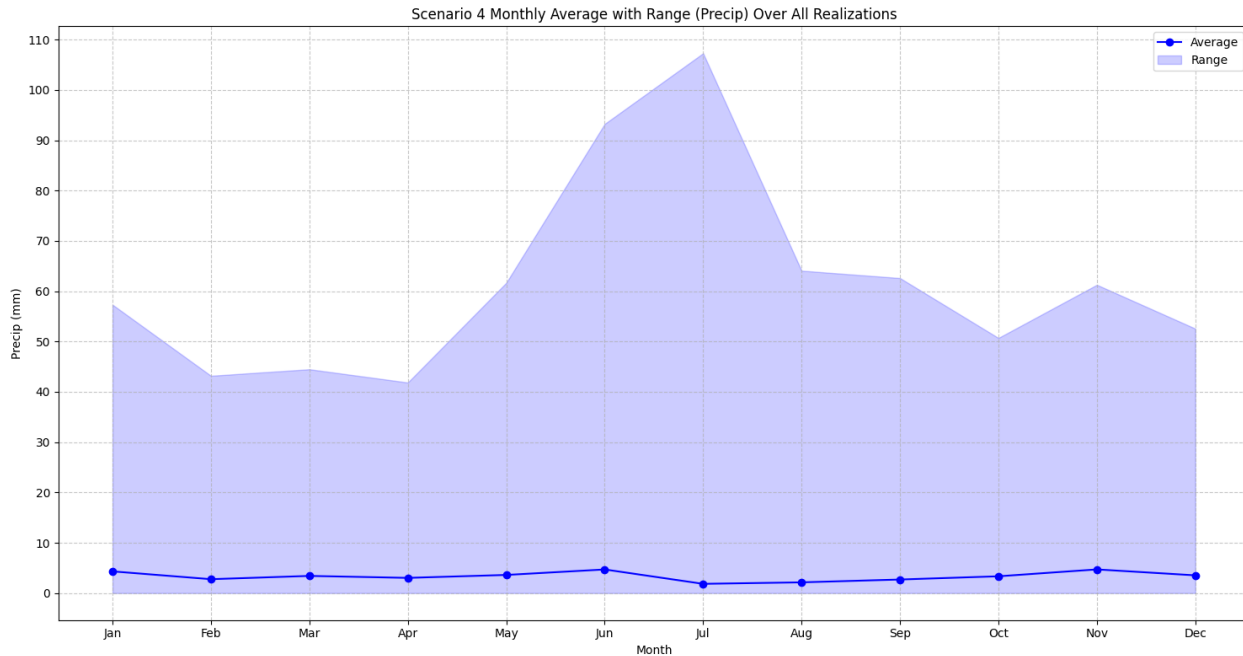


Figure 23 - Average Projected S4 Daily Precipitation per Month with Maximum

Figure 23 displays the projected future precipitation data from 2015-2100 for Scenario 4. The mean monthly precipitation per day fluctuates minorly from a low of approximately 2 mm in July to a high of approximately 5 mm in November. The maximum monthly precipitation event over this timeframe was approximately 107 mm in July followed by 92 mm in June. The monthly maximum precipitation was lowest in February, March, and April at around 42.5 mm.

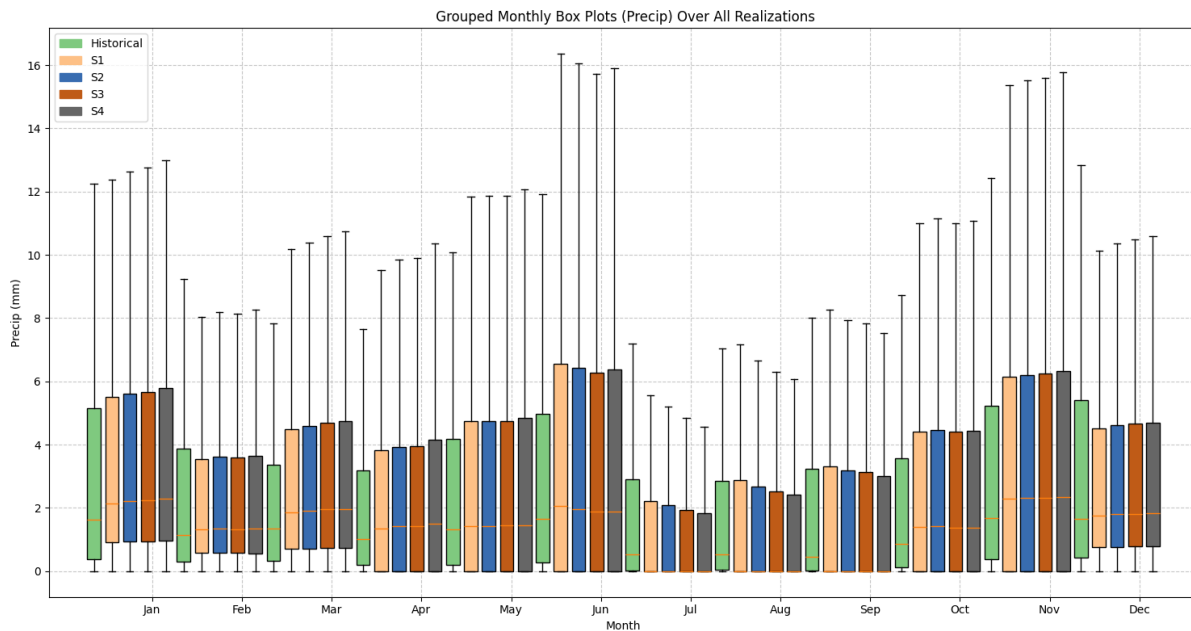


Figure 24 - Box Plot of Daily Precipitation per Month for All Scenarios Excluding Outliers

Figure 24 is a comparative box plot of the daily precipitation per month for all scenarios. The median precipitation line hovers around 2 mm for most of the year and is 0 mm in the TMCCP scenarios from July to September. This result is far different from the mean values displayed by the line graphs, and this is due to precipitation being bounded at zero but having a heavy tail. This statistical effect raises the mean while keeping the median low. The whiskers and IQR for the TMCCP scenarios show a trend developing. When climate change becomes more severe the wet months are projected to become wetter while the dry months are projected to become drier. December to March are the only months where the IQR does not extend to 0, which suggests it is common for precipitation to occur most days in the winter. In the line graphs, July often had the maximum precipitation event, however, in the box plot it has the smallest IQR which only extends to 6 mm. The highest IQR occurs in June and extends to 16 mm. The box plot whiskers will be artificially low due to the high number of 0 precipitation days, and a box plot showing precipitation outliers is in Appendix A.

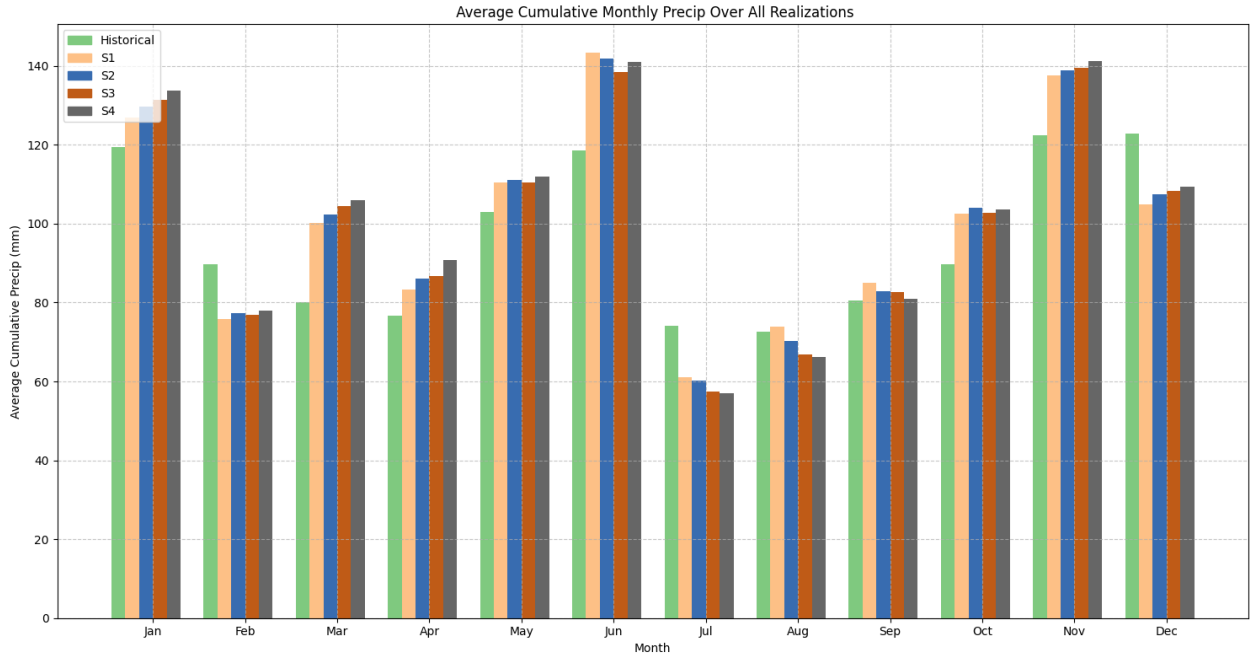


Figure 25 - Bar Graph of Average Cumulative Monthly Precipitation for All Scenarios

Figure 25 displays a comparative bar graph of the average cumulative monthly precipitation for all scenarios. January, June, and November are projected to have the largest cumulative precipitation values while July and August are projected to have the lowest. From October to May as the TMCCP scenario gets more extreme, precipitation is expected to increase on average. This trend is the opposite from July to September, which supports the notion that climate change makes wet months wetter and dry summer months drier. The historical data mostly follows this trend, with a few exceptions being increased historical precipitation predicted in February, July, and December. Overall, climate change is predicted to slightly

increase the total precipitation at Tent Mountain when compared to historical, which is favorable for the feasibility of the TM-PHES project.

All TMCCP future scenarios shared very similar daily mean precipitation values between 2.5 mm to 5 mm per month, as well as similar average cumulative monthly totals. This result predicts the total amount of rain experienced by the site will not change drastically due to climate change. However, the maximum daily precipitation events increased significantly in intensity in the TMCCP scenarios. The historical data showed a maximum daily precipitation value of 75 mm, while Scenario 2 predicts the largest overall daily precipitation value of 110 mm. The predicted 45 mm increase in maximum event intensity aligns with the expectation that climate change will escalate the severity of extreme precipitation occurrences, alongside a heightened frequency of rain-on-snow (ROS) events.

July had the maximum precipitation value for every TMCCP scenario, and yet it still had the lowest mean and cumulative values, which suggests July will have sparse, but very intense precipitation events. The line graphs for Scenarios 2, 3, and 4 (see Figure 21 - Figure 23) all provide similar values for mean and maximum daily precipitation. Therefore, if society maintains current emissions trends (Scenario 2), the climate change impact on precipitation at Tent Mountain is projected to be as severe as the impacts under the most extreme climate, Scenario 4. The TM-PHES project should thus consider the projected precipitation values of Scenario 2 for the design of risk mitigation features. This Scenario is the most likely scenario to occur based on current trends, and it is conservative compared to the precipitation values of worse climate change scenarios. Including projected precipitation values in the initial design will factor in the increasing severity of precipitation events, making the project robust to the changing climate and reducing the likelihood of capacity-based modifications and reconstruction in the future. This selection will reduce design risk regarding overtopping or dam failure, and it will increase the long-term sustainability of the project.

5.5 Projected Outflow

Flood-related disasters since 2000 have increased in occurrence by 134% compared to 1980-2000, and much of this change has been attributed to a more extreme climate [12]. As climate change progresses, flood-related disasters are expected to become more frequent and severe. Thus, it is vital the TM-PHES design account for flood scenarios that may occur due to the project releasing water to prevent dam failure/overtopping risks. An understanding of the basin outflow will be vital to inform the design of flood mitigation technologies. Reservoir outflow was estimated for the historic EMDNA data and the future climate change scenarios by using the historic EMDNA and future TMCCP realizations temperature and precipitation data as the input for the HEC-HMS model in Section 4. The output of this model was a realization-specific estimated outflow for the Upper and Lower Reservoirs. Due to model constraints, the outflow was calculated for the Upper and Lower Reservoirs independently, and these outflows were then

combined to estimate the total average outflow rate per day (Q_{total} in m^3/s) for the project. The TMCCP outflow realizations for each scenario were then compared to obtain the monthly outflow average and range. The following time series plots present the historical and projected daily outflow rate per month for the Tent Mountain basin. Appendix A includes boxplots of the same data broken up into 30-year time frames.

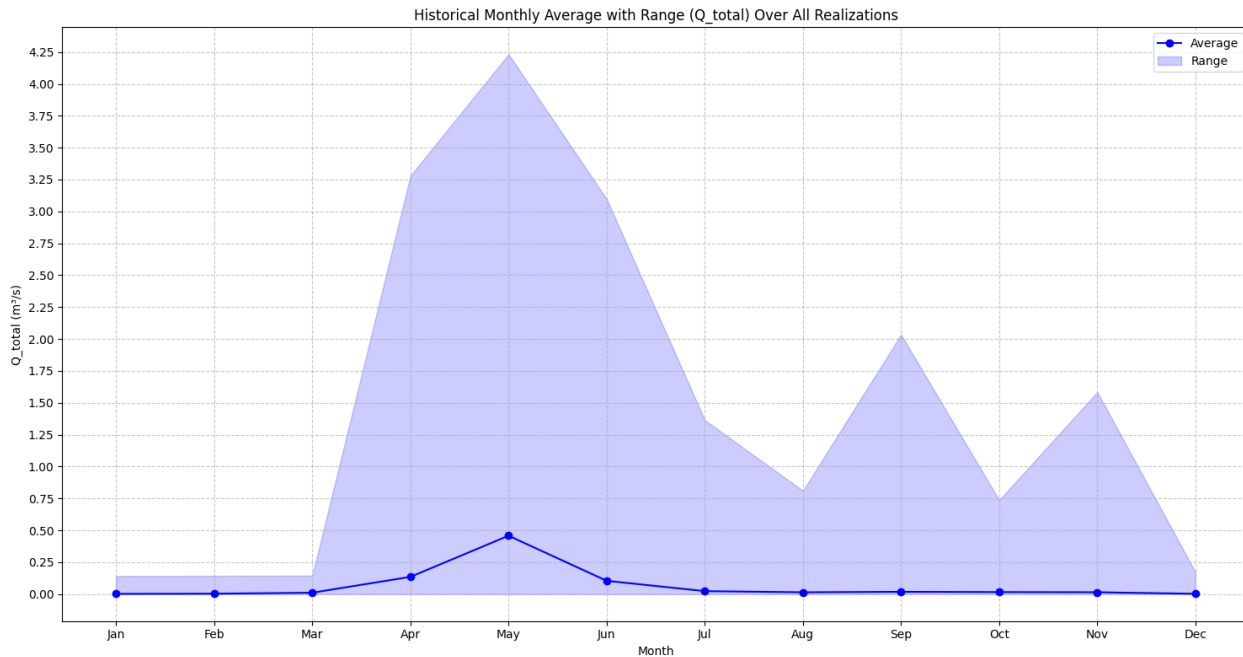


Figure 26 - Average Historical Daily Outflow per Month with Maximum

Figure 26 displays the estimated historic outflow data from 1979-2014. The mean monthly outflow per day peaks at a value of approximately $0.50 \text{ m}^3/\text{s}$ in May, while the months of July to March averaged near 0 outflow per day. The maximum daily outflow over this timeframe was approximately $4.25 \text{ m}^3/\text{s}$ in May while the winter months shared the lowest maximum outflow around $0.15 \text{ m}^3/\text{s}$.

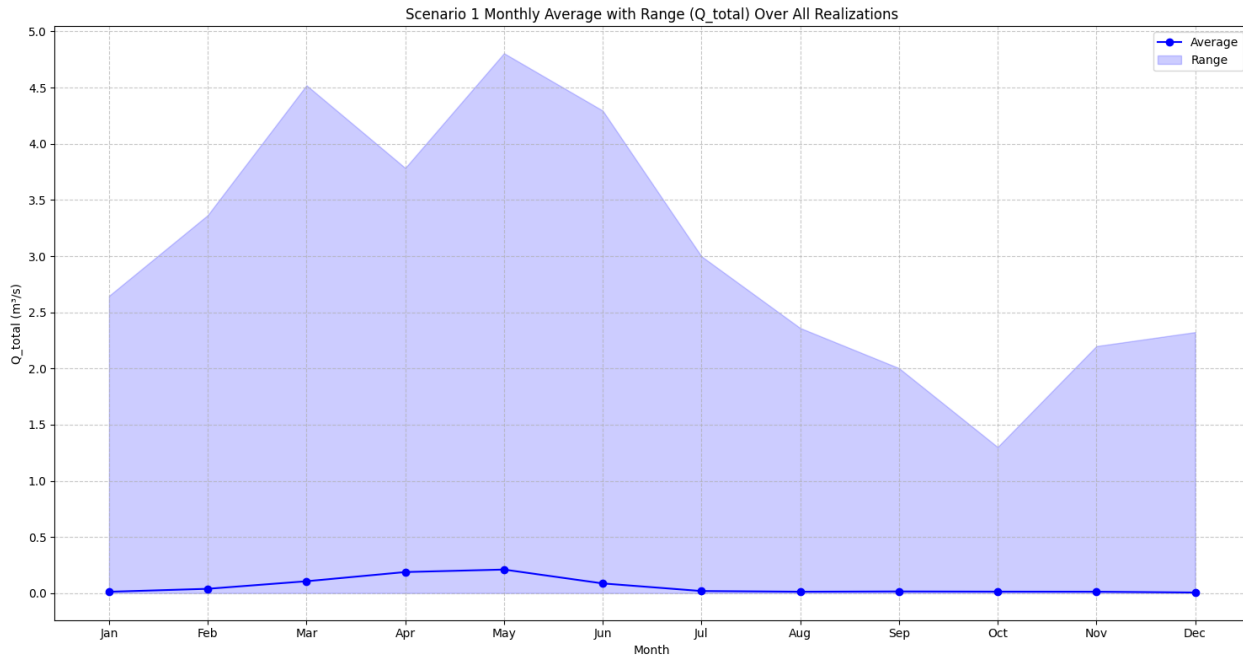


Figure 27 - Average Projected S1 Daily Outflow per Month with Maximum

Figure 27 displays the projected future outflow from 2015-2100 for Scenario 1. The mean monthly outflow per day peaks at a value of approximately $0.25 \text{ m}^3/\text{s}$ in April and May, while the months of July to January average near 0 outflow per day. The maximum daily outflow over this timeframe was approximately $4.75 \text{ m}^3/\text{s}$ in May with another peak of $4.5 \text{ m}^3/\text{s}$ in March. October had the lowest maximum at $1.35 \text{ m}^3/\text{s}$.

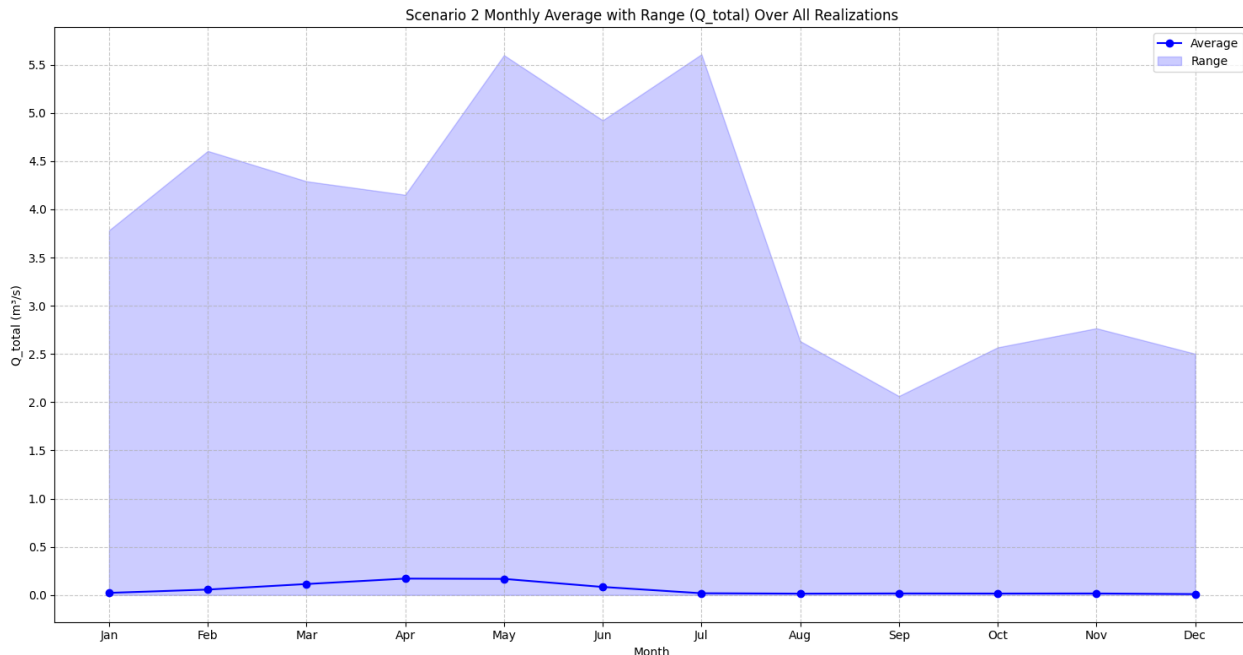


Figure 28 - Average Projected S2 Daily Outflow per Month with Maximum

Figure 28 displays the projected future outflow from 2015-2100 for Scenario 2. The mean monthly outflow per day peaks at a value of approximately $0.20 \text{ m}^3/\text{s}$ in April and May, while the months of July to January average near 0 outflow per day. The maximum daily outflow over this timeframe was approximately $5.5 \text{ m}^3/\text{s}$ in May and July. September had the lowest maximum outflow at approximately $2.0 \text{ m}^3/\text{s}$.



Figure 29 - Average Projected S3 Daily Outflow per Month with Maximum

Figure 29 displays the projected future outflow from 2015-2100 for Scenario 3. The mean monthly outflow per day peaks at a value of approximately $0.20 \text{ m}^3/\text{s}$ in April, while the months of July to January average near 0 outflow per day. The maximum daily over this timeframe was around $4.0 \text{ m}^3/\text{s}$ in April, May, and July. August had the lowest maximum outflow at approximately $1.35 \text{ m}^3/\text{s}$.

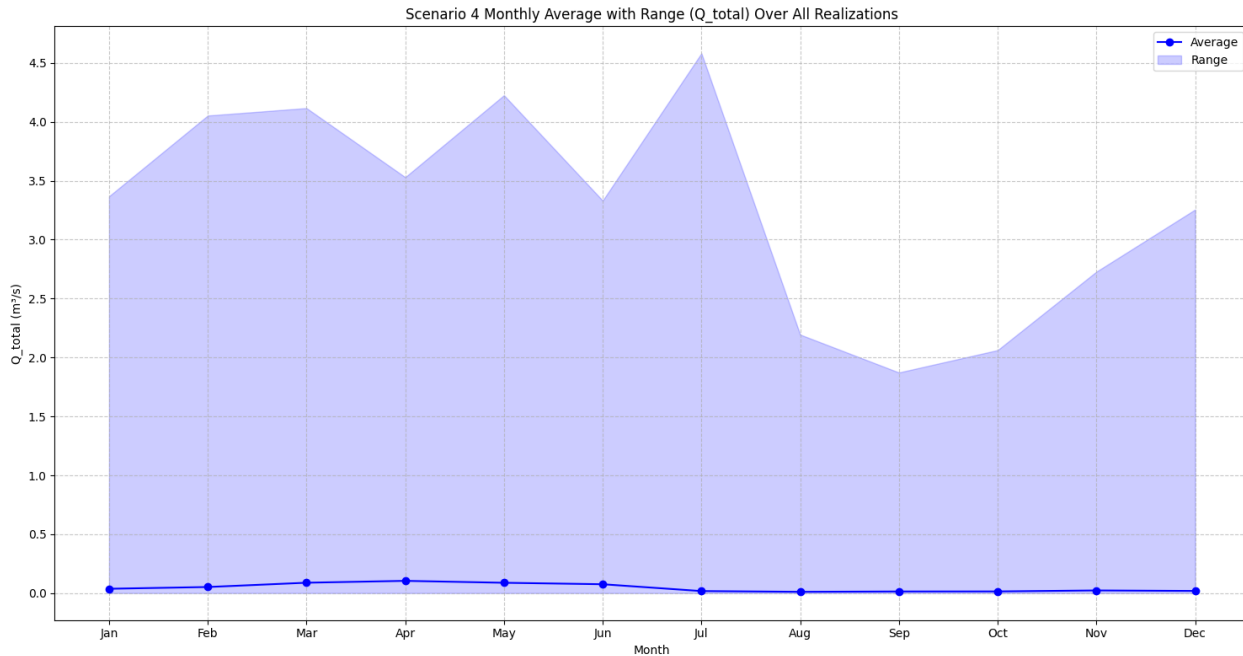


Figure 30 - Average Projected S4 Daily Outflow per Month with Maximum

Figure 30 displays the projected future outflow from 2015-2100 for Scenario 4. The mean monthly outflow per day peaks at a value of approximately $0.15 \text{ m}^3/\text{s}$ March to June, while the months of July to January average near 0 outflow per day. The maximum daily over this timeframe was approximately $4.5 \text{ m}^3/\text{s}$ in July, while the spring months peaked around $4.1 \text{ m}^3/\text{s}$. September had the lowest maximum outflow at approximately $1.85 \text{ m}^3/\text{s}$.

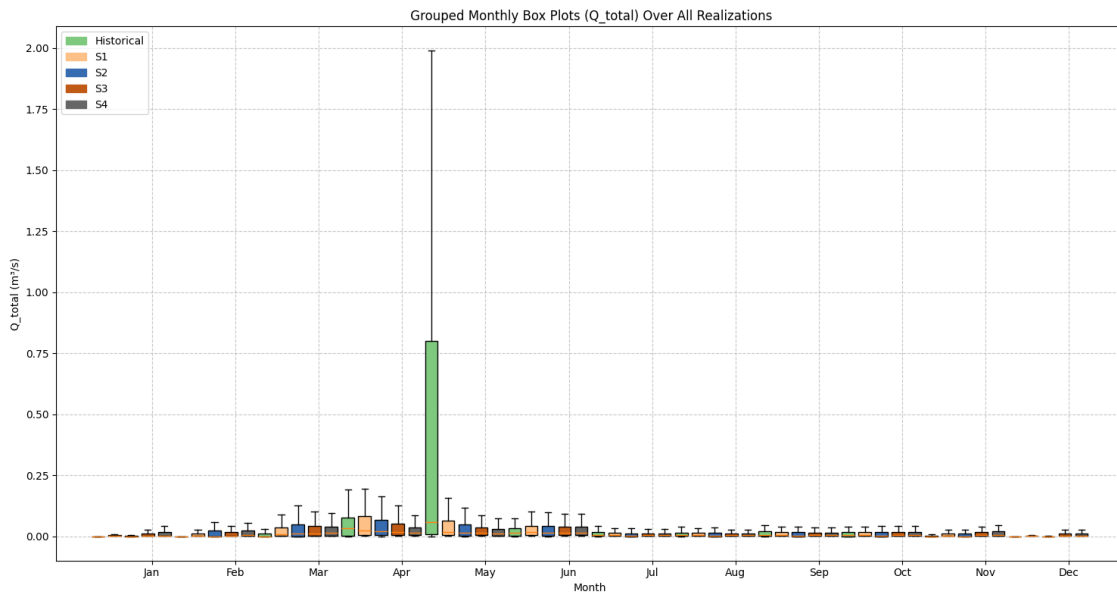


Figure 31 - Box Plot of Daily Outflow per Month for All Scenarios Excluding Outliers

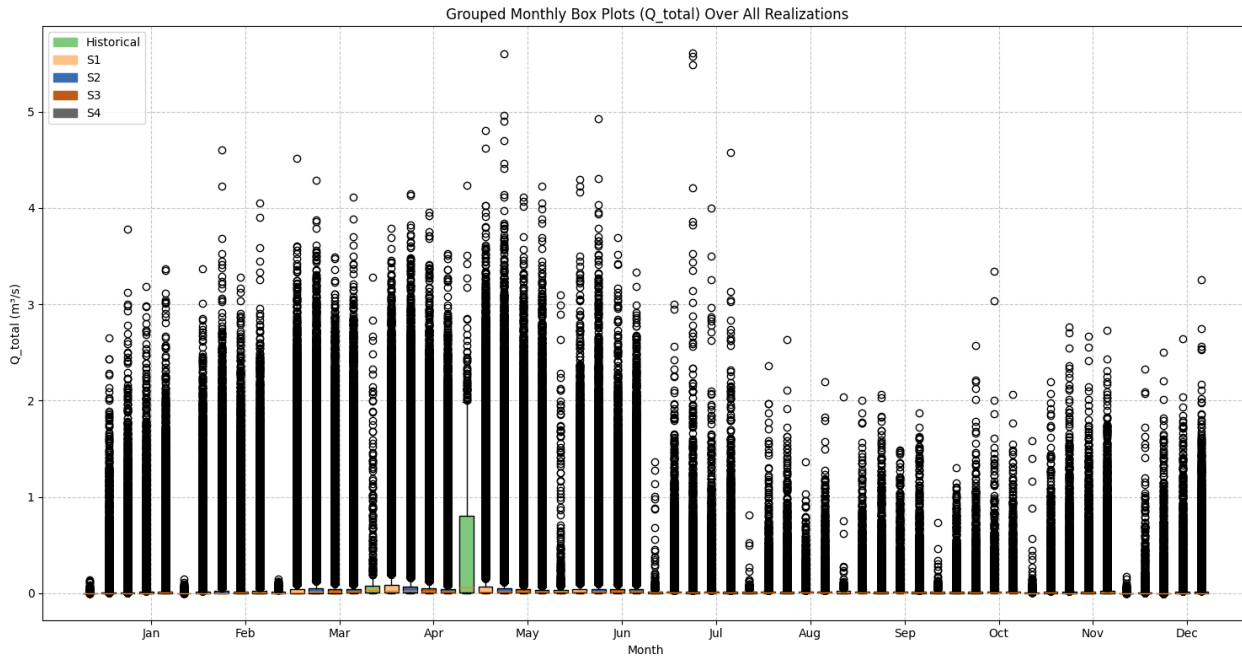


Figure 32 - Box Plot of Daily Outflow per Month for All Scenarios Including Outliers

Figure 31 is a comparative box plot of the daily outflow per month for all scenarios. The median outflow line hovers around $0.05 \text{ m}^3/\text{s}$ in the spring with higher values for lower TMCCP scenarios and is $0 \text{ m}^3/\text{s}$ for the rest of the year. The spring month medians are around $0.15 \text{ m}^3/\text{s}$ lower than the springtime means, suggesting the outflow data is highly influenced by outliers. The May historical IQR is an obvious anomaly in Figure 31, which is odd considering extreme outflow events are expected to increase in severity with climate change. Figure 32 shows this anomaly is no cause for concern, as when outliers are considered climate change scenarios produce much more severe outflow values. All scenarios predict more intense extreme outflow events than the historical data. An interesting result when considering outliers is that Scenario 2 has the largest predicted maximum outflow events occurring in May and July. August to October experience the lowest maximum outflow events which is expected due to the low cumulative and extreme precipitation values for these months.

There are several interesting trends revealed about the predicted outflow for the Tent Mountain basin. Every scenario predicts most months (July to January) are expected to experience an average daily outflow rate of approximately $0 \text{ m}^3/\text{s}$. April and May experience the highest average rate of outflow with a max of $0.5 \text{ m}^3/\text{s}$ from the historical data and a min of $0.15 \text{ m}^3/\text{s}$ from Scenario 4. Outflow peaks are also at their highest during the spring months, with the overall maximum outflow predicted at $5.5 \text{ m}^3/\text{s}$ in Scenario 2. Higher outflow averages and maximums occur in the spring because rain-on-snow (ROS) events are typically the most extreme hydrological scenarios for a mountainous watershed. ROS events carry the potential for substantial runoff, leading to both flooding and avalanches. Future scenarios are forecasted to witness a

decline in the occurrence of high peak flow ROS events in low (< 350 masl) and middle (350-1100 masl) elevation zones, while the frequency of ROS-linked peak flows is projected to rise in high elevation (>1100 masl) areas [13]. Furthermore, the shift from snow to rain precipitation during winter is likely to augment peak daily flows. The TM-PHES project is considered a high-elevation area, so increased ROS events can explain much of the increase in projected outflow severity. This consideration is supported by the cumulative monthly precipitation values in Figure 25 because most precipitation from December to March/April would be snow, which will not runoff until it melts, typically in April or May. As the climate change scenarios progress, larger average and maximum outflow values are seen from February to April, suggesting snowmelt events will occur earlier in the year. The increase in ROS events along with the predicted increase in precipitation intensity due to climate change can explain why the maximum predicted scenario outflow is 1.25 m³/s larger than the maximum outflow from the historical data. Scenario 2 predicts the most extreme outflow events. This is likely due to the scenario having similar precipitation intensity as Scenarios 3 and 4, but less extreme temperature increases, resulting in more ROS events than the more extreme climate change scenarios. Since Scenario 2 predicts the most extreme outflow events and it is the scenario most likely to occur under current climate trends it will be the scenario used to inform the design of flood mitigation infrastructure.

5.6 Projected Storage

Sufficient stored water is critical for the operation of any pumped hydro storage project. Tent Mountain was designed to have enough live storage to produce 320 MW of electricity for 16 hours straight, corresponding to 7,107,000 m³ of water (Section 1.2). The exact volume of water stored at any given time will fluctuate around this number due to seepage, evaporation, outflow, and precipitation. Drought is expected to become more severe in certain regions due to climate change, and drought-like conditions could have severe negative effects on the project's operability. Thus, it is useful to understand the projected extent of water storage fluctuation under climate change scenarios to inform facility operations, water loss mitigations, and the overall feasibility of the project.

Like outflow, storage was an output of the HEC-HMS model under different TMCCP realizations. However, due to time constraints, the model was calibrated to treat each reservoir independently, so both reservoirs' total storage values were created as outputs (Section 4). The actual pumped hydro storage system can only have one full reservoir at a time, so data transformation was performed to convert the storage outputs into system live storage. First, both total reservoir storage values were added and divided by 2 to approximate the total storage in one reservoir. Then 1,345,500 m³ was subtracted to account for the total dead storage in the system, this is slightly larger than the sum of the designed dead storage (1,285,900 m³) because it made the mean system live storage equal to the design value of 7,107,000 m³. This transformation may have

inaccuracies, but it is a good approximation to understand projected fluctuations around the design live storage volume. The line graphs created to show the mean and range of fluctuations for each climate change scenario start in 2030 because this is when the model predicts all scenarios will have full reservoirs (see Figure 33). This is longer than the approximately 3.1 years predicted to gain 7,107,000 m³ of live storage based on the historically based water balance. This discrepancy is due to the model calculating the time required to fill both reservoirs rather than until the live storage value is achieved. A further study could be conducted to understand storage fluctuations with a circular routing model.

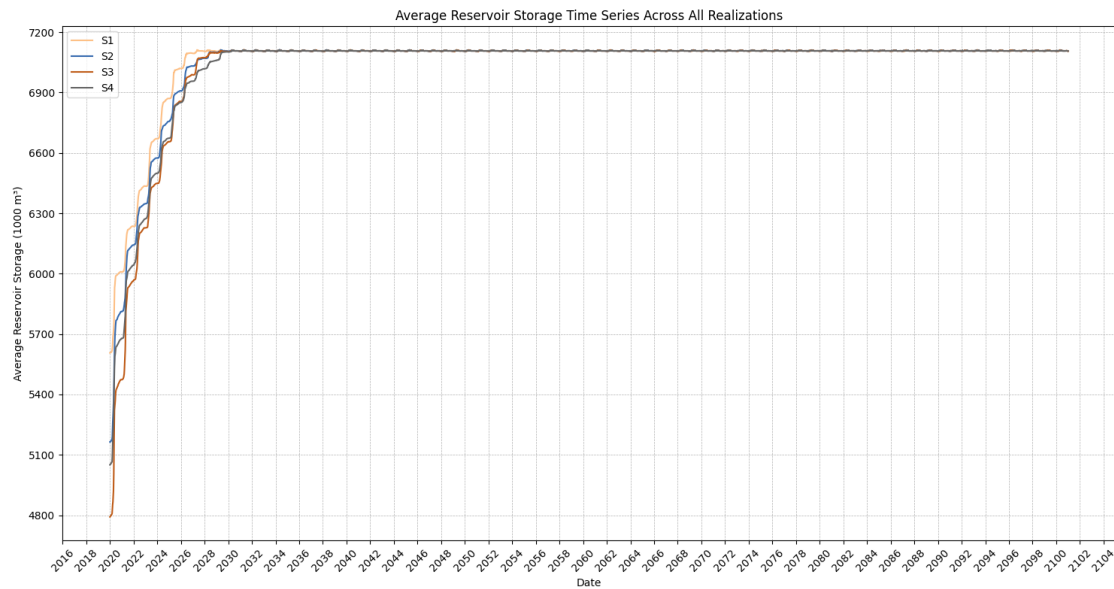


Figure 33 - Reservoir Storage for All Scenarios 2020-2100

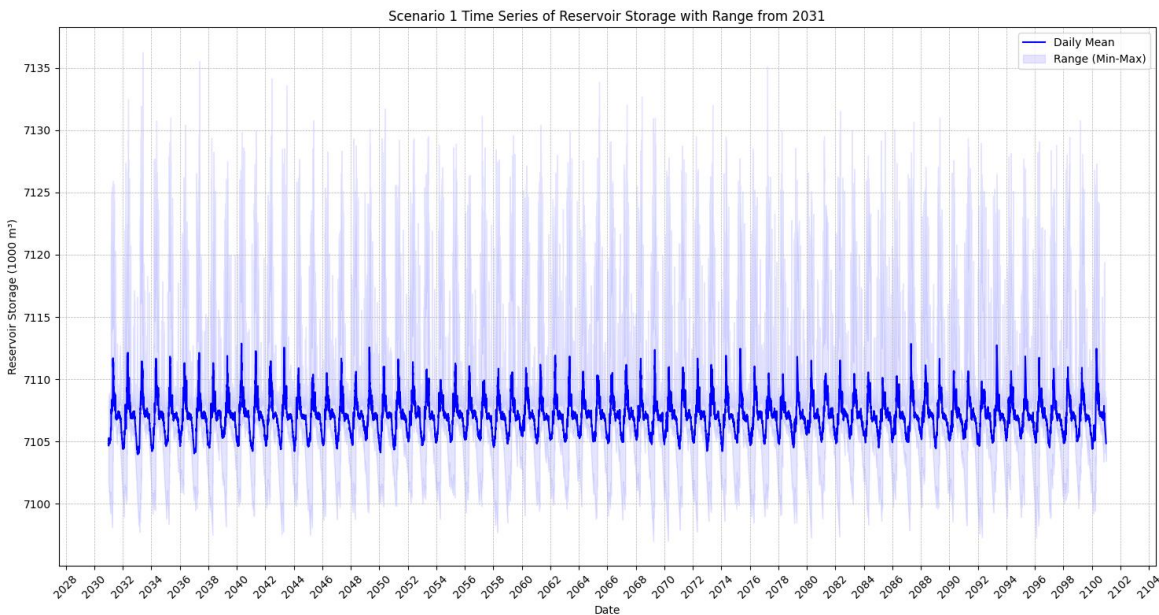


Figure 34 - Daily S1 Projection of Average Reservoir Storage with Range from 2031-2100

Figure 34 displays the projected future storage from 2015-2100 for Scenario 1. The daily mean storage value appears to fluctuate between a high of 7,112,000 m³ and a low of 7,104,000 m³. The total range appears to show the system reaching a max storage of volume of 7,136,000 m³ and a low of 7,098,000 m³.

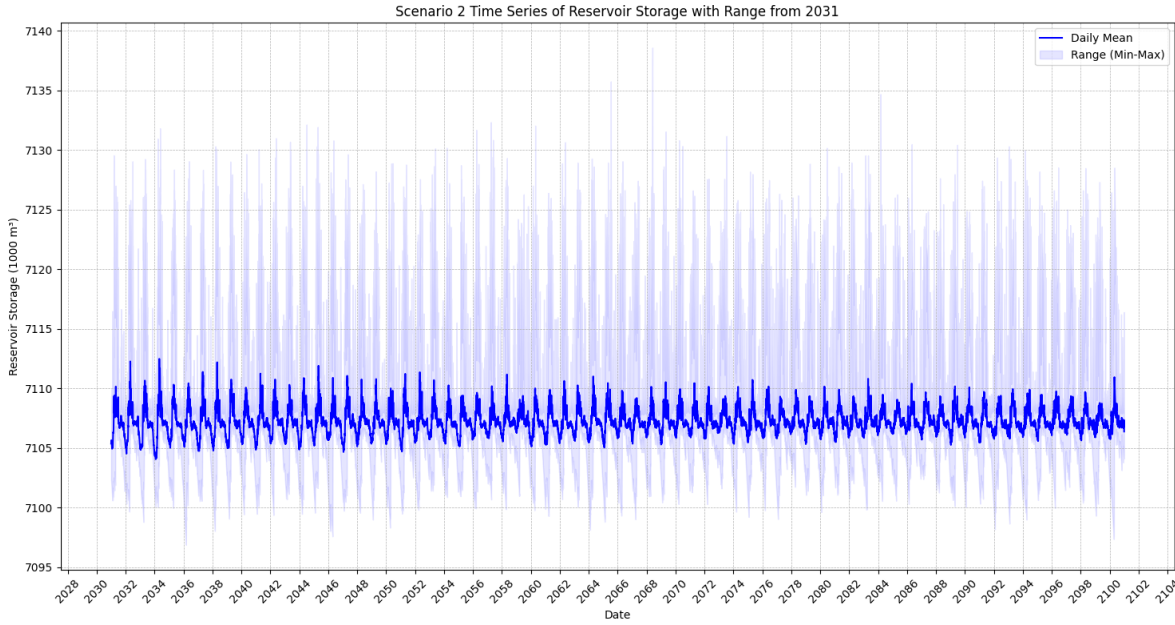


Figure 35 - Daily S2 Projection of Average Reservoir Storage with Range from 2031-2100

Figure 35 displays the projected future storage from 2015-2100 for Scenario 2. The daily mean storage value appears to fluctuate between a high of 7,112,000 m³ and a low of 7,105,000 m³. The total range appears to show the system reaching a max storage of volume of 7,139,000 m³ and a low of 7,097,000 m³.

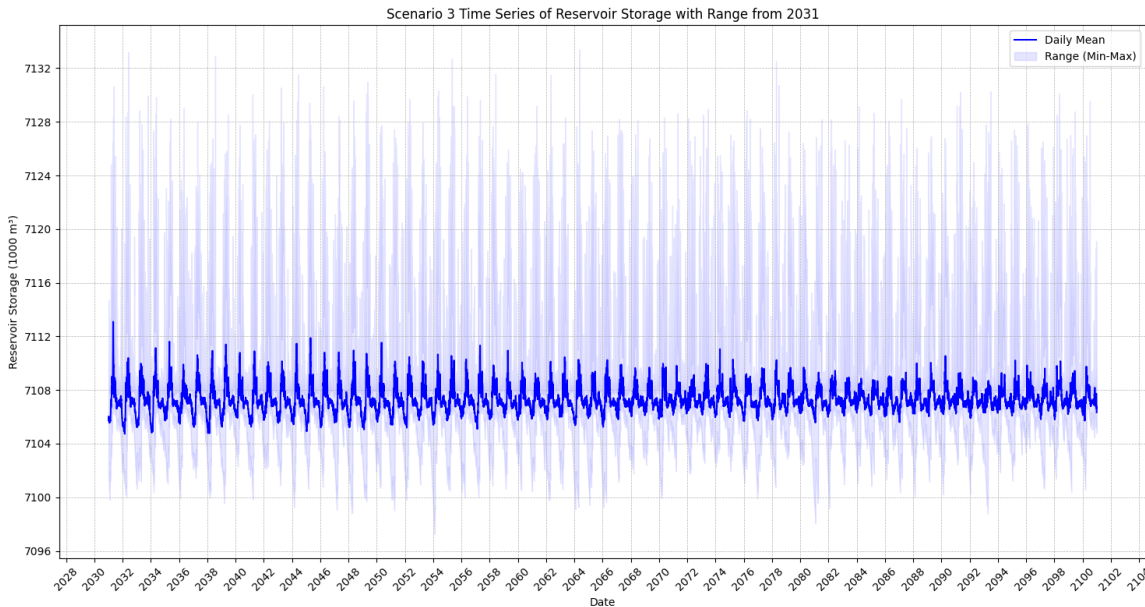


Figure 36 - Daily S3 Projection of Average Reservoir Storage with Range from 2031-2100

Figure 36 displays the projected future storage from 2015-2100 for Scenario 3. The daily mean storage value appears to fluctuate between a high of 7,110,000 m³ and a low of 7,106,000 m³. The total range appears to show the system reaching a max storage of volume of 7,133,000 m³ and a low of 7,098,000 m³.

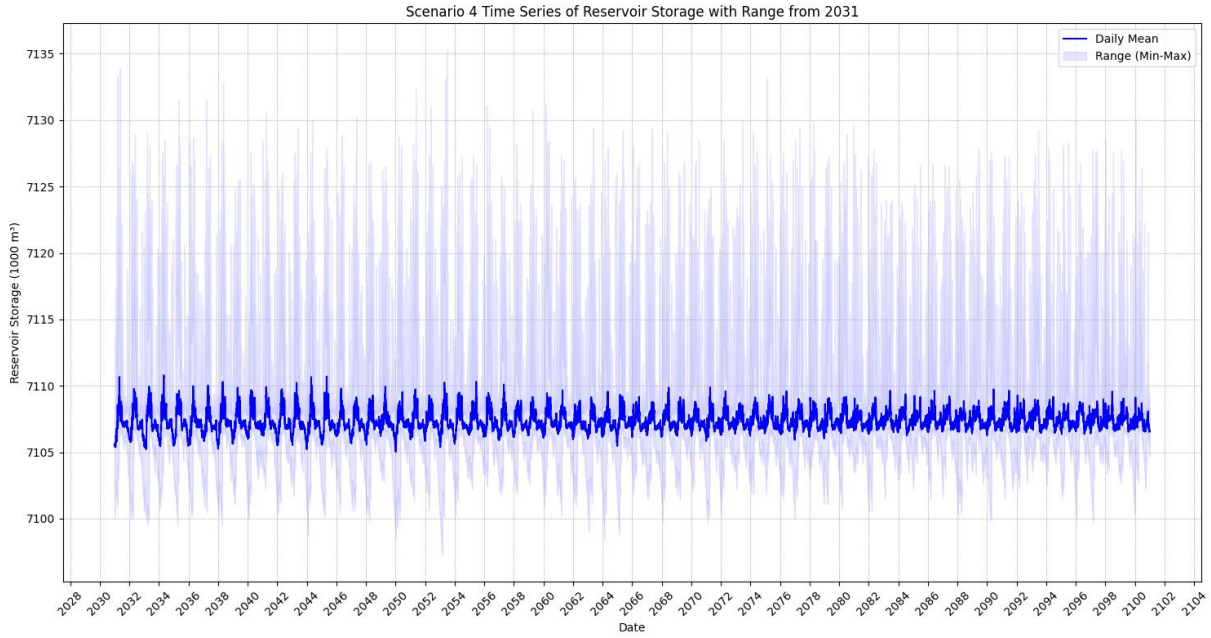


Figure 37 - Daily S4 Projection of Average Reservoir Storage with Range from 2031-2100

Figure 37 displays the projected future storage from 2015-2100 for Scenario 4. The daily mean storage value appears to fluctuate between a high of 7,110,000 m³ and a low of 7,105,000 m³. The total range appears to show the system reaching a max storage of volume of 7,135,000 m³ and a low of 7,097,000 m³.

Table 9 - Summary of Storage Fluctuations

Situation	Scenario	Volume (m ³)	Operational Time (h)	Δ Upper Reservoir Water Level (mm)
Overall Max.	S2	7,139,000	16.07	116.03
Highest Max. Mean	S1	7,112,000	16.01	18.3
Lowest Max. Mean	S1	7,104,000	15.99	-10.88
Overall Min.	S2	7,097,000	15.97	-32.26

Table 9 summarizes the mean and overall maximum and minimum storage values from all four TMCCP scenarios. Scenario 1 had the most fluctuation in mean storage, while Scenario 2 had the most fluctuation in overall storage. This makes sense because Scenario 2 was found to have the most extreme outflow events. Operational time was calculated from each storage value using the equation 7:

$$Operational\ Time(h) = \frac{Volume(m^3)}{123.4 \frac{m^3}{s}} * \frac{1\ h}{3600\ s} \quad (7)$$

A design discharge rate of $123.4\ m^3/s$ was adopted, as it is the value specified by Hatch in their prefeasibility study corresponding to the details of the generation system, which specifies $4 \times 80\ MW$ fixed-speed reversible Francis turbines and two $4\ m$ diameter penstocks [1]. Change in water level was calculated with equation 8:

$$\Delta\ Water\ Level\ (mm) = \frac{New\ Volume\ (m^3) - 7107000\ m^3}{275800(m^2)} * \frac{1000\ mm}{1\ m} \quad (8)$$

The Upper Reservoir area of $275,800\ m^2$ was used because it is smaller than the Lower Reservoir so it would have a more pronounced change in depth. Despite the projected $42,000\ m^3$ range in water storage, the operational capacity of the plant fluctuated a maximum of 0.1 hours, while the water level fluctuated a maximum of $148.29\ mm$. Thus, according to the simulated reservoir storage analysis completed in this report, Tent Mountain should not suffer from impactful storage issues due to drought.

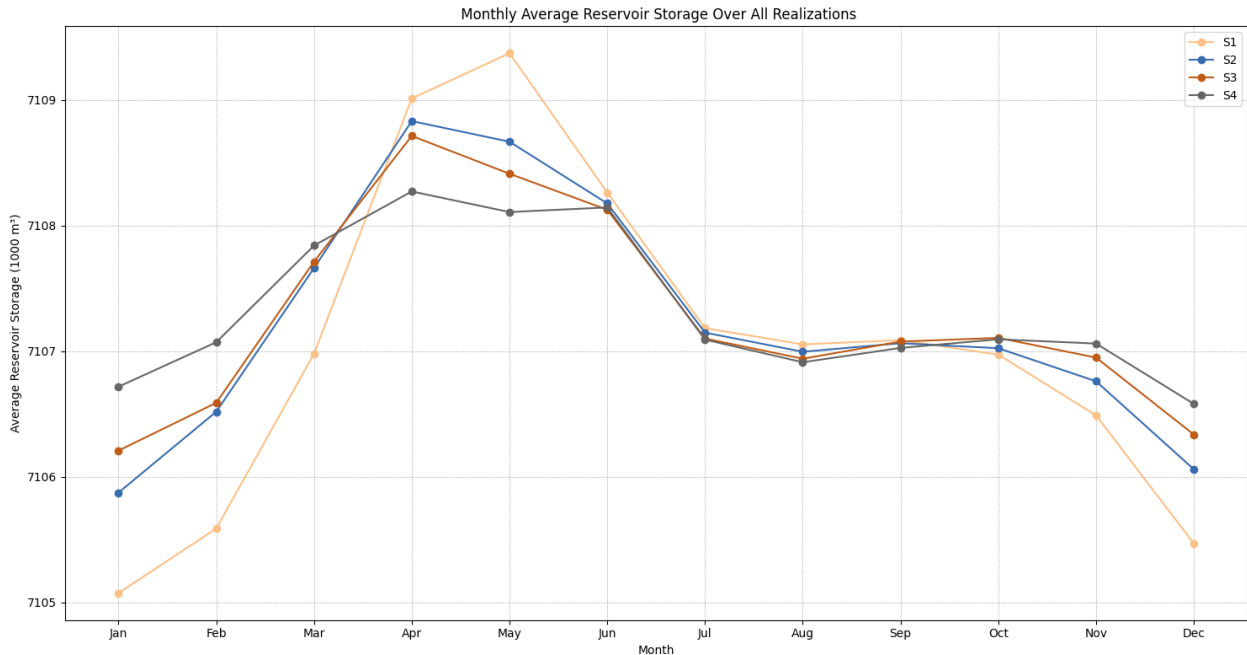


Figure 38 - Monthly Average Reservoir Storage for All Scenarios

Figure 38 displays the average storage value by scenario for each month. Scenario 1 is seen to have the largest fluctuation in average storage, which is also seen in the daily time series figures. All scenarios have below design storage in winter, and above design storage in spring. The chart also shows that as scenarios increase in climate change intensity, the average storage variability decreases. This output corresponds to

the increase in total precipitation predicted by the TMCCP data. Thus, the TM-PHES project should be resilient to the challenges imposed by climate change and should have enough water storage to be feasible.

6 Design Event Estimation

6.1 Frequency Analysis

A frequency analysis was performed using the historical and projected future (Scenario 2) annual maximum daily precipitation and streamflow values. Scenario 2 was the chosen climate change scenario because it is the most likely scenario to occur based on current emissions trends, and it produced the largest extremes in precipitation and outflow. The results of these analyses are presented in Table 10.

Table 10 – Frequency Analysis Summary

Return Period (years)	Historical Data		Projected Future Data	
	Precipitation (mm)	Runoff (cms)	Precipitation (mm)	Runoff (cms)
2	38.0	1.6	57.3	3.3
5	43.9	2.5	67.6	3.8
10	53.6	3.0	75.4	4.2
25	30.3	3.6	85.6	4.7
50	64.8	4.0	93.4	5.0
100	69.1	4.3	101.1	5.3
1000	82.0	5.1	126.8	6.4
Selected Distribution	Gamma	Generalized Extreme Value	Pearson Type III	Pearson Type III
Kolmogorov-Smirnov Test Result	0.327	0.219	0.484	0.364

Each of the data sets were fit to a curve using the Kolmogorov-Smirnov (K-S) test as a marker of best fit. This test is a nonparametric statistical method used to assess correlation between a sample and a specific probability distribution. In this case, Gamma, Generalized Extreme Value (GEV), Pearson Type III (PE3), and Normal distributions were evaluated. Typically, hydrological data does not conform to normal distributions; however, it was included to assess the HEC-HMS model's capability of producing data that matches typical hydrological patterns. The K-S test result represents the maximum absolute difference between the empirical cumulative distribution function (ECDF) of the input data and the cumulative distribution function (CDF) of the selected distribution. Therefore, smaller values indicate a better goodness-of-fit.

As shown in Table 10, the precipitation and runoff for each return period using the projected future data is increasingly larger; however, the increase in runoff is not proportional to the increase in precipitation. This result is likely due to the increased evapotranspiration associated with the higher temperatures in Scenario

2, as compared to the historical data, which affects annual peak runoff by reducing antecedent soil moisture prior to heavy precipitation events.

It is apparent from the results of the streamflow frequency analysis that the model, as set up for the continuous simulation, is not an effective predictor of extreme high flows. Nevertheless, the findings serve as a broad reference point for estimating the Probable Maximum Precipitation (PMP) and Probable Maximum Flood (PMF), which are expected to exceed their respective 1:1000-year counterparts in magnitude. As discussed in the Fall Report, the consequence classification of the project is assumed to be “extreme” due largely to the project’s upstream position relative to Highway 3 and several communities in the Municipality of the Crowsnest Pass [14]. The PMF is therefore designated as the Inflow Design Flood (IDF).

6.2 Probable Maximum Precipitation

The PMP is defined as the greatest depth of precipitation for any given duration meteorologically possible for a given size storm area at a particular location at a particular time of year, with no allowance made for long term climatic trends [15]. Oftentimes, area reduction factors are used for large basins; however, this does not apply to this project’s basin due to its small size (5.557 km^2). Moreover, larger basins often see higher peak flows from PMP events longer than 24 hours due to longer lag times. Due to the relatively short lag time of this basin, it is assumed that the 24-hr PMP will generate the highest peak flow.

Robust PMP estimation is commonly accomplished using at least one of the following methods:

1. **Theoretical Storm:** This method begins with selecting a storm pattern characteristic of the most severe regional conditions. This pattern may be derived historically, using meteorological theory, or stochastically, using parameters from other similar basins. Storm duration, as well as temporal and spatial distribution are calculated based on the chosen method. Ultimately, using these parameters, precipitation depths are computed for various durations, thus the PMP is derived.
2. **Hydrometeorological:** This approach involves the conversion of historical meteorological data, such as humidity, temperature, wind, and air pressure, to scenarios with potential to generate extreme precipitation. Statistical techniques, such as frequency analysis, are used to calculate the probability distribution of precipitation events. Complex hydrological models are often used to simulate precipitation events under the specified meteorological conditions, and the PMP depth is specified based the model results.
3. **Stochastic Storm Transposition:** As with all methods, this technique requires the analysis of historical storm events in the general region of interest. Relationships are developed between storm characteristics and antecedent meteorological conditions. Employing these relationships, synthetic storm events are formulated for the target location by spatially transposing historical storm data

using the statistical models. The most extreme events are selected from the generated storms, and from these the PMP is estimated.

Due to the time constraints of this project, an in depth PMP estimation was not possible. However, a literature review was conducted, which informed a PMP estimate sufficient for a feasibility-level report. It is recommended that subsequent phases of work independently verify this estimate.

Typical Annual Exceedance Probability (AEP) for PMP events on the eastern slopes of the Rockies are on the order of 10^{-7} to 10^{-8} (equivalent to 1:10,000,000 to 1:100,000,000 years) [16]. Assuming similar distributions were used to make this estimate and based on the historical and future projected (Scenario 2) data, respectively, the precipitation associated with an event of AEP 10^{-8} is 125 mm and 255 mm.

A 1980 publication from the University of Alberta, which employed both hydrometeorological and stochastic methods, estimates the Banff PMP at approximately 210 mm [17]. This result is significant because of the similar orographic conditions between Banff and Tent Mountain. However, its relevance is constrained by the occurrence of numerous high precipitation events in the basin since the publication, which would likely skew the statistical methods' results towards the higher end. A Government of Canada publication from 1999, again using both meteorological and stochastic methods, posits that a 295 mm 24-hr event at Spionkop Creek in the foothills, about 60 km southeast from Tent Mountain, may have approximated a PMP event for that area [18]. This estimate is relevant due to its proximity; however, its usefulness is limited by the basin's lower elevation and somewhat flatter topography. Based on a spatial distribution of stochastic PMP estimates across the eastern Rockies reported in a BC Government publication, 201 mm and 275 mm represent the lower and upper bounds, respectively, of the reasonable PMP range for the Tent Mountain site [16]. This spatial distribution is shown in Figure 39.

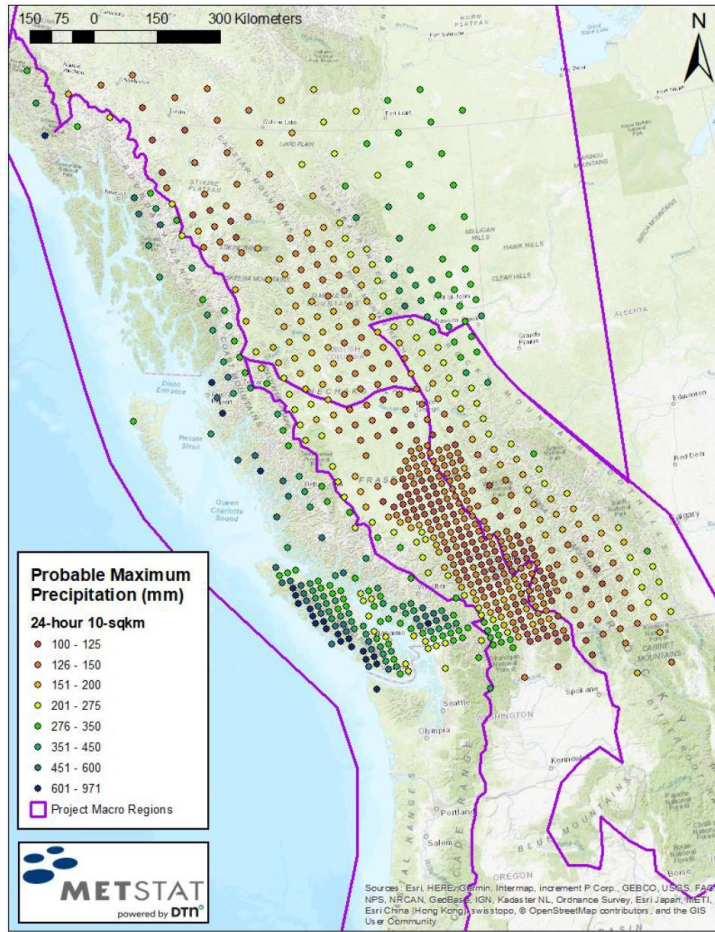


Figure 39 - Spatial Distribution of PMP Values at 24-hour, 10 km²

Alberta Environment and Protected Areas (then Alberta Environment) commissioned a PMP study for the Chain Lakes Reservoir, located in the foothills of the Livingstone Range, roughly 80 km northeast of Tent Mountain, in 2002. This report complied with the World Meteorological Organization (WMO) guidelines for PMP estimation, which involves the use of theoretical storm method, and returned a PMP value of 420 mm for that basin [19]. This outcome is significantly higher than other estimates and has since been superseded by an even higher estimate following high magnitude storm events in 2005 and 2013. The Chain Lakes Reservoir region is visible on Figure 39 as the darker green dot southwest of Calgary; this distribution lends validity to this region's higher PMP being considered an outlier.

Except for the historical AEP-based estimate for Tent Mountain and the Chain Lakes estimate, all relevant PMP estimates fall in the range of 200-300 mm. Considering an equal weighting for each of the four estimates within this range, including the Scenario 2 AEP-based estimate for Tent Mountain, the average value is 247 mm. Consequently, this value has been chosen as the PMP value for generating the Probable Maximum Flood (PMF).

6.3 Probable Maximum Flood

It is common industry practice for the physically or statistically estimated PMP to be input to an event-based hydrological model to provide an estimate of the PMF peak flow [16]. The HEC-HMS model setup is described in Section 4.2. Due to time constraints, only a rain-driven event was modelled. It is recommended that future analysis include a rain-on-snow (ROS) event as this is typically the governing case in mountainous basins. Climate change's influence is expected to cause typical timing of ROS events to shift somewhat earlier in the year, as well as somewhat decreasing their magnitude as less time will be available for snow to accumulate. However, it is still prudent to evaluate.

Two possible PMF scenarios were modelled:

1. The Upper Reservoir is at its NMOL and the Lower Reservoir is at its DSL.
2. The Lower Reservoir is at its DSL and the Lower Reservoir is at its NMOL.

Table 11 summarizes the model results with a spillway width of 30 m. Time zero is equal to start of the IDF.

Table 11 – IDF Event-Based Model Results

Parameter	PMF 1		PMF 2	
	Upper Reservoir	Lower Reservoir	Upper Reservoir	Lower Reservoir
Initial water level (masl)	1,803.3	1,480.0	1,760.0	1,509.0
Peak inflow (m ³ /s)	41.5	152.1	41.5	130.4
Peak inflow time (hr)	12.5	12.9	12.5	12.5
Peak outflow (m ³ /s)	22.6	0.0	0.0	46.1
Peak outflow time (hr)	13.1	-	-	14.2
Peak water level (masl)	1,803.7	1,489.9	1,763.4	1,510.6
Total inflow volume (dam ³)	318.5	1,348.7	318.5	1,348.7

Figure 40, Figure 41, Figure 42, and Figure 43 provide a graphic representation of each PMF scenario for the Upper and Lower Reservoirs, computed by the calibrated HEC-HMS model.

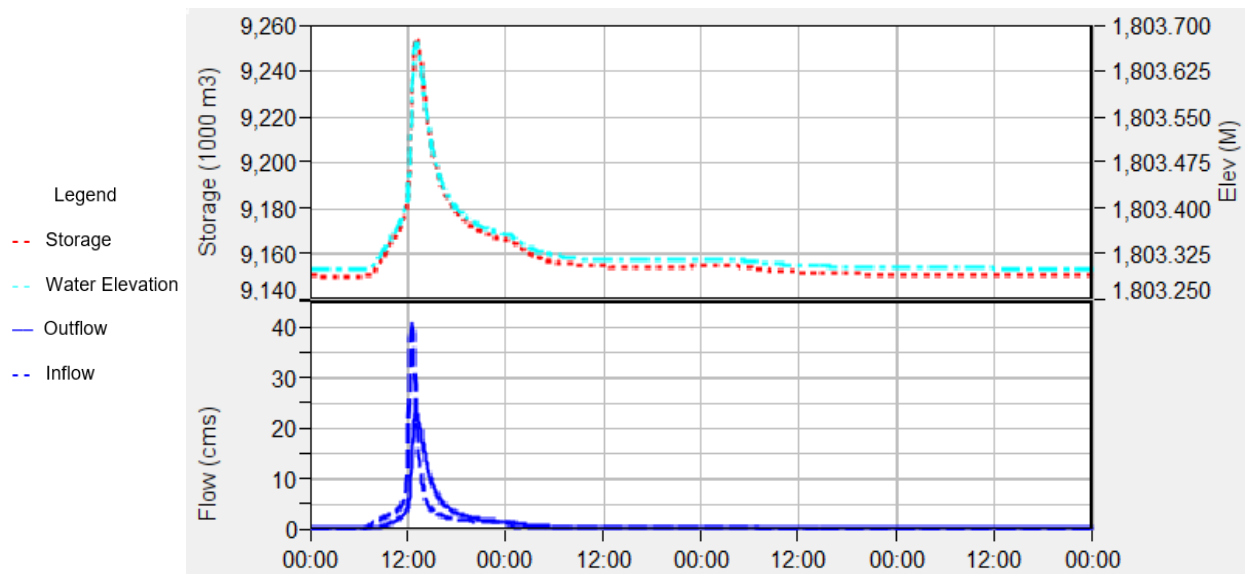


Figure 40 – Upper Reservoir Storage, Flow, and Water Elevation (PMF 1)

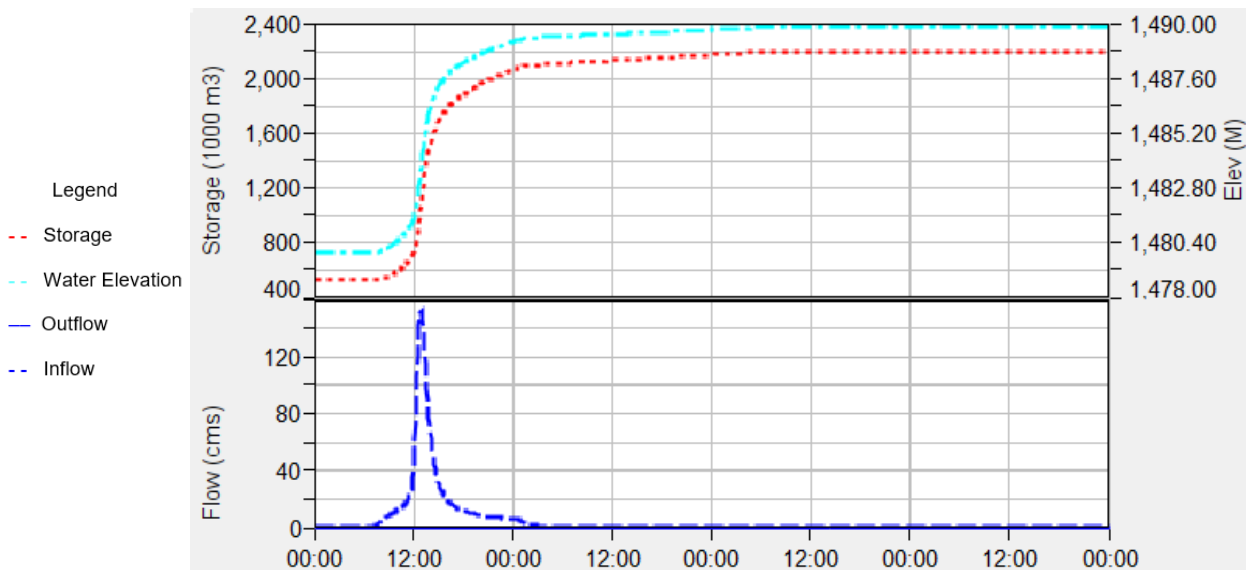


Figure 41 – Lower Reservoir Storage, Flow, and Water Elevation (PMF 1)

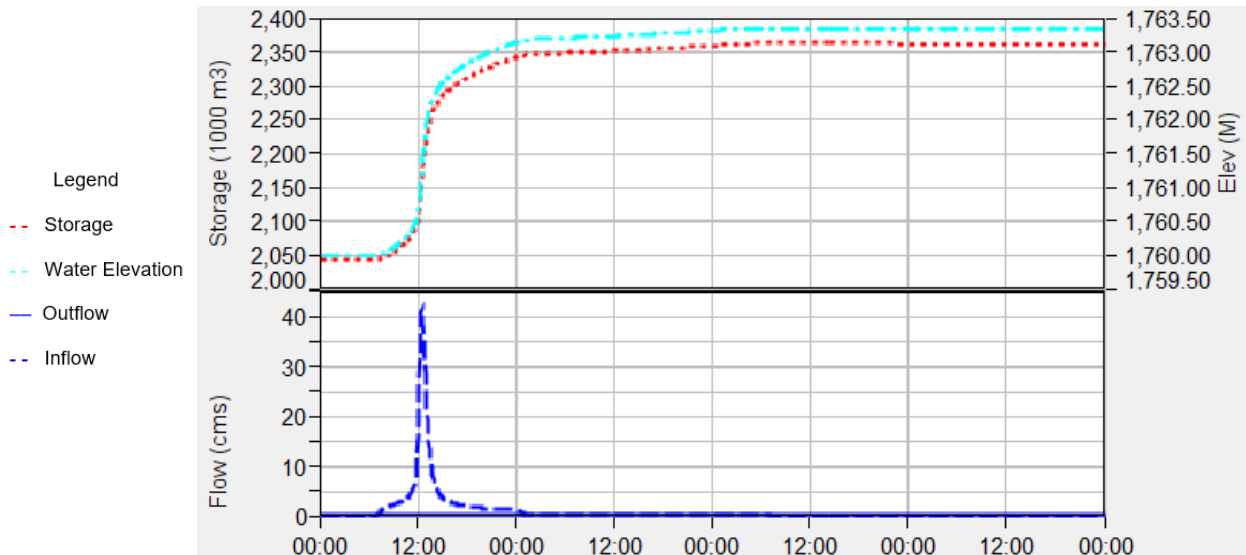


Figure 42 – Upper Reservoir Storage, Flow, and Water Elevation (PMF 2)

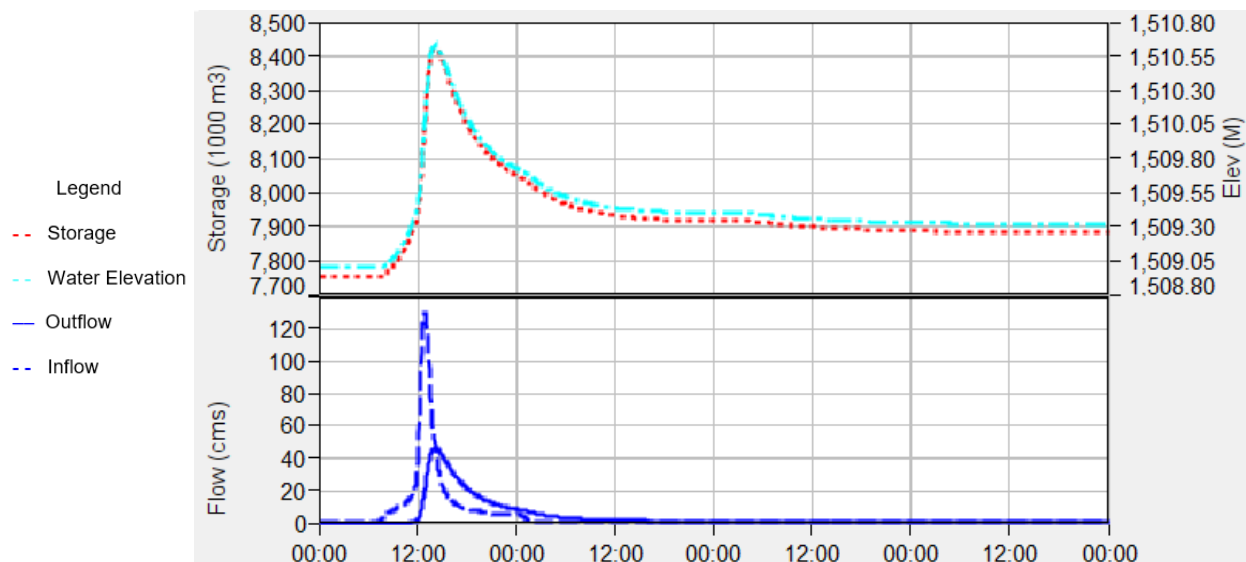


Figure 43 – Lower Reservoir Storage, Flow, and Water Elevation (PMF 2)

PMF 1 is the governing scenario for the Upper Reservoir. Since the Upper Reservoir's IDF peak outflow rate ($22.6 \text{ m}^3/\text{s}$) is much less than the operating flow rate for the penstocks during power generation ($98.0 \text{ m}^3/\text{s}$), it is assumed that the Upper Reservoir can fully attenuate the IDF with only trivial impacts on its retaining structures or the Lower Reservoir.

Due to the effect of spillway width on inflow-outflow relationships and peak water levels, the reservoirs' PMP attenuation capabilities are explored in Section 7.1 alongside spillway design. Although the peak inflow at the Lower Reservoir is higher for PMF 1, its starting water level allows it to fully attenuate the

flood. Despite its lower peak inflow (due to no contribution from the Upper Reservoir) PMF 2 is the governing scenario for the Lower Reservoir as it results in a higher peak outflow and will be used hereafter to guide spillway design.

7 Design Updates

7.1 Spillway

The Lower Reservoir's North Dam will be equipped with a spillway that is intended to remain inoperative, except in case of major flood events. The modelled spillway was based on a broad-crested configuration with a coefficient of $1.0 \text{ m}^{0.5}/\text{s}$ and a crest elevation of 1509.3 m.

Table 12 – Lower Reservoir Spillway Width Sensitivity Analysis

Parameter	Spillway width (m)			
	15	20	25	30
Initial water level (masl)	1,509.0	1,509.0	1,509.0	1,509.0
Peak inflow (m^3/s)	130.4	130.4	130.4	130.4
Peak inflow time (hr)	12.5	12.5	12.5	12.5
Peak outflow (m^3/s)	29.6	35.9	41.3	46.1
Peak outflow time (hr)	14.5	14.4	14.3	14.2
Peak water level (masl)	1510.9	1510.8	1510.7	1,510.6
Total inflow volume (dam^3)	1,348.7	1,348.7	1,348.7	1,348.7

For every 5 m decrease in the spillway width, the time to peak outflow is increased by approximately 6 minutes, the peak water level is increased by approximately 0.1 m, and the peak outflow is decreased by approximately $5 \text{ m}^3/\text{s}$. The minimum crest elevation of 1512.5 m is 1.6 m above the maximum peak water level. A wind and wave analysis is recommended in subsequent phases to confirm that this freeboard is sufficient to avoid overtopping under CDA-specified conditions.

These marginal differences in time to peak and peak water level are trivial; much to the contrary, the marginal differences in peak flow are significant. By halving the spillway width, the peak outflow is reduced by approximately 35%. The sensitive riparian environment of the Crowsnest Creek tributary downstream of the site would likely experience much more severe negative impacts from a peak flow of $46.1 \text{ m}^3/\text{s}$, as compared to a peak flow of $29.6 \text{ m}^3/\text{s}$.

Another important consideration between these alternatives is cost. Detailed cost estimation is outside the scope of this report, but assuming construction cost is proportional to spillway width, the narrowest spillway would be the most cost effective.

The spillway width is therefore set at 15 m for the following reasons:

1. To minimize construction costs.
2. To minimize peak outflow and downstream externalities in case of flooding.
3. It yields sufficient freeboard (assuming no wind and wave effects).

A graphical representation of the PMF attenuation with a 15 m spillway on the Lower Reservoir is presented in Figure 44.

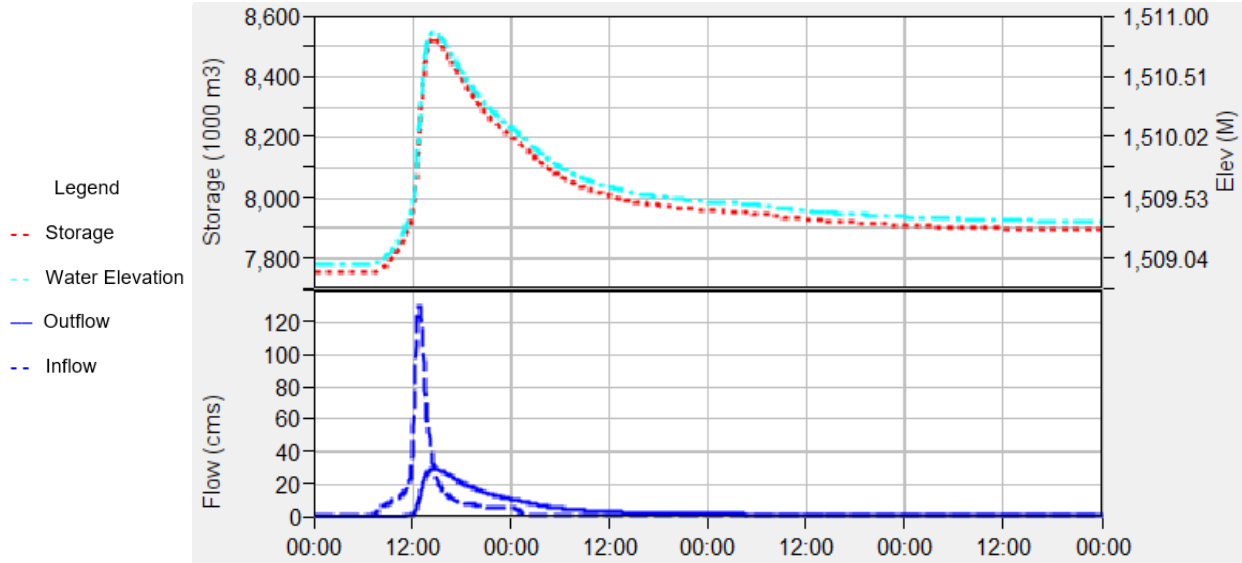


Figure 44 – Lower Reservoir Storage, Flow, and Water Elevation (PMF 2, 15 m Spillway)

7.2 Riparian Outlet

In addition to the main spillway, the Lower Reservoir North Dam structure will include a gated riparian outlet intended to operate year-round. Riparian and aquatic health parameters adapted from the Bow River Basin Council indicate that flows between 0.667 and 1.296 times the seasonal means are within natural, expected fluctuations [20]. It is important to note that no such guidelines are available at the time of writing for the Oldman River Basin, but given the ecological similarities between the basins, it is assumed that these guidelines are applicable. Monthly mean outflow values were calculated using outputs from the historical and Scenario 2 simulations and are summarized in Table 13 and

Table 14 respectively.

Table 13 – Monthly Riparian Flow Summary - Historical

Month	Jan	Feb	Mar	Apr	May	Jun	Jul	Aug	Sep	Oct	Nov	Dec
0.667 (m³/s)	0.001	0.002	0.007	0.090	0.305	0.069	0.015	0.009	0.012	0.010	0.010	0.001
Mean (m³/s)	0.002	0.003	0.011	0.135	0.458	0.104	0.023	0.014	0.018	0.016	0.015	0.002
1.296 (m³/s)	0.002	0.004	0.014	0.175	0.593	0.135	0.030	0.018	0.023	0.020	0.019	0.003

Table 14 – Monthly Riparian Flow Summary – Scenario 2

Month	Jan	Feb	Mar	Apr	May	Jun	Jul	Aug	Sep	Oct	Nov	Dec
0.667 (m ³ /s)	0.015	0.037	0.076	0.113	0.095	0.055	0.012	0.009	0.011	0.010	0.010	0.006
Mean (m ³ /s)	0.022	0.056	0.114	0.170	0.143	0.083	0.018	0.014	0.016	0.015	0.015	0.009
1.296 (m ³ /s)	0.029	0.073	0.148	0.220	0.185	0.108	0.023	0.018	0.021	0.019	0.019	0.012

The maximum and minimum mean monthly flows from the historical simulation are 0.458 m³/s (May) and 0.002 m³/s (January and December), respectively. The outflows generated by the Scenario 2 simulation do not affect the upper and lower limits of mean flow and thus, do not affect the riparian outlet design. The outlet gate and flow measurement structure should therefore be built to operate between 1.0 m³/s and 0.0 m³/s, with an adjustment sensitivity of 0.0005 m³/s.

Actual operational flows will be governed by total storage volume between the two reservoirs but should remain compliant with these guidelines for the vast majority of the time.

8 Operational Plan

8.1 Project Initialization

The following three-phased approach is necessary to initialize the project:

1. **Reservoir Filling:** outflow is maintained at the minimum environmental rate (see Section 7.2) until the required live storage volume of 7,107,000 m³ has accumulated between the Upper and Lower Reservoirs. This phase is expected to take approximately 3.1 years (see Section 3.8)
2. **Settling the Water Debt:** outflow is maintained as close to the maximum environmental rate (see Section 7.2) as possible without reducing water storage until the net diversion reaches zero.
3. **Regular Operations:** the total volume between the two reservoirs is maintained constant such that outflow is equal to runoff. The length of this phase is indefinite.

This phased approach is necessary due to the temporary diversion license (TDL) governing the project's access to water. As the name suggests, the license holder is not entitled to any permanent diversion or export of water and must therefore maintain a net zero diversion quantity over time. The outflow referred to above will occur primarily through the Lower Reservoir's North Dam riparian outlet.

8.2 Power Generation in Alberta

The Tent Mountain site can accommodate a PHES with an 80-year lifetime and a 320 MW installed capacity [21]. The turbine configuration within the powerhouse consists of 4 x 80 MW fixed-speed reversible Francis turbines [21], to be utilized during the 16-hour continuous generation duration. At the normal maximum

operating level of the Upper Reservoir of 1803 m, the storage capacity offered is 5120 MWh and the maximum gross head is 294 m.

Energy storage provides the flexibility to balance electricity supply and demand in real-time [21], where generation can be optimized to occur during periods of high demand. In essence, this project will make use of the collected water in the Upper Reservoir by releasing it when electricity demands spike, to flow through a penstock down to the powerhouse through the four turbines that rotate the generators which produce the electricity. The water will then collect in the Lower Reservoir and be pumped back up through the second penstock to the Upper Reservoir using low-cost energy when electricity demand is low.

Alberta utilizes a unique regulatory framework, unlike the rest of Canada, where it is the only fully deregulated or unbundled electricity market in the country. Most Canadian provinces and territories have utilities that are vertically integrated Crown corporations, which operate as regulated monopolies. However, Alberta's unbundled system makes private capital investments in generation and storage assets very attractive [21]. In Alberta, the wholesale power prices are set by a market run by the Alberta Electric System Operator (AESO), where:

1. Generators submit bids to the AESO on a per-minute basis that are then sorted from lowest to highest, creating a merit order [22].
2. The power offered at the lowest bid will be highest on the merit order and dispatched first, the power is then dispatched in accordance with the merit order and demand at the time [22].
3. At the end of each minute, the last price purchased from the merit order is recorded as the System Marginal Price (SMP) and the average price across each hour is calculated to determine the pool price [22].
4. This pool price is then utilized to determine the average price of power in the province and the rate formula that determines the amount consumers pay on their electricity bills [22].

Building upon this framework, wind and solar producers commonly submit bids to the power pool at lower prices compared to competitors utilizing alternative energy sources. This practice tends to reduce the System Marginal Price (SMP) and consequently lowers the overall pool price of power. When the pool price is lowest, which often occurs due to an abundance of wind and solar generation, it is the optimal time for the water collected in the Lower Reservoir to be pumped back up to the Upper Reservoir. An example of this concept is illustrated below in Figure 45 with the wind and solar generation in relation to the daily average pool price visualized for April 2023, using data from the AESO. Thus, from the predictive standpoint, wind and solar generation forecasts from the AESO could potentially be utilized to predict optimal times to pump and generate.

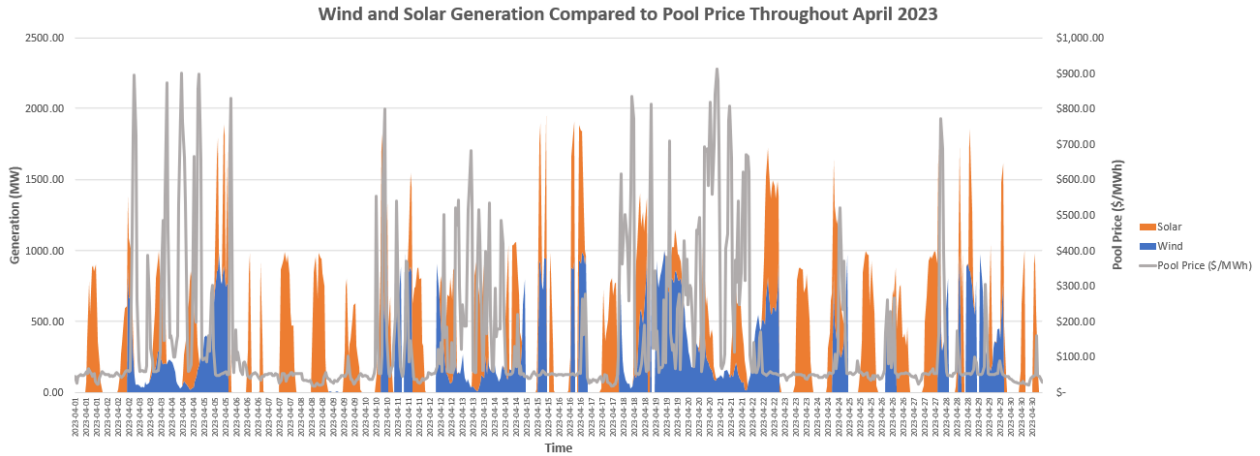


Figure 45 – Wind and Solar Generation as a Function of Pool Price (April 2023)

8.3 Production and Pumping Plan

The TM-REX will consist of a 320 MW pumped hydro energy storage system, a 100 MW green hydrogen electrolyzer, and a 100 MW offsite wind farm. It can be noted that with the primary energy source utilized for power generation in Alberta being natural gas, diversifying the energy mix with more renewable sources, such as hydro energy, will contribute to the decarbonization efforts of the sector.

1. The Upper Reservoir water level, sitting at an elevation of 1803 m, effectively acts as a large battery, providing power stably and reliably to the Albertan grid during periods of high demand and recharging during periods of low demand. Moreover, during periods when the renewable energy capacity is low (such as when the wind is not blowing and sunlight is unavailable), the TM-PHES will play a vital role in filling supply gaps and sustaining the presence of renewable energy in the electricity generation mix [21].
2. The ideal generation period for the TM-PHES is in the mornings and evenings when electricity demand and prices are typically high [21]. The water will be released via the surface pipes (penstock) and collected in the Lower Reservoir below (1509 m El., 294 m average head). As water passes through turbines in the powerhouse, electricity will be generated that will be sold into the power grid or used to power the green hydrogen facility.
3. When renewable energy is in excess and energy prices are low (around mid-day), the turbines can be reversed to pump the water collected in the Lower Reservoir back up to the Upper Reservoir. For the turbine to behave as a pump, electricity is supplied to the generator rather than the generator producing the electricity, resulting in the generator and turbine spinning in the opposite direction to effectively pump the water back up the penstock [23].
4. Powerlines are to be constructed to connect the PHES to the nearby electric grid to send and receive power, depending on the operation occurring. The intention is to have the PHES be at least partially

powered by the clean wind energy produced at the offsite wind farm (100 MW) to be constructed (the second element of the TM-REX). Powerlines will also connect the offsite wind and PHES facilities to the onsite green hydrogen electrolyzer production facility (the third element of the TM-REX).

8.4 Operating Schedule

The operations schedule was designed to help give the client insight into the best ways to operate the PHES to maximize revenue. Note, the turbine has a pumping volumetric flowrate that is 80% of the generating volumetric flow rate; therefore, it is necessary to maintain a 4:5 ratio of generating to pumping to sustain the equilibrium between the Upper and Lower Reservoirs (see Table 15) [21]. Although this design has the capacity to generate for 16 hours consecutively, it is expected that optimal operations will involve varied generation runtimes and will only infrequently make use of the entire 16-hour capacity as dictated by the energy market. In keeping with this, the following three options were explored to provide a point of reference for future operations:

Option 1: 10.66 hours of generation and 13.33 hours of pumping.

Option 2: 8 hours of generation and 10 hours of pumping.

Option 3: 6 hours of generating and 7.5 hours of pumping.

Table 15 - Turbine design discharges [1]

Operation Mode	Design Discharge (m³/s)
Turbine	123.4
Pump	98.0 (80% of generating flow)

For each of the three options, a maximum possible net revenue was calculated, based on the option's operating hours and assuming the facility was operating on standard hours every day of the year. For all maximum net revenue values, it was assumed that each option was generating during the most profitable hours each day and pumping during the least profitable hours. Based on the 2022 pool prices in Alberta all set prices were calculated by finding the most profitable average hours over the course of the year (see Table 16) [24].

Based on this table, the facility would be generating electricity during the most profitable hours, pumping water during the least profitable hours, and remaining on standby during middle hours if applicable. For the set hours, Option 1 would be generating from 11:20 am-10 pm and pumping from 10 pm-11:20 am. Option 2 would be generating from 1-9 pm, not operating between 6-7 am, 8-9 am, 10 am-1 pm, and 9-10 pm, and then pumping from 7-8 am, 9-10 am, and 10 pm-6 am. Lastly, Option 3 would be generating from 3-9 pm,

not operating from 6 am-3 pm, 9-10 pm, and 11-11:30 pm, and then pumping from 10-11 pm and 11:30 pm-6 am.

Table 16 – List of most profitable pool price hours in Alberta for 2022 [24]

Rank	2022 Pool Price Hours in Alberta	Average Daily Pool Price (\$/MWh)
1	5pm - 6pm	292.83
2	6pm - 7pm	260.88
3	4pm - 5pm	256.05
4	7pm - 8pm	246.58
5	8pm - 9pm	220.42
6	3pm - 4pm	211.85
7	2pm - 3pm	190.44
8	1pm - 2pm	188.39
9	noon - 1pm	176.48
10	9pm - 10pm	170.75
11	11am - noon	169.81
12	8am - 9am	150.38
13	6am - 7am	145.41
14	10am - 11am	145.29
15	7am - 8am	145.01
16	9am - 10am	132.48
17	11pm - midnight	131.94
18	10pm - 11pm	116.37
19	5am - 6am	103.98
20	midnight - 1am	95.21
21	1am - 2am	91.24
22	2am - 3am	87
23	4am - 5am	85.59
24	3am - 4am	84.91

The net revenue for all three options was calculated using pool price data in Alberta from 2022, so these values won't necessarily match year-to-year, but they provide a benchmark. Option 1 had a maximum possible net revenue of \$102 million and a net revenue of \$61.5 million with set operating hours. Option 2 had a maximum possible net revenue of \$154 million and a net revenue of \$69.9 million with set operating hours. Option 3 had a maximum possible net revenue of \$140 million and a net revenue of \$73.1 million with set operating hours (see Table 17). The net revenue of each option was also associated with a percent difference between generating and pumping pool prices. These differences went as follows for Option 1 the max difference was 19.15% and the set difference was 10.24%, for Option 2 the max difference was 29.28% and the set difference was 12.03%, and for Option 3 the max difference was 27.09% and the set difference

was 12.79%. Therefore, based on 2022 pool prices in Alberta, operating using Option 2, with 8 hours of generation to 10 hours of pumping, would be the most effective due to it having the highest maximum possible net revenue and a positive stable set net revenue. However, it's worth noting that TransAlta would also have the possibility to sign a power purchase agreement (PPA) with a power purchaser to have a set price for the electricity, regardless of the pool price, which could change the operating hours of the facility.

Table 17 – Net revenue and annual % difference of the maximum and set options.

Options (generating - pumping)	Net Revenue (\$)	Annual percent difference between generating and pumping pool prices (%)
Max Option 1 (10.66-13.33)	102,427,340.48	19.15
Set Option 1 (10.66-13.33)	61,563,407.47	10.24
Max Option 2 (8-10)	154,697,133.12	29.28
Set Option 2 (8-10)	69,986,023.06	12.03
Max Option 3 (6-7.5)	140,851,346.39	27.09
Set Option3 (6-7.5)	73,131,677,06	12.79

Additionally, the turbines are designed to generate 320 MW per hour, but it takes 378 MW per hour to pump the water back to the Upper Reservoir. Although it takes more energy to pump water back up, the facility will only be pumping water during the non-peak hours of the day and won't increase the demand on the grid during the peak hours. With set operating hours, it's also important to note the varying profitability of certain months throughout the year. During 2022 in Alberta, the months of August, July, and September were the most profitable, while March, April, and May were the least profitable (see Table 18). Additionally, during March and April, the projections of all three set options had the facility operating at negative net revenue. Therefore, without a PPA, it doesn't make financial sense to operate the facility year-round based on 2022 pool prices. With one of the main goals of the facility being to help manage electricity added to the grid, there might be times of the year when the facility will be operating at maximum capacity for all 16 hours and other times when the facility won't be operating at all due to a lower need for electricity.

Table 18 – Monthly % difference between generating and pumping pool prices for Alberta in 2022

Max Option 1		Set Option 1		Max Option 2		Set Option 2		Max Option 3		Set Option 3	
Month	% Difference										
8	37.67	8	44.57	8	52.06	8	39.16	8	44.62	8	31.06
12	30.77	9	28.17	9	45.31	7	26.28	9	40.78	9	23.02
11	26.97	7	27.39	7	33.84	9	25.14	10	31.91	7	22.85
9	26.63	6	12.04	10	33.80	6	12.93	7	31.12	2	13.93
2	25.31	2	9.69	12	31.08	2	12.38	11	29.18	6	11.68
1	20.96	12	6.08	11	30.91	12	8.41	12	28.27	1	9.39
7	17.54	1	5.70	6	26.78	1	7.17	6	25.01	11	9.33
6	14.59	11	4.73	2	26.19	11	6.26	2	24.81	12	9.28
10	11.94	5	2.00	1	22.26	5	3.11	1	21.55	10	8.42
5	7.43	10	1.13	5	19.86	10	2.50	5	19.15	5	4.39
3	6.10	3	-7.40	4	16.67	3	-4.05	4	16.26	3	-1.06
4	4.40	4	-11.56	3	12.40	4	-8.59	3	12.23	4	-4.17

9 Mitigation and Adaptation

By implementing a range of mitigation and adaptation strategies, pumped hydro energy storage systems can proficiently handle excess water during flood occurrences and reduce evaporation during drought periods. It is crucial to prioritize risk mitigation for the project infrastructure and downstream facilities, including neighbouring communities. This approach ensures the ongoing dependability and robustness of the system against the backdrop of climate change and variability. Several of these strategies are explored generally below, and recommendations are made as to which are most compatible with the TM-PHES.

9.1 Extreme Drought Events

9.1.1 Surface Covers

Installing floating covers or geomembranes on the surface of the reservoir can significantly reduce evaporation rates by creating a physical barrier between the water surface and the atmosphere. These covers can be made from materials such as plastic, rubber, or geotextiles and are effective at minimizing water loss due to evaporation. Options such as Shade Balls or Aquacaps can be considered but upfront price, the frequency of high evaporation times during the year, and constant water level fluctuations need to be investigated further. Shade balls are plastic eco-friendly balls that could be used in lakes, ponds, streams, and dams as shown in Figure 46.



Figure 46 – Shade Balls [25]

The Department of Water and Power (LADWP) first implemented shade balls in California, specifically in Los Angeles, in 2011. Their primary purpose was to mitigate evaporation and block UV rays, thus preventing the formation of harmful organisms, algae, and carcinogens. In a study conducted in the Nehru Pond located in the Namakkal district of India, researchers evaluated the effectiveness of using shade balls to decrease evaporation from the water surface. The study utilized 4-inch black balls made from high-density polyethylene (HDPE) and carbon black to cover the reservoir. Results indicated that the shade balls led to a reduction in reservoir evaporation by 43-45% [25].

Floating discs (Aquacaps), as shown in Figure 47, are round, dome-shaped floating modules of about 1.1 m in diameter and made up of polypropylene and high-density polyethylene (HDPE), which both satisfy food grade standards.



Figure 47 – Aquacaps on Reservoir [26]

A study was carried out with a laboratory scale to estimate the efficiency of floating elements in reducing evaporative losses from water reservoirs. The Aquacaps were shown to cover 91% of the water surface. The influence of wind and shortwave radiation on the evaporation rates from water surface was considered in the experiment. The results show that evaporation from the covered reservoir was reduced by about 80% relative to the uncovered water surface. However, changes in cover color did not significantly modify the evaporative rate [26].

9.1.2 Shading

Planting vegetation or installing shade structures around the reservoir perimeter can help reduce evaporation by blocking direct sunlight and reducing the temperature of the water surface. This natural shading can be particularly effective in areas with high levels of solar radiation and can also provide additional ecological benefits such as habitat restoration and erosion control with the implementation of trees or shrubs around the perimeter of the reservoir. Natural versions of the Aquacaps could be investigated as well, such a lily pads or similar vegetation. However, this idea was abandoned due to Tent Mountain's climate, as floating plants would most likely die during the winter months. Some shading is naturally provided by the area the TM-PHES reservoirs are located. The Upper Reservoir sees shading from its steep banks on the East, South, and especially West sides. While the Lower Reservoir is situated in a natural valley, that of which contains many trees on all the shores of the reservoir.

9.1.3 Windbreaks

Constructing windbreaks or wind barriers along the shoreline of the reservoir can help reduce wind-induced turbulence and, therefore, evaporation. Windbreaks can be made from natural materials such as trees, shrubs, or grasses, or from man-made structures on the reservoir such as fences or barriers and are designed to intercept and deflect wind currents away from the water surface. Furthermore, implementing windbreaks near the reservoirs would prevent moisture levels of the nearby soil from decreasing. This option would be very economical, however could be ignored as the Upper Reservoir currently sits in a fairly protected location from high wind speeds. Similarly, the Lower Reservoir also lies in a natural valley with trees serving as a natural windbreak.

9.1.4 Chemical Treatments

Applying chemical treatments such as monolayer films or evaporation retardants to the water surface can form a thin, insoluble layer that inhibits evaporation. These treatments work by reducing surface tension and suppressing the diffusion of water molecules into the atmosphere, effectively slowing down the rate of evaporation. Additionally, monolayer films can reduce the heat absorbed on the water surface by reflecting sunlight. This strategy is a possible alternative; however, the main concern of this strategy is the containment of these films to the reservoir. For instance, if these films were in the outflow of the facility, they could affect downstream runoff.

9.1.5 Water Level Management

Adjusting the water level of the reservoir to minimize exposed surface area during periods of high evaporation can help reduce water loss. Through the implementation of a drought prevention limiting water level (DPLWL), operators can mitigate the effects of drought events on reservoir operations. The DPLWL can be developed after considering drought conditions based on long term hydrological and meteoritical

data. This water level acts as the minimum water level during extreme drought cases to ensure reliable resource utilization. By strategically controlling water levels based on seasonal variations in evaporation rates and water demand, operators can optimize reservoir storage capacity while minimizing evaporative losses.

9.1.6 Engineered Features

Incorporating engineered features such as baffles, berms, or contouring within the reservoir can help create sheltered areas and reduce wind-induced wave action, thereby decreasing evaporation rates. These engineering interventions are designed to modify the hydrodynamics of the reservoir and minimize water loss due to surface turbulence.

9.2 Extreme Excess Water Events

9.2.1 Spillway Management

Ensuring that spillways are properly designed and maintained to safely discharge excess water during flood events is crucial. Regular inspection and maintenance of spillway infrastructure, including gates, channels, and control structures, can help prevent overflow and mitigate the risk of dam failure [27].

9.2.2 Emergency Preparedness

Developing and implementing comprehensive emergency response plans for flood events can help minimize the impact of excess water on pumped hydro systems. This program includes establishing protocols for monitoring weather forecasts, coordinating with local authorities, and activating emergency response teams to manage flood risks and ensure the safety of personnel and surrounding communities.

9.2.3 Reservoir Capacity Expansion

Investing in infrastructure upgrades to increase the storage capacity of reservoirs can help accommodate surplus water during periods of high precipitation. This development may involve constructing additional reservoirs, expanding existing storage facilities, or implementing temporary water storage solutions such as inflatable dams or retention ponds to capture and retain excess runoff.

9.2.4 Managed Release

Implementing managed release strategies to gradually discharge excess water from reservoirs during flood events can help prevent sudden surges in downstream flows and mitigate the risk of downstream flooding. By carefully controlling discharge rates and coordinating with downstream water users and stakeholders, operators can optimize water management and minimize adverse impacts on ecosystems and communities.

9.2.5 Floodplain Management

Implementing floodplain management measures such as vegetation restoration, wetland preservation, and land use planning can help mitigate the impact of flood events on pumped hydro systems. By preserving natural floodplains and enhancing their capacity to absorb and attenuate floodwaters, operators can reduce the risk of reservoir inundation and minimize damage to infrastructure and surrounding areas.

9.2.6 Sedimentation Control

Implementing sedimentation control measures such as erosion control structures, sediment traps, and sedimentation basins can help minimize the accumulation of sediment in reservoirs during high precipitation events. Dredging can also be useful to optimize long-term storage.

9.3 Recommendations

9.3.1 Drought

To increase the drought resilience of the PHES, it is recommended that physical surface cover strategies such as shade balls or Aquacaps be implemented. These are chosen, and other options rejected, for the following reasons:

1. Water level management is not feasible due to the nature of the PHES and its dynamic water levels.
2. The constantly dynamic reservoir water levels will not result in potential ground contamination if physical barriers become beached, as would potentially occur with a chemical surface cover.
3. They produce proven substantial reductions in evaporation rates.
4. Physical surface cover strategies are much more cost-effective than engineered baffles or other structural solutions.
5. The Upper Reservoir is already shaded to a great extent, as the peak of Tent Mountain is south of it and blocks a great deal of direct sunlight. Especially at its lower water levels, the Upper Reservoir will also find significant wind relief from the topography of the pit in which it lies. The Lower Reservoir is surrounded by shade- and wind cover-providing trees.

9.3.2 Flood

Spillway management, emergency preparedness, managed release are recommended to be prioritized for flood mitigation at the PHES. Other strategies are conditionally recommended as well, for the reasons explained below:

1. Spillway management, emergency preparedness, and managed release are inextricably linked and are the foundation of dam safety, as mandated by the CDA.
2. The high slope and general dearth of natural wetlands in the Crowsnest Pass pose challenges to floodplain management. However, Crowsnest and Emerald Lakes, downstream of the project but

upstream of the municipality, is expected to provide some attenuation of large flood events. These features provide natural floodplain management.

3. Sedimentation control is not expected to be a concern for either reservoir due to their small catchment areas and the associated limited overland flow speeds and potential erosion. Conversely, the soils in the catchment are generally coarse grained, increasing their resistance to erosion and subsequent sedimentation of the reservoirs. Periodic bathymetric surveys are recommended to ensure that these expectations are met.
4. While the intent of this design is to provide long-term robustness and resilience in the face of a changing climate, it is acknowledged the ability of science to accurately project future climates is limited. In light of this, reservoir capacity expansion or spillway redesign may be required in the future, should the PMP and associated PMF estimates increase significantly.

10 Conclusion

Ultimately, this feasibility study on the economic, climate, and operational analyses of the TM-PHES project support the resilience and viability of the proposed design amidst evolving environmental dynamics. Therefore, it is recommended that the TM-PHES project advances to the next phase of development, which involves detailed component design, increased stakeholder engagement, and a final investment decision. Table 19 summarizes the final design components and recommendations produced throughout this capstone feasibility investigation of the TM-PHES project.

Table 19 – Design Summary (Fall and Winter Terms)

Parameter	Value
Recommended Operation Plan – Option 2	8-hour production, 10-hours pumping
Projected Net Revenue – Option 2 Set Operations 2022	\$ 69,986,023.06
Recommended Drought Mitigation Strategy	Physical surface covers
Recommended Flood Mitigation Strategies	Spillway, emergency preparedness and managed release
Upper Reservoir	
Drainage Area (km ²)	1.311 km ²
Live Storage Volume (million m ³)	7.107 E06 m ³
NMOL (masl)	1803.3 masl
NMOL Reservoir Footprint (km ²)	0.2758 km ²
Dead Storage Volume (million m ³)	2.045 E06 m ³
DSL (masl)	1760.0 masl
Seepage Reduction Strategy	Grout curtain and grouted cutoff wall
Containment Structure Minimum Elevation (masl)	1806.8 masl
Lower Reservoir	
Drainage Area (km ²)	5.557 km ²
Live Storage Volume (million m ³)	7.107 E06 m ³
NMOL (masl)	1509.0 masl
Dead Storage Volume (million m ³)	0.5268 E06 m ³
DSL (masl)	1480.0 masl
South Dam	
Dam Crest Elevation	1513.0 masl
Dam Type	Asphalt core rockfill embankment
Spillway Crest Elevation	1509.3 masl
Spillway Width	15 m
Spillway Type	Broad crested
IDF Peak Flow	130.4 m ³ /s
Riparian Outlet Flow Capacity	0.0-1.0 m ³ /s
North Dam	
Dam Crest Elevation	1512.5 masl
Dam Type	Asphalt core rockfill embankment

This design report has been provided for the exclusive use of TransAlta, Evolve Power, and the Schulich School of Engineering. All designs have been developed using the best information available at the time of writing. This report does not provide any guarantees that are not explicitly written herein. Next steps for the continuation of this project could include:

- Analysis of recently installed hydrometric gauges at the site.
- Updates to the hydrological model calibration upon receipt of new information.
- Continued testing of geological site conditions.
- Detailed design and ultimately construction of the project.

We are pleased to have contributed to the Pre-Feasibility Studies of the Tent Mountain Pumped Hydro Energy Storage Project.

Sincerely,

HydroVault Engineering

Mr. Andrew Szjoka, P.Eng

Specialist, Hydro, Growth,
TransAlta Corporation

Alain Pietroniro, P.Eng, PhD

Professor, Department of Civil Engineering,
University of Calgary
alain.pietroniro@ucalgary.ca

Simon Papalexiou, PhD

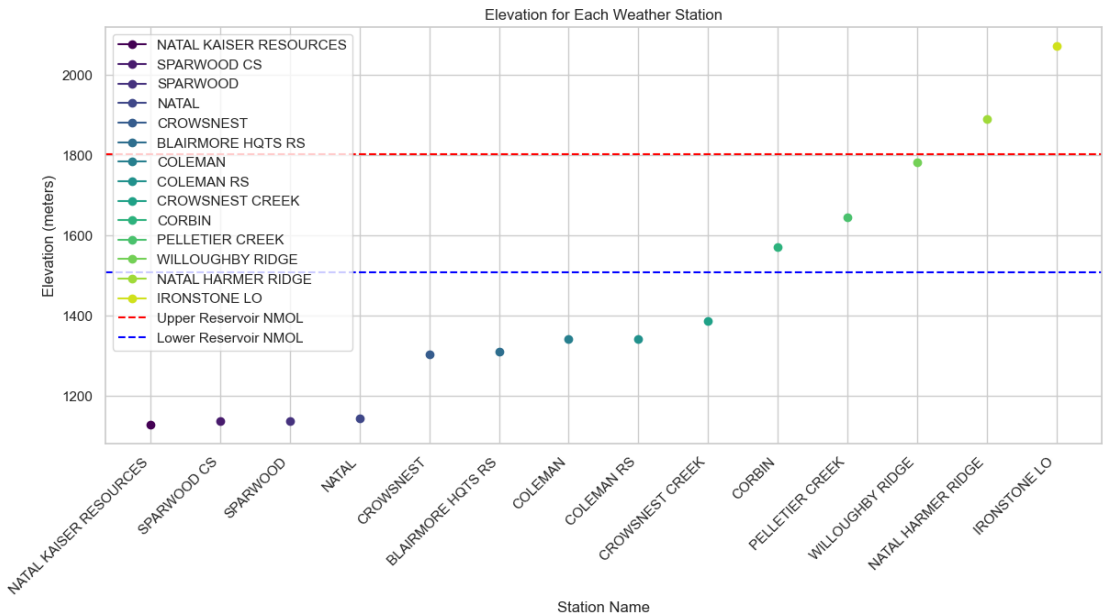
Professor, Department of Civil Engineering,
University of Calgary
simon.papalexiou@ucalgary.ca

11 References

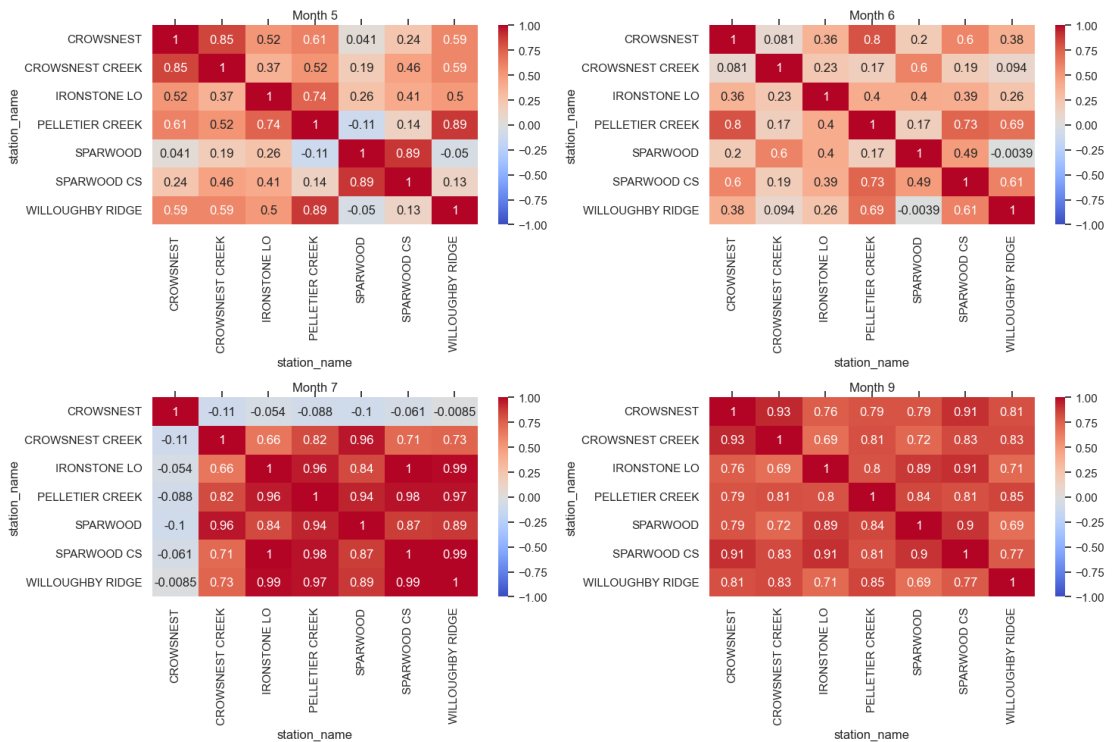
1. Hatch, "Montem Resources Tent Mountain PSP Prefeasibility: Hydrological Assessment," TransAlta, 2022. [Online].
2. Hatch, "Montem Resources Tent Mountain PSP Prefeasibility: Geological and Geomechanical Assessment," TransAlta, 2022. [Online].
3. Matrix, "Tent Mountain Hydrology Basis," Montem, 2019. [Online].
4. Guoqiang T., "EMDNA: an Ensemble Meteorological Dataset for North America." Earth System Science Data, 2021. doi:10.5194/essd-13-3337-2021.
5. O'Neill, B. C., "The Scenario Model Intercomparison Project (ScenarioMIP) for CMIP6", European Geosciences Union, 2016. doi:10.5194/gmd-9-3461-2016.
6. Eyring, V., "Overview of the Coupled Model Intercomparison Project Phase 6 (CMIP6) experimental design and organization", European Geosciences Union, 2016. doi:10.5194/gmd-9-1937-2016.
7. Alberta Environment and Sustainable Resource Development, Evaporation and Evapotranspiration in Alberta, <https://agriculture.alberta.ca/acis/docs/mortons/mortons-evaporation-estimates.pdf>. Accessed: Feb. 2024.
8. Linacre, E. T. (1977). A simple formula for estimating evaporation rates in various climates, using temperature data alone. *Agricultural Meteorology*, 18, 409–424.
9. Q. Li, Z. Jia, and Y. Zhao, "Laboratory evaluation of hydraulic conductivity and chemical compatibility of bentonite slurry for grouting walls," *Environ. Earth Sci.*, vol. 80, no. 569, p. 1, Aug. 18, 2021.
10. CivilGEO. "Precipitation Type (SCS Storm)." CivilGEO Knowledge Base. [Online]. Available: <https://knowledge.civilgeo.com/kb/precipitation-type-scs-storm/>. Accessed: March 8, 2024.
11. U.S. Department of Agriculture, "NRCS Part 650 Engineering Field Handbook, National Engineering Handbook, Chapter 2 Estimating Runoff Volume and Peak Discharge 210-650-H, 2nd Ed.," Feb. 2021. Available: <https://directives.sc.egov.usda.gov/46253.wba>. Accessed: Mar 3, 2024.
12. Climate Action, "Climate Action Fast Facts" United Nations, 2024.
<https://www.un.org/en/climatechange/science/key-findings>
13. C. G. Surfleet and D. Tullos, "Variability in effect of climate change on rain-on-snow peak flow events in a temperate climate," in *Journal of Hydrology*, vol. 479, pp. 24-34, 2013, ISSN 0022-1694. [Online]. Available: <https://doi.org/10.1016/j.jhydrol.2012.11.021>. Accessed: Mar. 15, 2024.
14. Alberta Environment and Parks, "CDA Classification Ratings Dams - April 2016," Government of Alberta, 2016. [Online]. Available: <https://open.alberta.ca/dataset/e598d71f-9baa-4f33-98d1-2417f9bf7d93/resource/08db72bd-6fef-48d4-8c62-72c33c44d9a3/download/cda-classificationratingsdams-apr2016.pdf>. Accessed: Jan. 29, 2024.
15. Hopkinson, R. F., "Point Probable Maximum Precipitation for the Prairie Provinces", Atmospheric & Hydrologic Sciences Division, Atmospheric Environment Branch, Government of Canada, 1999. [Online]. Available: https://publications.gc.ca/collections/collection_2020/eccc/en56/En56-268-1999-eng.pdf. Accessed: Mar 3, 2024.
16. British Columbia Ministry of Environment and Climate Change Strategy, "Bulletin 2020-3-PMP, British Columbia Extreme Flood Project Probable Maximum Precipitation Guidelines – Technical Report." Available: https://a100.gov.bc.ca/pub/acat/documents/r59232/Bulletin_2020_3_PMP_Technical_Report_1625625266636_A9BFA45679.pdf. Accessed: Mar 3, 2024.
17. J. P. Verschuren and L. Wojtiw, "Estimate of the maximum probable precipitation for Alberta river basins," University of Alberta, June 1980. Available: <https://era.library.ualberta.ca/items/34487031-1dda-46c1-b4c7-894503256f3d/view/06387d34-2bb0-4dce-8b63-b730f9046155/Verschuren-201980.pdf>. Accessed: March 6, 2024.
18. R.F. Hopkinson, "Point Probable Maximum Precipitation for the Prairie Provinces," Atmospheric and Hydrologic Sciences Division, Prairie Section, Atmospheric Environment Branch, Environment Canada, July 1999.

19. C. Walford, "Probable Maximum Flood Willow Creek at Chain Lakes Reservoir," Alberta Environment, Dam Safety and Water Projects Branch, March 2002.
20. Bow River Basin Council, "Conditions and Indicators," Bow River Basin Council, [Online]. Available: <https://ecr.brbc.ab.ca/>. Accessed: Jan. 29, 2024.
21. Hatch, "Montem Resources Pre-Feasibility Report" TransAlta, 2022. [Online].
22. AESO, "Understanding the market," AESO, <https://www.aeso.ca/market/market-participation/understanding-the-market/> Accessed: Jan. 18, 2024.
23. A. Blakers, A review of pumped hydro energy storage, <https://iopscience.iop.org/article/10.1088/2516-1083/abeb5b/pdf> [Accessed Jan. 20, 2024].
24. AESO, "Hourly Metered Volumes and Pool Price and AIL data," Hourly metered volumes and pool price and AIL data 2010 to 2023, <https://www.aeso.ca/market/market-and-system-reporting/data-requests/hourly-metered-volumes-and-pool-price-and-ail-data-2010-to-2023/>.
25. P. V. Kumar, S. V. Kumar, P. S. Kumar, S. Subash, and M. Sivaraja, "Reduction of Water Vapour by Using Shade Balls," International Journal of Engineering and Techniques, vol. 4, no. 2, pp. 596, Mar-Apr 2018. ISSN: 2395-1303. Available: <http://www.ijetjournal.org>
26. M. Aminzadeh, P. Lehmann, and D. Or, "Evaporation suppression and energy balance of water reservoirs covered with self-assembling floating elements," Hydrol. Earth Syst. Sci., vol. 22, pp. 4015–4032, 2018. [Online]. Available: <https://doi.org/10.5194/hess-22-4015-2018>
27. Y. Sharrab, M. El-shebli, M. Eljinini et al., "Extreme Weather and hydropower System: Production, Resilience, and Sustainability," May 2023, PREPRINT (Version 1) available at Research Square, Available: <https://doi.org/10.21203/rs.3.rs-2756965/v1>. [Accessed: April 2, 2024].

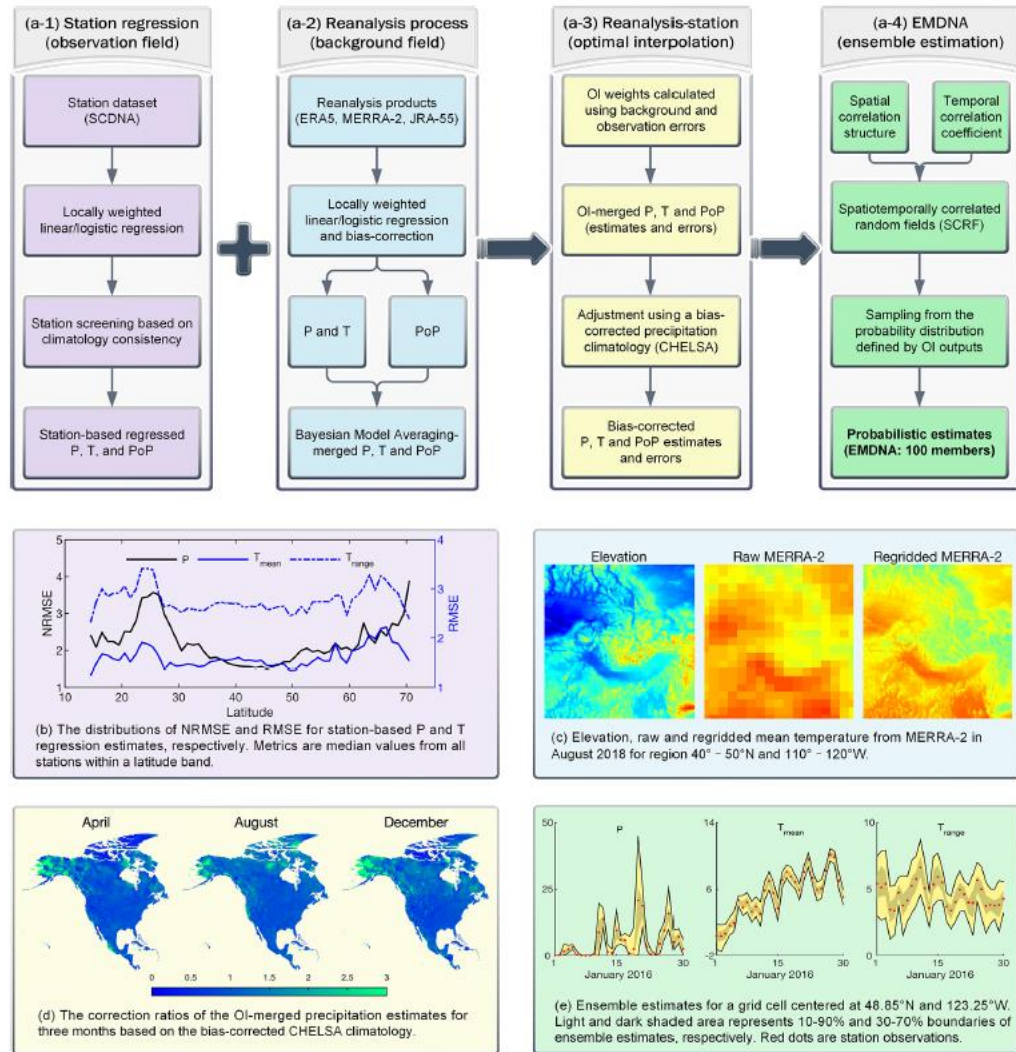
12 Appendix A



Appendix A Figure 1 - Elevation of ECCC Weather Stations



Appendix A Figure 2 - Monthly Correlation Stations with 5+ Years Overlapping Data



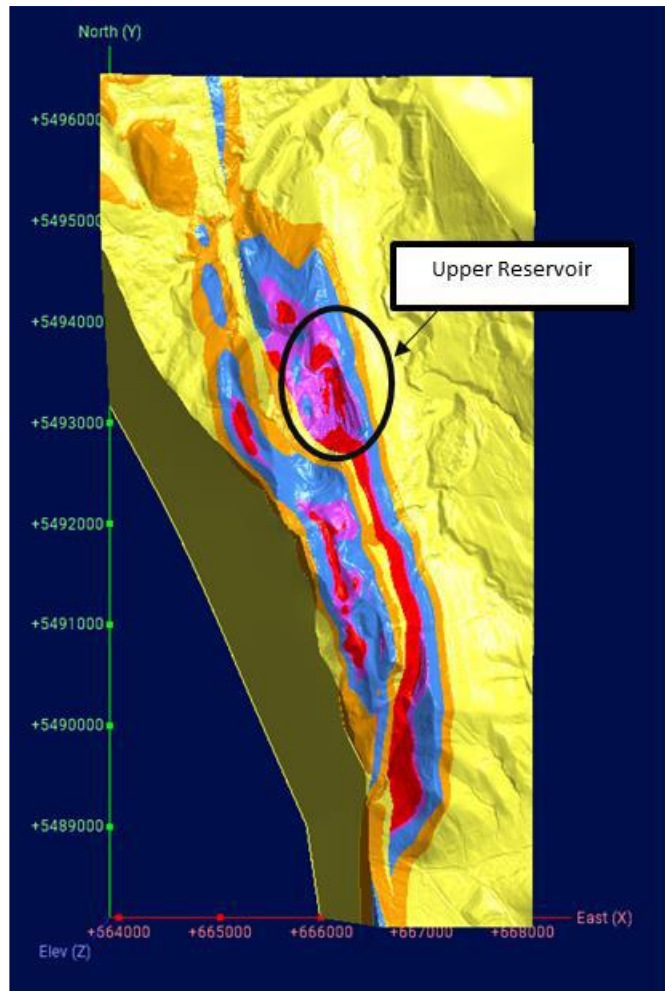
Appendix A Figure 3 - EMDNA Data Creation Methodology and Example [4]

Date	tmean	precip
1979-01-01	-24.9175	2.7711
1979-01-02	-21.8485	0.7097
1979-01-03	-22.255	0.11758
1979-01-04	-23.5575	0
1979-01-05	-21.4305	0.000486
1979-01-06	-20.391	0.17038
1979-01-07	-19.7835	0
1979-01-08	-18.441	0.048385
1979-01-09	-20.2805	0.24556
1979-01-10	-19.301	7.2842
1979-01-11	-18.6185	2.1399
1979-01-12	-19.1065	5.839
1979-01-13	-20.5515	3.151
1979-01-14	-22.4245	0.4275
1979-01-15	-20.669	0.42561

Appendix A Figure 4 - Sample of EMDNA Historic Data Tent Mountain

1	Date	precip	tmean	trange	evaporation
31382	2100-12-01	0	-8.87994194	9.102655411	0
31383	2100-12-02	1.216642261	-3.833276033	10.90546513	0
31384	2100-12-03	4.675139427	1.482396483	7.257365227	1.216553731
31385	2100-12-04	6.464138031	1.937180758	4.879348278	1.074335653
31386	2100-12-05	0.806223392	-1.717839956	2.679658413	0
31387	2100-12-06	1.125826955	-3.759391308	3.706907272	0
31388	2100-12-07	2.311118126	-7.365489006	4.945633411	0
31389	2100-12-08	0.873017073	-11.9424057	6.582952499	0
31390	2100-12-09	0	-9.811601639	13.30204105	0
31391	2100-12-10	0	-7.965694427	9.225187302	0
31392	2100-12-11	0.823690414	-6.28200531	8.801876068	0
31393	2100-12-12	0.783826828	-5.612553596	6.350090504	0
31394	2100-12-13	1.106826067	-5.200883865	5.449372292	0
31395	2100-12-14	3.621826172	-2.727208853	7.26286459	0
31396	2100-12-15	0.901927114	-1.431261778	5.129338741	0
31397	2100-12-16	0.993716955	0.080272913	3.426987648	0.534501191
31398	2100-12-17	2.254567623	0.446261108	3.639867306	0.631573659
31399	2100-12-18	2.811658621	0.997036278	3.420751572	0.725065866
31400	2100-12-19	2.453140497	-0.673957765	4.740801334	0
31401	2100-12-20	0.867902994	-1.325927019	5.514249325	0
31402	2100-12-21	0.961261153	-2.156065226	5.931359768	0
31403	2100-12-22	0.739236832	-6.204023361	7.547644138	0
31404	2100-12-23	0	-6.771417618	10.91883278	0
31405	2100-12-24	0	-7.148288727	8.796895981	0
31406	2100-12-25	1.040809751	-6.625031471	4.966884613	0
31407	2100-12-26	3.303374529	-7.094494343	3.212327003	0
31408	2100-12-27	0	-12.08595181	8.691358566	0
31409	2100-12-28	1.996977925	-8.53701973	5.036176205	0
31410	2100-12-29	4.419458389	-6.990920544	8.16397953	0
31411	2100-12-30	0	-6.893649578	8.394124031	0
31412	2100-12-31	0	-2.784130573	5.355337143	0

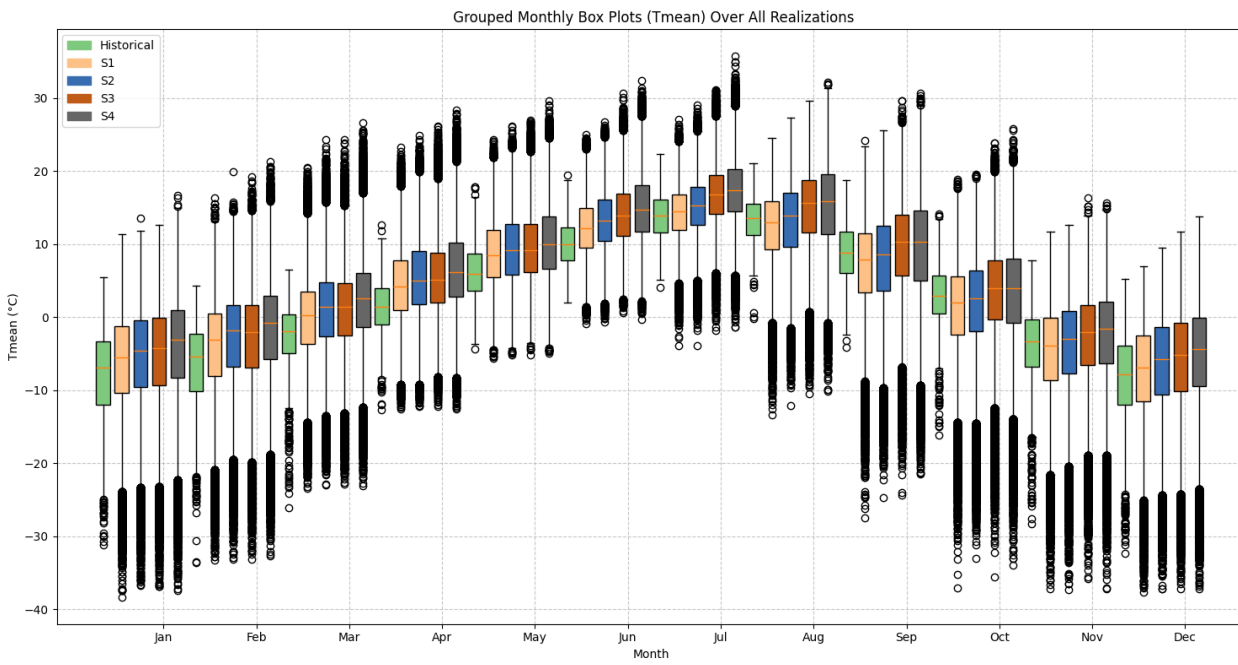
Appendix A Figure 5 - Sample Scenario Output Data with Calculated Evaporation



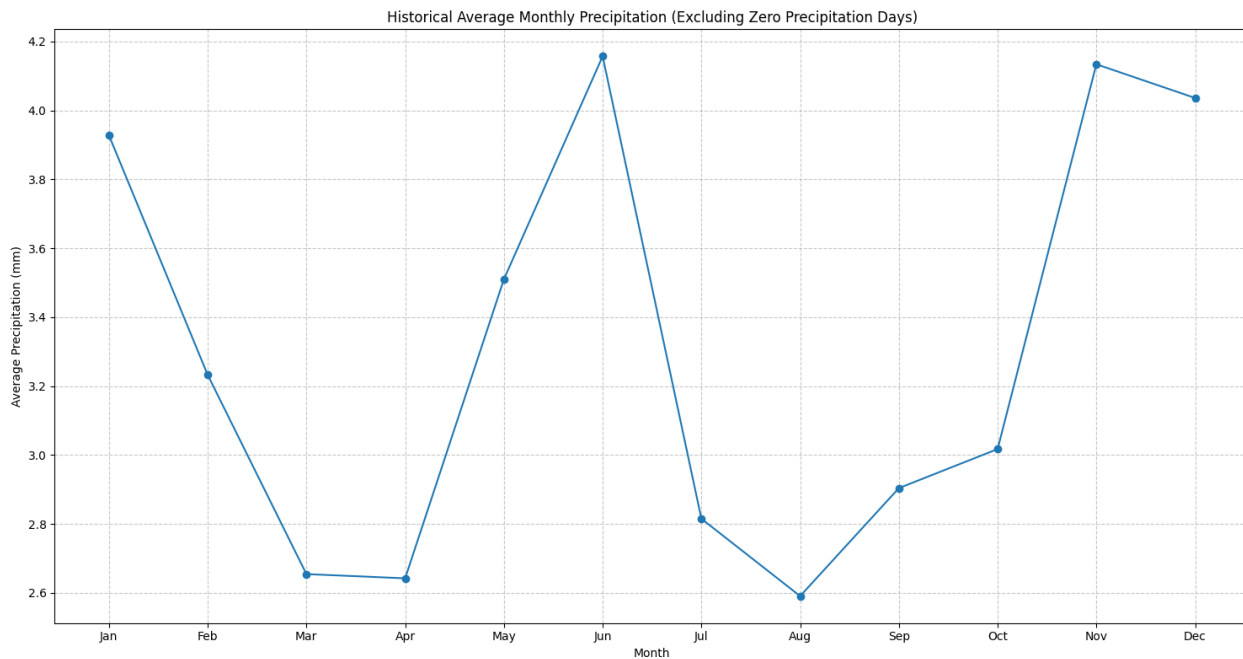
Appendix A Figure 6 - Overall Leapfrog Model of the Tent Mountain Site (Plan View)

1	date	time	q_in_uppi	stor_uppe	elev_uppe	q_out_upi	q_in_lowe	stor_lowe	elev_lowe	q_out_low	q_total
31382	01Dec.210	0:00	0	9148.786	1803.295	0.0014	0	7755.338	1509.002	0.01044	0
31383	02Dec.210	0:00	0	9148.665	1803.294	0.0014	0	7755.338	1509.002	0.01044	0
31384	03Dec.210	0:00	0	9148.544	1803.294	0.0014	0	7755.338	1509.002	0.01044	0
31385	04Dec.210	0:00	0.0168	9149.149	1803.296	0.0014	0.02803	7755.511	1509.003	0.01358	0.04483
31386	05Dec.210	0:00	0.00633	9150.027	1803.299	0.0014	0.01056	7755.776	1509.003	0.01889	0.01689
31387	06Dec.210	0:00	0.00138	9150.237	1803.3	0.00146	0.0023	7755.179	1509.002	0.00779	0.00368
31388	07Dec.210	0:00	0.00027	9150.185	1803.3	0.0014	0.00046	7754.831	1509.001	0.00302	0.00073
31389	08Dec.210	0:00	0.00002	9150.076	1803.3	0.0014	0.00003	7754.664	1509.001	0.00132	0.00005
31390	09Dec.210	0:00	0	9149.956	1803.299	0.0014	0	7754.58	1509	0.00066	0
31391	10Dec.210	0:00	0	9149.835	1803.299	0.0014	0	7754.535	1509	0.00038	0
31392	11Dec.210	0:00	0	9149.714	1803.298	0.0014	0	7754.508	1509	0.00023	0
31393	12Dec.210	0:00	0	9149.593	1803.298	0.0014	0	7754.492	1509	0.00016	0
31394	13Dec.210	0:00	0	9149.472	1803.297	0.0014	0	7754.48	1509	0.00011	0
31395	14Dec.210	0:00	0	9149.351	1803.297	0.0014	0	7754.472	1509	0.00008	0
31396	15Dec.210	0:00	0	9149.23	1803.296	0.0014	0	7754.466	1509	0.00006	0
31397	16Dec.210	0:00	0	9149.109	1803.296	0.0014	0	7754.461	1509	0.00005	0
31398	17Dec.210	0:00	0.00437	9149.177	1803.296	0.0014	0.00729	7754.702	1509.001	0.00167	0.01166
31399	18Dec.210	0:00	0.00838	9149.607	1803.298	0.0014	0.01399	7755.199	1509.002	0.00811	0.02237
31400	19Dec.210	0:00	0.00646	9150.127	1803.3	0.0014	0.01078	7755.412	1509.002	0.01173	0.01724
31401	20Dec.210	0:00	0.00162	9150.324	1803.3	0.00214	0.00271	7755.162	1509.002	0.00753	0.00433
31402	21Dec.210	0:00	0.00031	9150.249	1803.3	0.00152	0.00052	7754.841	1509.001	0.00313	0.00083
31403	22Dec.210	0:00	0.00005	9150.138	1803.3	0.0014	0.00008	7754.671	1509.001	0.00139	0.00013
31404	23Dec.210	0:00	0	9150.019	1803.299	0.0014	0	7754.585	1509	0.00007	0
31405	24Dec.210	0:00	0	9149.898	1803.299	0.0014	0	7754.538	1509	0.00039	0
31406	25Dec.210	0:00	0	9149.777	1803.298	0.0014	0	7754.51	1509	0.00024	0
31407	26Dec.210	0:00	0	9149.656	1803.298	0.0014	0	7754.493	1509	0.00016	0
31408	27Dec.210	0:00	0	9149.535	1803.298	0.0014	0	7754.481	1509	0.00011	0
31409	28Dec.210	0:00	0	9149.414	1803.297	0.0014	0	7754.472	1509	0.00008	0
31410	29Dec.210	0:00	0	9149.293	1803.297	0.0014	0	7754.466	1509	0.00006	0
31411	30Dec.210	0:00	0	9149.172	1803.296	0.0014	0	7754.461	1509	0.00005	0
31412	31Dec.210	0:00	0	9149.052	1803.296	0.0014	0	7754.458	1509	0.00004	0

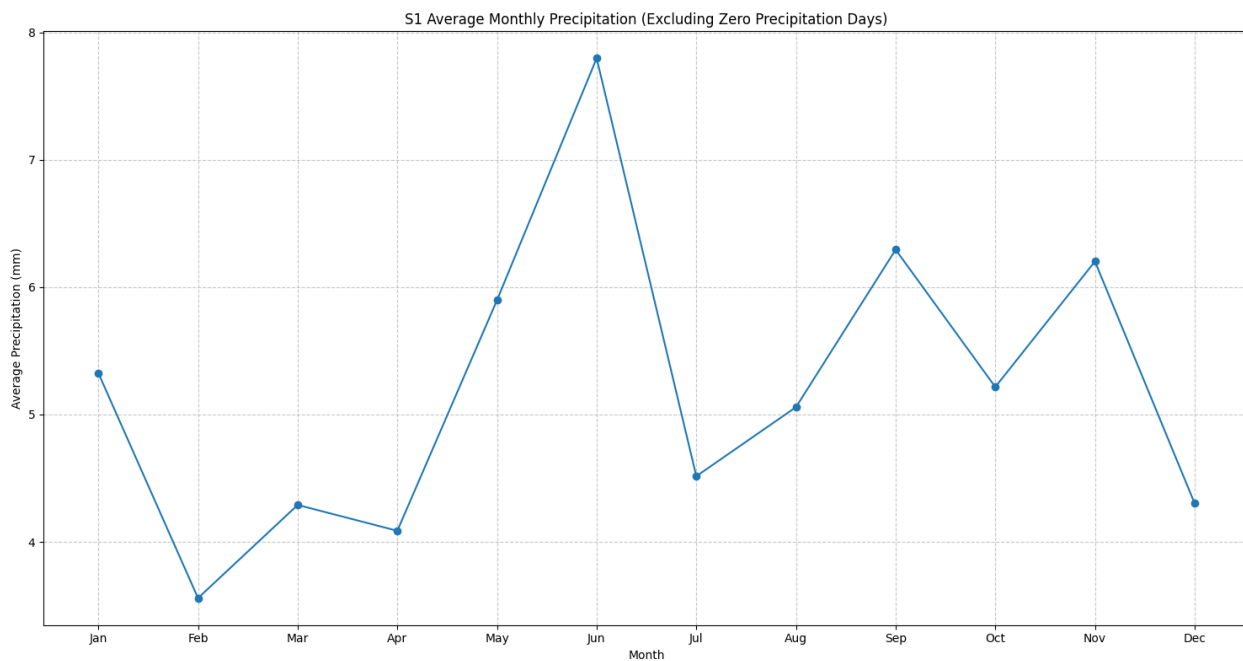
Appendix A Figure 7 - Sample HEC-HMS Output



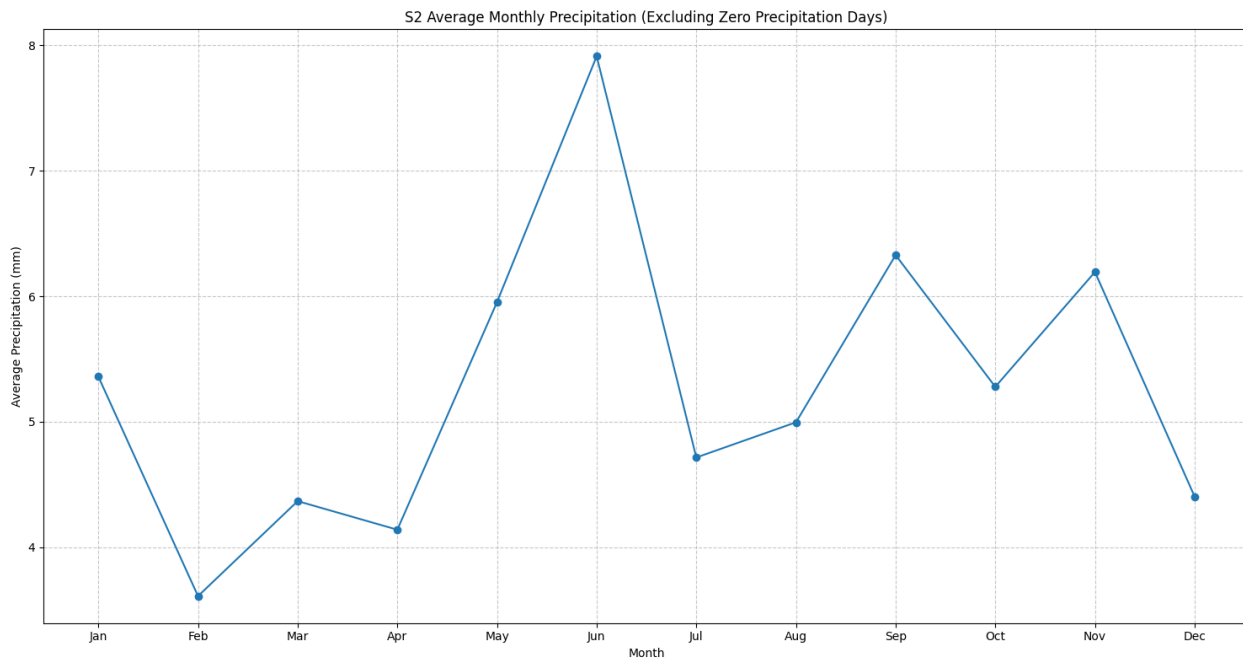
Appendix A Figure 8 -Box Plot of Monthly Temperature for all Scenarios with Outliers



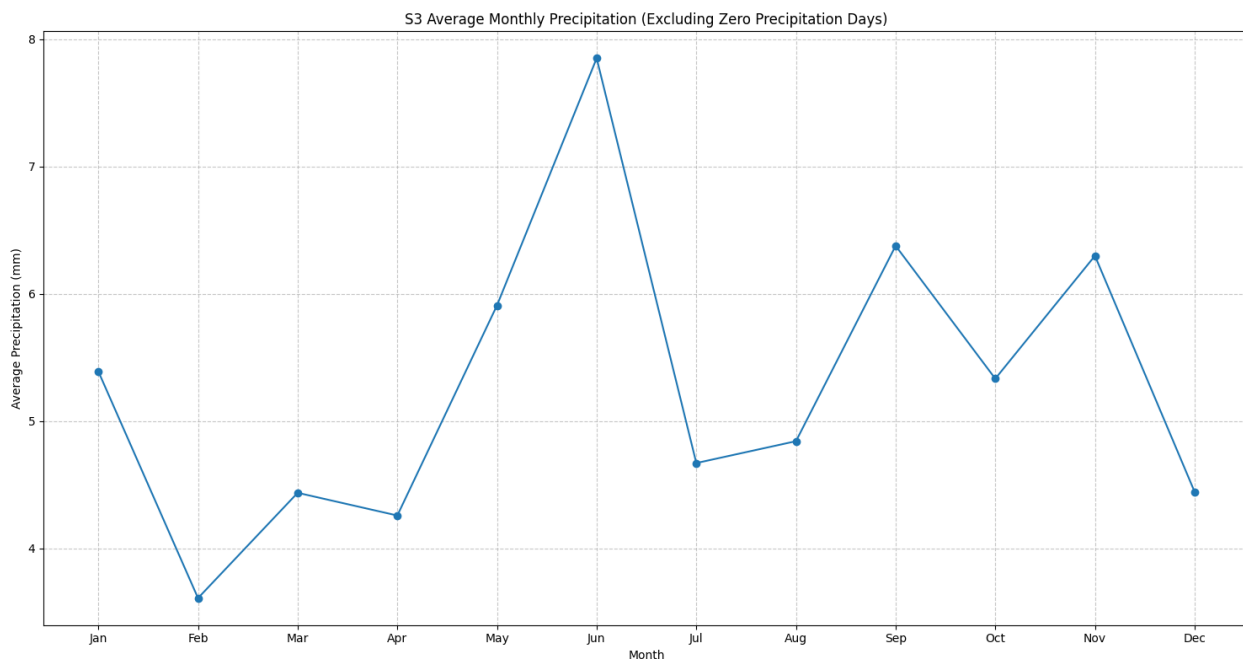
Appendix A Figure 9 - Average Historical Monthly Precipitation Excluding 0 Precipitation Days



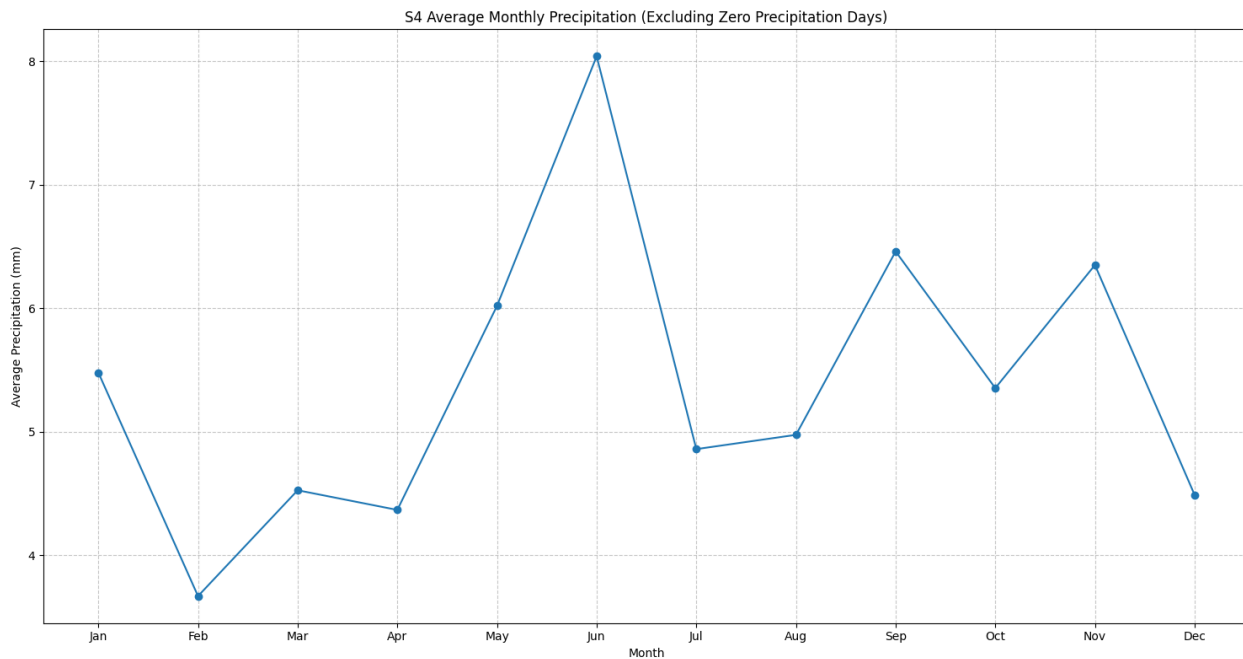
Appendix A Figure 10 - Average Projected S1 Daily Precipitation Excluding 0 Precipitation Days



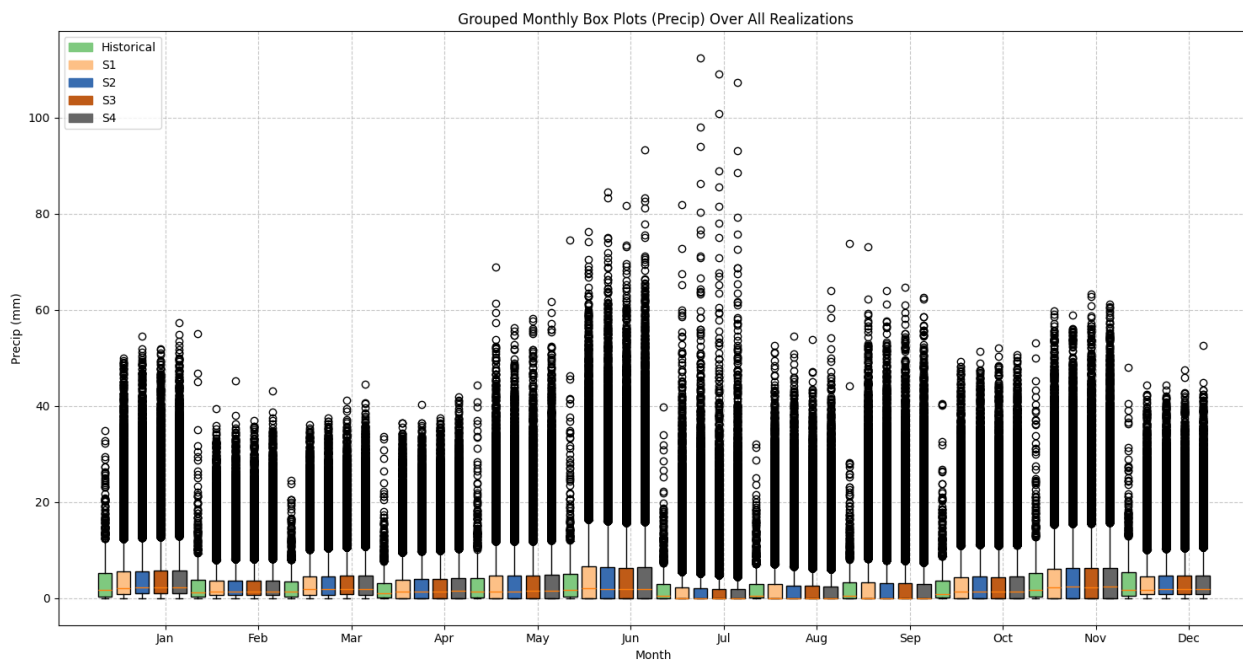
Appendix A Figure 11 - Average Projected S2 Daily Precipitation Excluding 0 Precipitation Days



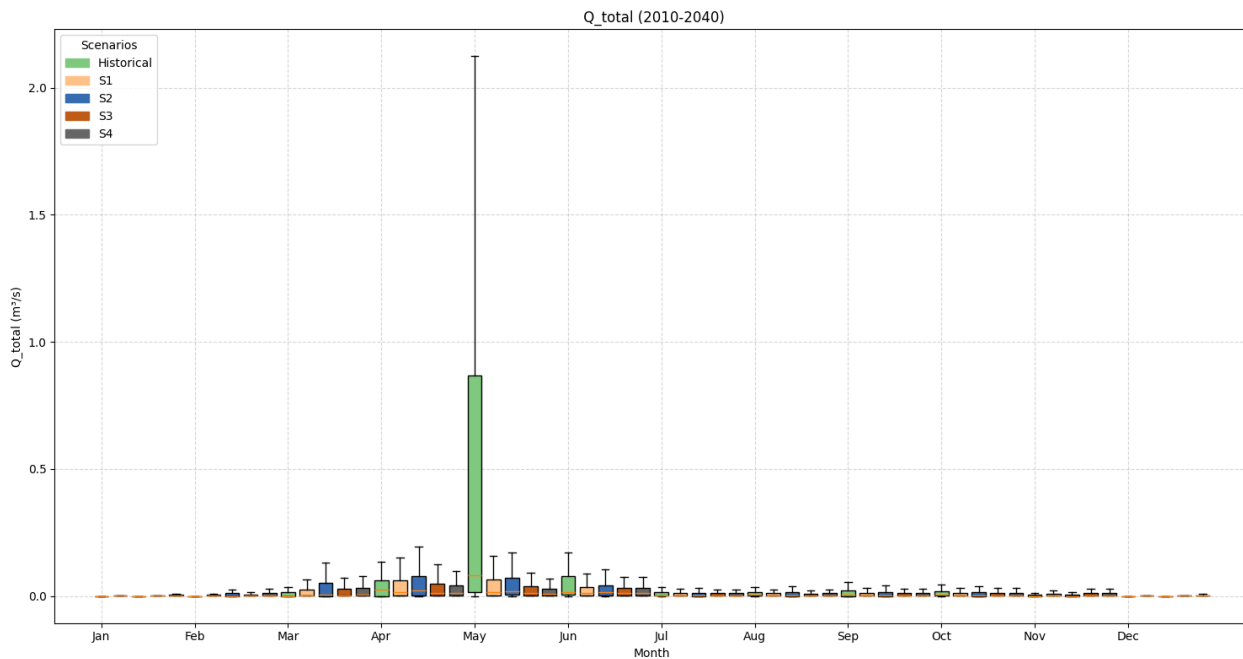
Appendix A Figure 12 -Average Projected S3 Daily Precipitation Excluding 0 Precipitation Days



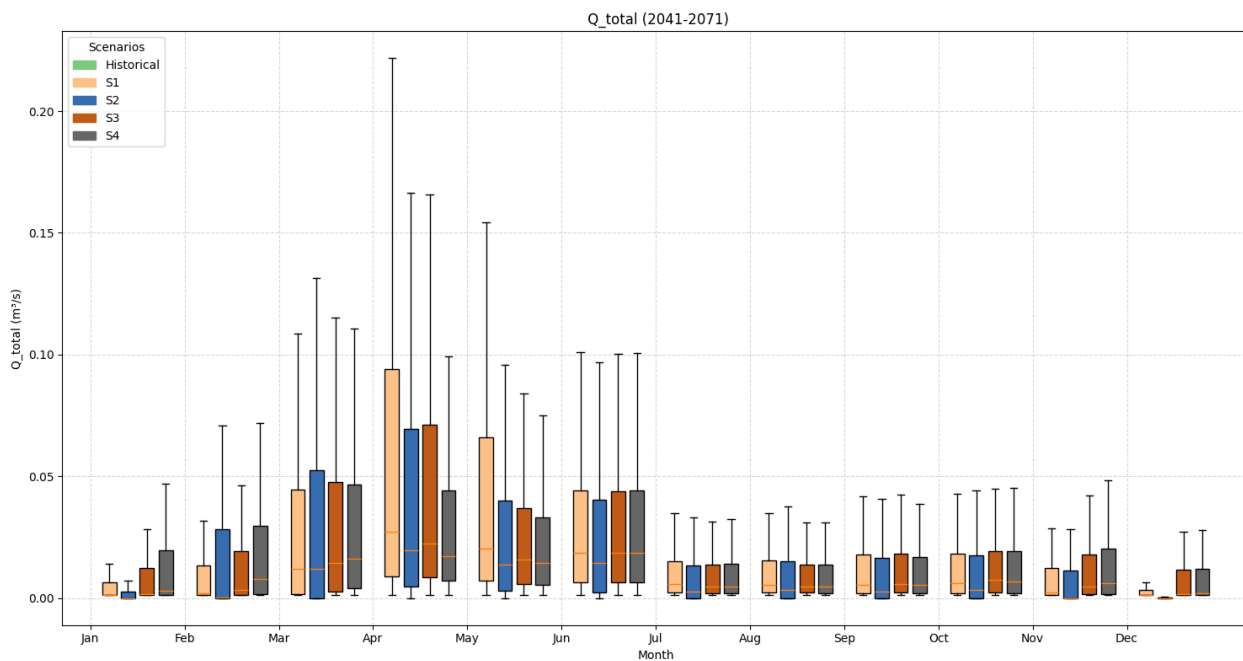
Appendix A Figure 13 - Average Projected S4 Daily Precipitation Excluding 0 Precipitation Days



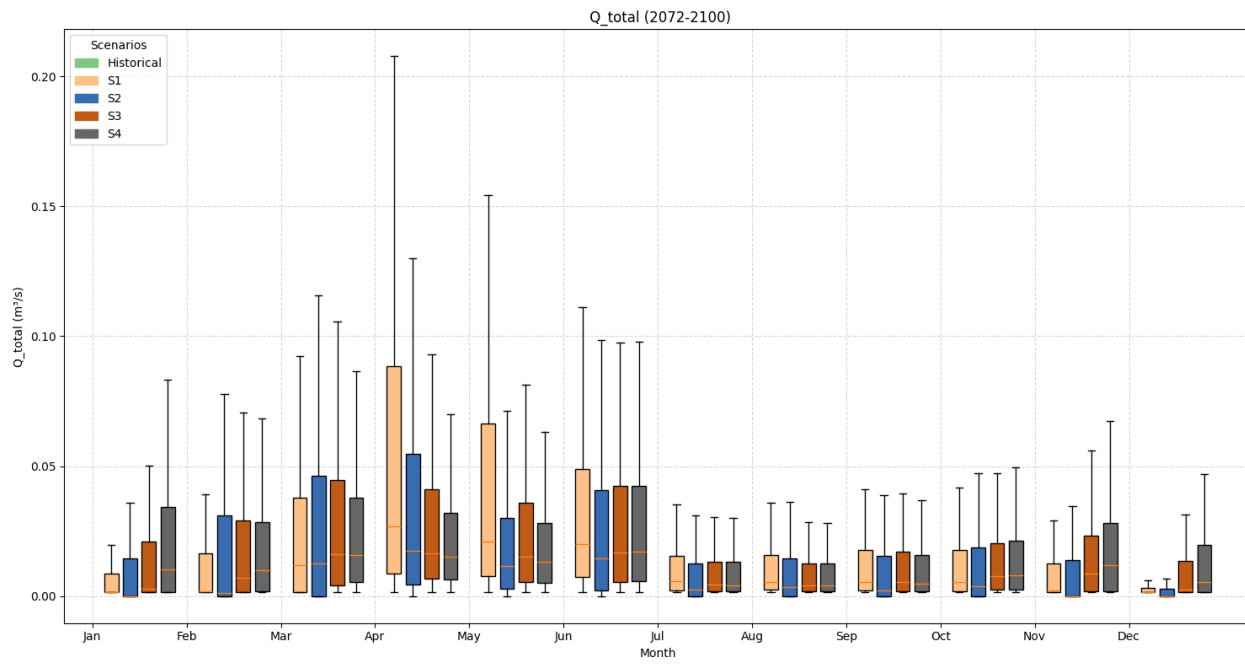
Appendix A Figure 14 - Box Plot of Daily Precipitation per Month, All Scenarios Including Outliers



Appendix A Figure 15 – Box Plot of Daily Outflow per Month Excluding Outliers (2010-2040)



Appendix A Figure 16 - Box Plot of Daily Outflow per Month Excluding Outliers (2041-2071)



Appendix A Figure 17 – Box Plot of Daily Outflow per Month Excluding Outliers (2072-2100)